Universidade Federal de Minas Gerais

Programa de Pós-Graduação em Engenharia Metalúrgica e de Minas

Tese de Doutorado

"Preparação e avaliação *in vitro* de nanofibras Gelatina/Policaprolactona com estrutura casca-núcleo obtidas por eletrofiação co-axial"

Autor: Ildeu Helênio Lazarini Pereira

Orientador: Prof. Rodrigo Lambert Oréfice, Dr.

Co-orientadora: Profa. Eliane Ayres, Dra.

Fevereiro 2013

Universidade Federal de Minas Gerais

Programa de Pós-Graduação em Engenharia Metalúrgica e de Minas

Ildeu Helênio Lazarini Pereira

PREPARAÇÃO E AVALIAÇÃO *IN VITRO* DE NANOFIBRAS GELATINA/POLICAPROLACTONA COM ESTRUTURA CASCA-NÚCLEO OBTIDAS POR ELETROFIAÇÃO CO-AXIAL

Defesa de tese a ser apresentada ao Curso de Pós-Graduação em Engenharia Metalúrgica e de Minas da Universidade Federal de Minas Gerais

Área de Concentração: Ciência dos Materiais

Orientador: Prof Rodrigo Lambert Oréfice, Dr.

Co-orientadora: Profa. Eliane Ayres, Dra.

Belo Horizonte

Escola de Engenharia da UFMG

Fevereiro 2013

Dedico este trabalho aos meus pais. Mesmo ausentes fisicamente, me ensinaram as lições básicas da vida.

AGRADECIMENTOS

Entre matérias isoladas, mestrado e doutorado, oito anos se foram sem mesmo que eu pudesse perceber. As realizações são infinitas e as propostas futuras foram completamente alteradas com o passar destes anos. Tenho orgulho desta etapa e de tudo que hoje quero para minha vida. Posso dizer que vivo intensamente e não me arrependo. Viver é uma arte, e a arte faz parte da minha vida. Todos os pontos se tornam infinitos, basta questionar. Tese é questionar, disciplinar, organizar e, muitas vezes, se sentir perdido. A sensação do término é de estar pronto para começar. Valeu a pena!

E, neste período e em todos os campos, levamos uma multidão conosco. Muitos andam juntos, outros atravessam, outros atrapalham, outros impedem, outros amam, compartilham e se deixam envolver. Posso ver de tudo, eu vi de tudo! Mas o crescimento é certeiro.

Agradeço a *Deus* por ser quem eu sou e estar sempre pronto para questionar e aprender com humildade. Muito obrigado!

Meus pais, minha dedicatória é eterna.

Ao *Renato Buratto*, sem ele o caminho seria ardiloso demais. Sem palavras para sempre te agradecer! Ao *Isaías Renato Buratto (Dzemba), Carmen Buratto, Stella e Gil, Felipe e Wally*, muito obrigado por tanto carinho.

Ao meu orientador, *Rodrigo Lambert Oréfice*, uma profunda admiração. Seria impossível agradecer todo o cuidado durante tantos anos. Impressionante! Você tem e disfruta do dom de ser professor e pesquisador. Meus parabéns e meu muito obrigado!

À *Eliane Ayres*, eu agradeço por tudo! Ela foi tudo que um aluno e um amigo precisa durante todos esses anos. Ela, sem mesmo perceber, e muitas vezes desacreditando, cria

uma redoma de proteção que nos conforta e nos faz acreditar que somos capazes. Do fundo do meu coração, não sei como te agradecer, e isto é inquestionável!

A todos os amigos e colegas do laboratório, muito obrigado por uma convivência tão fácil!

Ao Professor *Alfredo de Miranda Góes, Ana Cláudia Chagas* e equipe, um muito obrigado do fundo do coração!

Aos professores franceses *Guy Schlatter, Anne Hebraud, Luc Averous* e todos os colegas e amigos franceses, esta experiência foi maravilhosa e única. Muito obrigado!

Maria Aparecida Pacheco e *Nelson Azevedo.* Muito obrigado por me salvarem em todas as situações, vocês são sensacionais!

À Profa. *Rosário E. S. Bretas*, muito obrigado por me ajudar sempre prontamente!

À *Maria Cristina Monteiro de S. Costa*, amor eterno! À *Celeste Costa*, muito obrigado pelo meu primeiro livro de engenharia, "Ciência dos Materiais"! Foi realmente o início.

Sônia Lara, pra sempre vou te amar! Impressionante como você sempre está presente!

Roni Roland, André Bernardi e Rô, Gra, Lalá, Agnaldo e Vera, Agda Aline Rocha de Oliveira, vocês são muito especiais!

À minha família, e todos os que fazem parte da minha vida com um sentimento bom e real, meu muitíssimo obrigado!

Sumário

Índice de Figuras

Índice de Tabelas

Resumo

Neste estudo, nanofibras de policaprolactona (PCL) e de gelatina foram produzidas pela técnica de eletrofiação, e a associação destes dois polímeros formando uma estrutura casca-núcleo foi conseguida pela técnica de eletrofiação co-axial. Nanofibras com esta estrutura são ótimas candidatas para uso na Engenharia de Tecidos, pois são capazes de mimetizar a estrutura da matriz extra-celular, e, neste caso, combinando a bioatividade da gelatina (polímero natural) com a biodegradabilidade e melhores propriedades mecânicas da policaprolactona (polímero sintético). A hidrofilia da gelatina a torna solúvel em meio aquoso, por isso, para utilizá-la como biomaterial, uma reticulação das cadeias foi feita com glutaraldeído. Técnicas, como Infravermelho porTtransformada de Fourier (FTIR) e microscopias de Transmissão e Varredura revelaram a morfologia das fibras obtidas após mudanças nos parâmetros da solução e processamento durante a eletrofiação. Neste trabalho também foi mostrado a mineralização da superfície das nanofibras co-axiais após imersão em SBF10 (uma solução de óxidos para formar hidroxiapatita,) indicando que a presença da gelatina favorece a homogênea cobertura das nanofibras por fosfatos de cálcio. Resultados da Difração de Raios X revelaram que nesta composição mineral há Hidroxiapatita, principal constituinte da fase mineral dos ossos. Estudos in vitro revelaram a biocompatibilidade destas nanofibras com grande proliferação de células-tronco, assim como indícios de diferenciação destas em osteoblastos, tornando este biomaterial uma potencial candidato para uso na Engenharia de tecido ósseo.

Abstract

In this study, nanofibers containing polycaprolactone (PCL) and gelatin were produced by electrospinning. The combination of these two polymers in a core-shell structure was achieved by using a coaxial electrospinning technique. Nanofibers with this type of structure are good candidates for Tissue Engineering, since they are able to mimetize the structure of the extracellular matrix by combining the bioactivity of gelatin (natural polymer) with the biodegradability and high mechanical properties of polycaprolactone (synthetic polymer). Gelatin was submitted to a crosslinked reaction with glutaraldehyde in order to reduce its solubility in aqueous solutions Techniques such as FTIR, Transmission and Scanning Microscopies showed the morphology of the nanofiber obtained after changes in solution and electrospinning parameters were performed. In this work, it was also demonstrated the possibility of biomimetically coating the surface of the nanofibers with calcium phosphates after the immersion of the nanofibers in a SBF10 solution. The presence of gelatin as the shell material proved to be useful in favoring the deposition of the calcium phosphate surface layer. X ray diffraction results showed the presence of hydroxyapatite, one of the components of bone, in the composition of the obtained coating. In vitro studies confirmed the biocompatibility of the nanofibers. The mineralized nanofibers were able to favor both stem cell proliferation and differentiation of them in osteoblasts.

1 Introdução

A Nanotecnologia está crescendo rapidamente e nos afetará em alguma fase de nossas vidas. Pesquisas extensas estão sendo atualmente feitas nesta área para melhorar nossa qualidade de vida, sendo um atraente caminho para abordagens na área biomédica como regeneração tecidual, curativos e liberação controlada de fármacos.

Com o aumento numeroso da população idosa, a procura por enxertos ósseos tem gerado uma escassez na disponibilidade de tecidos doadores músculo-esqueletais [1]. Auto-enxertos apresentam muitas desvantagens para os pacientes, como o aumento no tempo de cirurgia, limitada quantidade de osso e dor no local doador [2]. Isto tem estimulado muito o interesse por materiais que possam ser substitutos de tecido ósseo.

Na Engenharia de Tecidos propõe-se a criação de um novo tecido para substituir em parte ou mesmo totalmente o tecido lesado. Muitos destes órgãos são estruturas fibrosas em escala nanométrica ou mesmo milimétrica. Quanto mais a estrutura artificial construída se assemelhar ao natural, melhores serão as respostas orgânicas.

Nanofibras podem servir de substrato para crescimento de tecidos devido à grande área superficial e poros interconectados em uma estrutura tridimensional. Elas podem mimetizar a forma fibrilar da matriz extracelular (MEC), que é um complexo de poliproteínas e polissacarídeos numa estrutura nanométrica [3]. Uma matriz de nanofibras deve também permitir a infiltração e proliferação celular [4].

A recuperação de tecidos requer uma função reparativa celular que é sustentada em uma rede tridimensional ao redor e dentro da matriz do biomaterial. Isto ocorre através de atividades celulares como adesão, migração, crescimento e diferenciação celular. Já foi demonstrado que a adesão e a taxa de proliferação de células aumentam em matrizes nanofibrosas quando comparado a filmes planos porosos de polímeros [5]. Origem celular apropriada, ótimos sinais de reconhecimento pelas células e uma estrutura

biodegradável que sirva como matriz extra-celular até a neoformação tecidual são três elementos básicos que se interagem para o sucesso da Engenharia de Tecidos em casos de cirurgia óssea reconstrutiva [1].

A demanda por novas nanoestruturas em biomateriais tem gerado um grande desenvolvimento técnico-cientifico nos últimos anos. Na eletrofiação, nanofibras poliméricas são produzidas como resultado de forças elétricas repulsivas que superam a tensão superficial do líquido polimérico carregado. Basicamente, o sistema de eletrofiação consiste em três partes: um gerador de alta tensão, uma seringa contendo a solução polimérica e um coletor [6]. Quando a intensidade do campo elétrico é aumentada, as cargas induzidas na superfície do líquido se repelem entre si criando uma instabilidade de cargas. Estas forças repulsivas agem em direção oposta a da tensão superficial, que resulta na extensão da gota na ponta da agulha numa forma cônica (Cone de Taylor) [7]. Quando estas forças repulsivas superam a tensão superficial do líquido, esta gota se alonga e se transforma em um jato estável que vai em direção ao coletor de carga oposta. Neste trajeto do jato, o solvente da solução evapora e fibras são formadas no coletor.

Parâmetros da solução (viscosidade, condutividade, tensão superficial, peso molecular do polímero e constante dielétrica), do processamento (campo elétrico, distância agulha-coletor e taxa de infusão) e do ambiente (humidade e temperatura) influenciam e direcionam o processo de Eletrofiação [4].

O uso efetivo de matrizes nanofibrosas poliméricas para engenharia de tecidos não está baseado somente na construção das fibras, mas também nas características dos materiais usados. Em particular, o processo de fabricação de nanofibras através de eletrofiação usando polímeros biodegradáveis sintéticos e naturais torna possível a construção de estruturas que se assemelham a elementos da matriz extracelular, além de melhorar a função de regeneração tecidual *in vitro*. Estudos com culturas celulares mostraram que a matriz é densamente povoada rapidamente por células que promovem uma infiltração celular na estrutura fibrilar. Além disso, a técnica de eletrofiação proporciona uma maneira barata e fácil de produzir nanofibras utilizando vários tipos de polímeros [8].

Nanofibras biocompatíveis e biodegradáveis são produzidas rotineiramente pela técnica de eletrofiação com uma enorme variedade de polímeros sintéticos e naturais, assim como compósitos contendo material inorgânico [9]. Os polímeros sintéticos geralmente criam a estrutura mecânica necessária, como resistência mecânica e degradação controlada. Já os polímeros naturais são mais biocompatíveis.

Dentre os polímeros sintéticos rotulados normalmente como biocompatíveis e biodegradáveis, a poli(caprolactona) (PCL) tem recebido uma atenção considerável. É um polímero hidrofóbico semi-cristalino com um grupo éster polar. Devido ao seu alto grau de cristalinidade e hidrofobia, o PCL degrada lentamente, mas não possui a mesma bioatividade de polímeros naturais [10].

Muito pertinente seria então criar estruturas nanométricas onde se combinem materiais sintéticos e naturais. O uso de polímeros naturais é importante porque estes são extremamente biocompatíveis, carregando proteínas especificas com grupamentos como RGD (arginina, glicina e ácido aspártico) com capacidade inerente de adesão celular [6].

Dentre os biopolímeros naturais, o colágeno, rico em RGD, que é um componente da matriz dérmica com fibras na dimensão de 50-500 nm, tem sido largamente usado como poliproteína na engenharia de tecidos pela excelente biocompatibilidade e não-imunogenicidade, mas as propriedades mecânicas ainda não foram alcançadas como as requeridas pela matriz extracelular [11].

A gelatina, biopolímero natural formado a partir da hidrólise controlada do colágeno, possui a mesma sequência de proteínas (RGD), tem mais baixa antigenicidade do que o colágeno, além de ser de baixo custo. Ela pode ser retirada de tecido animal como pele, músculo ou osso [11]. Entretanto a gelatina degrada rapidamente em contato com fluidos corporais, necessitando de um tratamento de reticulação para não limitar sua utilização como matriz para regeneração tecidual [12].

Recentemente, um sistema de eletrofiação utilizando seringas com capilares coaxiais foi criado para eletrofiar duas soluções poliméricas ao mesmo tempo, formando fibras em

estrutura casca-núcleo [13]. O emprego desta tecnologia avançada de eletrofiação coaxial proporciona inúmeros benefícios. Por exemplo, os materiais do núcleo podem fornecer determinadas propriedades requeridas pelo tecido a ser reparado, ao passo que os materiais da casca podem ser projetados para incluir propriedades adicionais, tais como biocompatibilidade ou propriedades hidrofílicas.

A principal vantagem da nanoestrutura núcleo-casca obtida pela técnica de eletrofiação coaxial é o potencial para obter uma combinação de propriedades de diferentes tipos de materiais. Esta técnica é interessante não só no desenvolvimento de nanofibras multifuncionais, mas também matrizes com diferentes taxas de degradação em diferentes períodos de uso no corpo humano. A performance mecânica de nanofibras, com específicas concentrações de polímeros no núcleo e na casca, produzidas por tal processo, geralmente é melhor do que aquelas produzidas somente com um polímero [14]. Esta técnica também é estudada para a produção de nanofibras com liberação controlada de fármacos, onde o polímero da casca impede a liberação inicial acelerada do fármaco encapsulado no polímero do núcleo [15].

A incorporação de minerais, como fosfato de cálcio nas nanofibras eletrofiadas é um excelente caminho para a fabricação de matrizes para a Engenharia de Tecido ósseo [9]. O osso é constituído de uma fase mineral com 60-70% de hidroxiapatita carbonatada cristalina e de uma matriz orgânica rica em fibras de colágeno [16]. Compósitos poliméricos contendo Hidroxiapatita podem aprimorar o crescimento de osteoblastos [17]. Tendo em vista que a associação entre hidroxiapatita e colágeno são os mais promissores substitutos dos ossos [16] e que a presença de gelatina facilita o recobrimento homogêneo das nanofibras por fosfato de cálcio, várias técnicas têm sido desenvolvidas para incorporar minerais em matrizes poliméricas a fim de ajudar na indução de diferenciação óssea [18].

Neste contexto, esta pesquisa pretende elucidar características de nanofibras que associam polímeros sintéticos e naturais, PCL e gelatina, respectivamente, processadas através da técnica de eletrofiação coaxial em uma estrutura núcleo-casca. Pretende-se mostrar também a interessante deposição de hidroxiapatita em tais nanofibras, que pode

beneficiar a reparação óssea. A construção destas nanoestruturas tridimensionais citocompatíveis *in vitro e in vivo* as tornaria perfeitamente capaz de funcionar como matrizes para crescimento celular, além de serem capazes de se degradar conjuntamente à reparação tecidual.

Os objetivos específicos e da tese em geral são apresentados no capítulo 2. Os resultados desta Tese serão descritos e discutidos nos capítulos 3, 4 e 5. No terceiro e quarto capítulos serão retratadas a produção de nanofibras de Policaprolactona e gelatina obtidas pela técnica de Eletrofiação e a produção de nanofibras coaxiais destes mesmos polímeros obtida pela técnica de Eletrofiação coaxial. Estas produções foram realizadas em conjunto com a Universidade de Strasbourg – França, no contexto do projeto CAPES – Cofecub. Estudos preliminares *in vitro* de citotoxicidade destas nanofibras coaxiais após cobertura com fosfatos de cálcio serão mostrados no terceiro capítulo, assim como indícios de osteogênese e angiogênese em células-tronco cultivadas nestas nanofibras. Os estudos biológicos foram feitos em parceria com o laboratório do Prof. Alfredo Góes de Miranda (Instituto de Ciências Biológicas - UFMG). Com exceção dos capítulos de introdução, objetivos e conclusão (capítulo 6), o conteúdo da Tese foi escrito em inglês, no formato de artigos, e dividido em capítulos.

Referências

1. Yang F, Wolke JGC, Jansen JA. Biomimetic calcium phosphate coating on electrospun poly (ε-caprolactone) scaffolds for bone tissue engineering. Chem. Eng. J 2008; 137:154-161.
2. Phipps MC, Clem WC, Grunda JM, Clines GA, Bellis SL. Increasing the pore sizes of bone-mimetic electrospun scaffolds comprised of polycaprolactone, collagen I and hydroxyapatite to enhance cell infiltration. Biomaterials 2012; 33:524-534.
3. Kim SH, Shin C, Min SK, Jung SM, Shin HS. In vitro evaluation of the effects of electrospun PCL nanofibers mats containing the microalgae Spirulina (Arthrospira) extract on primary astrocytes. Colloids and Surfaces B: Biointerfaces 2012; 90:113-118.
4. Chakrapani VY, Gnanamani A, Giridev VR, Madhusoothanan M, Sekaran G. Electrospinning of Type I collagen and PCL nanofibers using acetic acid. Journal of Applied Polymer Scienve 2012; 125:3221-3227.
5. Kim YJ, Park MR, Kim MS, Kwon OH. Polyphenol-loaded polycaprolactone nanofibers for effective growth inhibition of human cancer cells. Materials Chemistry and Physics 2012; 133:674-680.
6. Bhardwaj N, Kundu SC. Electrospinning: A fascinating fiber fabrication technique. Biotechnol. Adv 2010; 28:325-47.
7. Baji A, Mai YW, Wong SC, Abtahi M, Chen P. Electrospinning of polymer nanofibers: Effects on oriented morphology, structures and tensile properties. Compos. Sci. Technol 2010; 70:703-18.
8. Chong EJ, Phan TT, Lim IJ, Zhang YZ, Bay BH, Ramakrishna S, Lim CT. Evaluation of electrospun PCL/gelatin nanofibrous scaffold for wound healing and layered dermal reconstitution. Acta Biomaterialia 2007; 3:321-30.
9. Li X, Xie J, Lipner J, Yuan X, Thomopoulos S, Xia Y. Nanofiber scaffolds with gradations in mineral content for mimicking the tendon-to-bone insertion site. Nano Letters 2009; 9(7):2763-2768.
10. Woodruff MA, HutmacherDW. The return of a forgotten polymer-Polycaprolactone in the 21st century. Prog. Polym. Sci 2010; 35(10):1217-56.
11. Ki CS, Baek DH, Gang KD, Lee KH, Um IC, Park YH. 2005 Characterization of gelatin nanofiber prepared from gelatin–formic acid solution. Polymer 2005; 46:5094-102.
12. Wu SC, Chang WH, Dong GC, Chen KY, Chen YS, Yao CH. Cell adhesion and proliferation enhancement by gelatin nanofiber scaffolds. Journal of Bioactive and Compatible Polymers 2011; 26(6):565-577.
13. Zhao P, Jiang H, Pan H, Zhu K, Chen W. Biodegradable fibrous scaffolds composed of gelatin coated poly(ε-caprolactone) prepared by coaxial electrospinning. Journal of Biomedical Materials Research 2007; 83:372-382.
14. Huang ZM, Zhang YZ, Ramakrishna S. Double-layered composite nanofibers and their mechanical performance. J Polymv Sci Part B: Polym Phys 2005; 43:2852-2861.

15. Meinel, AJ, Germershaus O, Luhmann T, Merkle H, Meinel L. Electrospun matrices for localized drug delivery: current Technologies and selected biomedical applications. European Journal of Pharmaceutics and Biopharmaceutics 2012; 81:1-13.
16. Bigi A, Boanini E, Panzavolta S, Roveri N, Rubini K. Bonelike apatite growth on hydroxyapatite-gelatin sponges from simulated body fluid. 2002; 59:709-714.
17. Campos DM, Anselme K, Soares GDA. In vitro biological evaluation of 3D hydroxyapatite/collagen (50/50 wt. (%)) scaffolds. Material Research 2012; 15(1):151-158.
18. Tas AC, Bhaduri SB. Rapid coating of Ti6Al4V at room temperature with a calcium phosphate solution similar to 10× simulated body fluid. J. Mater. Res 2004; 19:2742-49.

2 Objetivos

2.1 Objetivo geral:

Preparação e avaliação *in vitro* de nanofibras Gelatina/Policaprolactona com estrutura casca-núcleo obtidas por eletrofiação co-axial para uso em Engenharia de Tecidos.

2.2 Objetivos específicos:

- Obtenção de nanofibras de Policaprolactona pela técnica de eletrofiação.
- Obtenção de nanofibras de Gelatina pela técnica de eletrofiação.
- Obtenção de nanofibras de Gelatina/Policaprolactona em estrutura casca-núcleo pela técnica de eletrofiação co-axial.
- Caracterização e análise das nanofibras após mudanças nos parâmetros da solução e de processamento.
- Análise da mineralização da superfície das nanofibras com estrutura casca-núcleo após cobertura por hidroxiapatita.
- Avaliação preliminar de citotoxicidade destas nanofibras.
- Avaliação precoce de diferenciação angiogênica e osteogênica de células-tronco cultivadas nas nanofibras.

3 Influence of solution and processing parameters in electrospinning of single Poly(ε-Caprolactone) (PCL) nanofibers and co-axial PCL/Gelatin nanofibers

Abstract. *In the electrospinning process, polymer nanofibers with submicron-scale diameters are formed when a droplet of a viscoelastic polymer solution is subjected to a high-voltage electrostatic field. In this paper, we report the experimental work on the electrospinning process in which the influence of different process and solution parameters were evaluated. The effect of the electrospinning solvent on poly(ε-caprolactone) (PCL) fiber morphology was evaluated. The replacement of 2, 2, 2-trifluoroethanol (TFE) with a mixture of acetic acid and formic acid significantly reduced the diameter of the fibers. Solutions of PCL and gelatin in acetic acid/formic acid were electrospun in fibers by co-axial electrospinning. The ratio of the viscosities* η_{core}/η_{shell} *was found to be of critical importance to achieve stable core–shell nanofibers.*

Keywords: *Electrospinning; PCL; Gelatin; Solvent dielectric constants; Rheology*

3.1 Introduction

Electrospinning has been widely used for the fabrication of polymeric nanofibers [1]. The basic electrospinning setup includes a polymer solution or melt reservoir and a grounded collector with a high-voltage between them. When the voltage is high enough to overcome the surface tension of the polymer solution/melt, a charged jet is generated towards the grounded collector and the solvent evaporates/melt solidifies along the jet to form solid thin fibers [2].

Numerous studies have shown that the optimal electrospinning configuration and operational conditions differ drastically from one polymer to another, with process parameters (applied electric field, needle-to-collector distance, flow rate, type of collector) and solution properties (viscosity, surface tension, conductivity) being the main factors influencing the transition of a polymer solution into ultrafine fibers [3]. In this paper, some of these parameters have been explored, particularly the effect of replacing 2, 2, 2-trifluoroethanol (TFE) by a mixture 1:1 (v/v) of acetic acid and formic acid in the solution for electrospinning.

Polycaprolactone (PCL) is a polyester with a semicrystalline linear structure and excellent mechanical strength. It is non-toxic in nature and found to be cyto-compatible with several body tissues, making it an ideal material for tissue engineering [4]. PCL degrades, in the first instance, by random chain scission of the ester groups via hydrolysis [5]. Polymers capable of undergoing hydrolytic degradation initially absorb water, hydrating the molecular chains. The type of functional group presented along the length of the polymer chain affects the rate of water absorption, its subsequent hydrolysis and, ultimately, its rate of degradation. Thus, the hydrophobic nature of the PCL backbone leads to a much slower degradation than most of the other biodegradable synthetic polymers. To overcome this shortcoming, PCL-based co-axial nanofibers, in which a polymer with faster degradation rate is used as either the core or shell of the nanofiber, can be used [6].

In this study, the effects of some parameters involved in the electrospinning of polycaprolactone nanofibers, as well as of gelatin/polycaprolactone coaxial nanofibers, on the morphology of the fibers were investigated. Gelatin, a protein derived from partial hydrolysis of collagen, was chosen because of its biological origin, biocompatibility, bioresorbability, non-immunogenicity, biodegradability and commercial availability [7].

3.2 Materials and Methods

3.2.1 Materials

The materials used for nanofiber fabrication were poly(ε-caprolactone) (PCL) (Sigma-Aldrich, St. Louis, MO, USA, Mn = 80,000 g/mol), gelatin powder (type A from porcine skin, gel strength approx. 300 g Bloom) (Sigma-Aldrich, St. Louis, MO, USA), 2,2,2-trifluoroethanol (TFE) (99%) (Sigma-Aldrich, St. Louis, MO, USA), acetic acid (98-100%) (Riedel de Haën) and formic acid (99.8%) (Sigma Aldrich). All the chemicals were used without any further treatment.

3.2.2 Electrospinning of PCL nanofibers

To prepare spinnable solutions, the PCL was dissolved in TFE under stirring for 24 h. Alternatively, PCL was dissolved in a 1:1 (v/v) mixture of acetic acid and formic acid. The experimental setup used for electrospinning process consisted of an adjustable DC power supply (Gamma High Voltage Research, USA), a syringe pump in which the syringe was connected to a stainless steel needle (D=2 mm) and a static collector wrapped with aluminum foil. During the electrospinning process, the solution was ejected from the tip of the positively charged needle to generate ultrafine fibers on the collector that was connected to the ground with a zero or a negative polarity. Different PCL concentrations ranging from 10% to 17% w/w were prepared and electrospun at different feed rates. Electrospinning parameters such as applied voltage and distance from the tip of the needle to the collector were varied. All experiments were conducted at room temperature and below 40% relative humidity. After the electrospinning process, the nanofibrous cloth was carefully peeled off from the collector and stored in a sealed desiccator for further investigations.

3.2.3 Co-axial electrospinning of PCL/gelatin nanofibers

The two polymer solutions were independently fed through concentrically configured needles. The outer and inner diameters of the needles were 2.0 and 1.5 mm, respectively. The solution concentrations of PCL and gelatin in acetic acid/formic acid 1:1 (v/v) were maintained at 15% w/w. Both PCL and gelatin solutions were delivered with a programmable syringe pump. A collecting plate was placed on a grounded static

collector wrapped with aluminum foil. Both polymer solutions were electrospun by combining different feed rates. The needle was positively charged with voltages of 25 or 30 kV. The collector was connected to the ground with a zero polarity. The distance from the tip of the needle to the collector was maintained at 15 cm. All experiments were conducted at room temperature and below 40% relative humidity. After the electrospinning process, the nanofibrous membrane was carefully peeled off from the collector and put into a sealed desiccator to further investigations.

3.2.4 Characterization of electrospun mats

Morphology and diameter of the nanofibers were analyzed by scanning electron microscopy (SEM) (JEOL JSM 5600, Japan) at an accelerating voltage of 15 kV. Samples for SEM were mounted on metal stubs and coated with gold using a sputter coater (JEOL JFC-1200 fine coater, Japan). Non-woven nanofiber mats were analyzed with 50 individual measurements of nanofiber diameters taken from SEM micrographs using image analysis software (Image J, National Institutes of Health, USA). This was repeated for a single electrospun fiber mat fabricated under a single set of constant conditions to calculate the average nanofiber diameter and standard deviation.

The nanofibrous mats were also characterized by attenuated total reflectance Fourier transform infrared (ATR-FTIR), using a Golden Gate single reflection ATR in a Bruker IFS-spectrometer at a resolution of 4 cm^{-1} and 256 co-added scans. The spectra were collected between 400 and 4,500 cm^{-1}.

A Physica MCR 301 Rheometer (Anton Paar, Austria) equipped with a cone and plate (CP 50-1) was used for viscosity measurements. Shear measurements were performed in a range of shear rates from 0.05 to 90 s^{-1}.

Transmission electron microscopy (TEM) (TOPCON 002B) at 200 kV was used to observe the core-shell structure of the fibers. The samples for the TEM observation were prepared by directly depositing the as-spun fibers onto copper grids. The samples were dried in a vacuum oven for 48 h at room temperature prior to TEM images.

3.3 Results and Discussion

3.3.1 Nanofibers of PCL in TFE

Optimization of the electrospinning processing conditions for each particular polymer/solvent is crucial to obtain electrospun fibers with characteristics that meet specific application needs [1]. The effect of variations in many parameters, such as the applied voltage, the solution flow rate and the needle-to-collector distance at different concentrations on the fiber morphology were analyzed. Table 3.1 shows the various parameters used and their effect on fiber diameter when TFE was used as solvent for PCL.

Table 3.1: Electrospinning conditions for PCL solutions in TFE

Sample	C%(wt)	U (kV)	d (cm)	FR	D (nm)	SD (nm)
PCL-12	10	18/0	12	0.8	170	94
PCL-13	10	20/0	12	0.8	140	33
PCL-14	10	22/0	12	0.8	200	94
PCL-15	10	25/0	12	0.8	160	69
PCL-16	10	18/0	15	0.8	300	301
PCL-17	10	20/0	15	0.8	180	147
PCL-18	10	22/0	15	0.8	140	57
PCL-19	10	25/0	15	0.8	160	90
PCL-20	12	18/0	12	0.8	460	36
PCL-21	12	20/0	12	0.8	590	29
PCL-22	12	22/0	12	0.8	610	43
PCL-23	12	25/0	12	0.8	950	350
PCL-24	12	18/0	15	0.8	340	319
PCL-25	12	20/0	15	0.8	200	141
PCL-26	12	22/0	15	0.8	230	156
PCL-27	12	25/0	15	0.8	400	326
PCL-28	14	18/0	12	0.8	690	372
PCL-29	14	20/0	12	0.8	720	436

PCL-30	14	22/0	12	0.8	780	322
PCL-31	14	25/0	12	0.8	1120	287
PCL-32	14	18/0	15	0.8	550	352
PCL-33	14	20/0	15	0.8	530	391
PCL-34	14	22/0	15	0.8	610	444
PCL-35	15	15/-15	15	0.8	970	427
PCL-69	7	10/-10	15	0.2	Failed	
PCL-70	7	15/-15	15	0.2	100	30
PCL-71	7	20/-20	15	0.2	110	39
PCL-72	7	30/0	15	0.2	110	46
PCL-73	7	15/-20	15	0.2	120	44
PCL-74	12	10/-10	15	0.2	Failed	
PCL-75	12	15/-15	15	0.2	450	285
PCL-76	12	20/-20	15	0.2	330	300
PCL-77	12	30/0	15	0.2	430	343
PCL-78	12	15/-20	15	0.2	450	386
PCL-79	15	10/-10	15	0.2	Failed	
PCL-80	15	15/-15	15	0.2	870	369
PCL-81	15	20/-20	15	0.2	680	526
PCL-82	15	30/0	15	0.2	560	398
PCL-83	15	15/-20	15	0.2	690	577
PCL-114	7	30/0	15	0.2	Failed	

C% (wt): solution concentration of PCL

d (cm): distance from needle to collector

U (kV): Voltage

FR: PCL solution feed rate (mL/h)

D (nm): Average fiber diameter

SD (nm): Standard deviation

ATR-FTIR analysis was conducted to characterize the PCL nanofibers. Figure 3.1 shows the FTIR spectra of PCL nanofibrous mats. This includes 2951 cm^{-1} (asymmetric CH_2 stretching), 2951 / 2865 cm^{-1} (CH_2 stretching), 1722 cm^{-1} (carbonyl stretching), 1293 cm^{-1} (C–O and C–C stretching), 1239 cm^{-1} (asymmetric COC stretching) and 1176 cm^{-1} (symmetric COC stretching) [8].

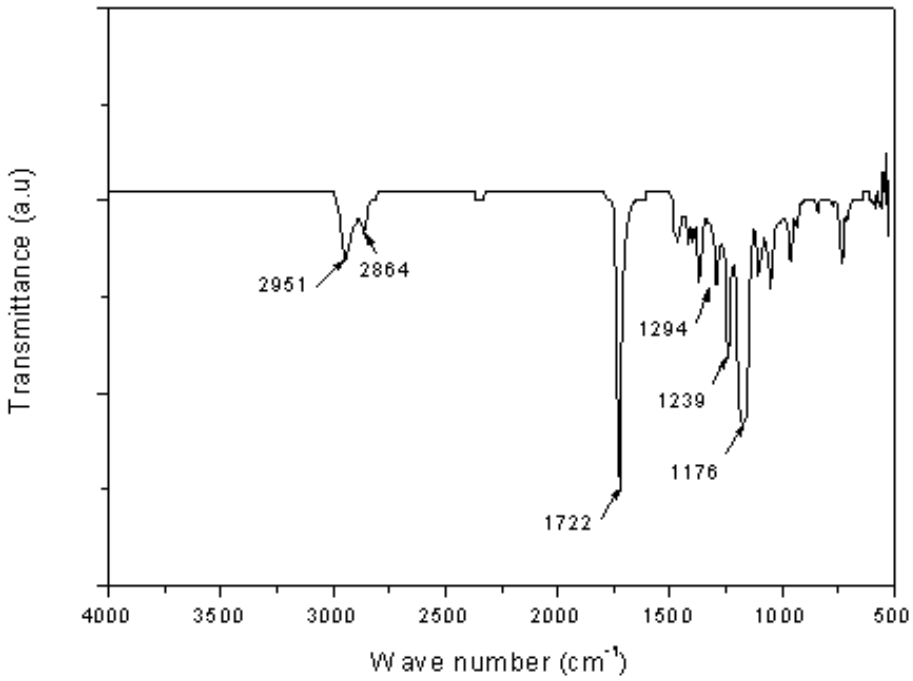

Figure 3.1: FTIR spectrum of PCL nanofiber mats. Sample used: PCL-20.

The effect of voltage on electrospun fiber morphology was investigated at different PCL solution concentrations (Figure 3.2). A crucial element in the electrospinning process is the voltage applied to the solution. According to Bhardwaj *et al*. [1], fiber formation occurs only after the threshold voltage is obtained. This induces the necessary charges on the solution along with electric field and initiates the electrospinning process. However, electric field instabilities are detected above the threshold voltage [9].

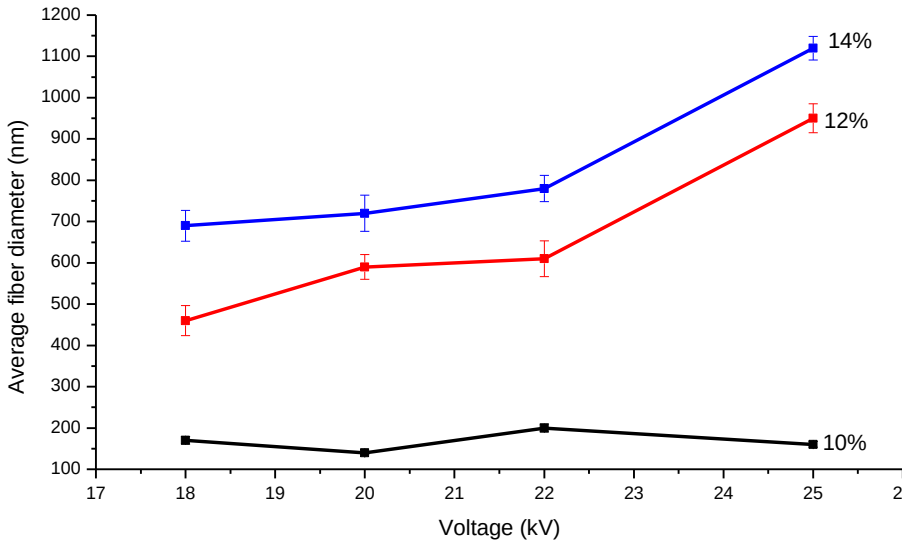

Figure 3.2: Graph showing fiber diameter vs. applied voltage for 10, 12 and 14% solutions of PCL in TFE. Samples used: PCL-12, PCL-13, PCL-14, PCL-15, PCL-20, PCL-21, PCL-22, PCL-23, PCL-28, PCL-29, PCL-30 and PCL-31. Distance from needle to collector of 12 cm and feed rate of 0.8 mL/hr. Error bars are ± standard deviation of sample population.

Studies have suggested that when higher voltages are applied, there is more polymer ejection, which facilitates the formation of a larger diameter fiber [1]. This effect can be observed in Figure 3.2, although most of the studies have found the opposite effect [1]. As can be seen in Figure 3.2, the effect of voltage on fiber diameter is more pronounced at higher concentrations. Thus, the voltage influences the fiber diameter, but the polymer solution concentration has a much more profound effect on it. Figure 3.3 (a-d) shows SEM images of some nanofibers used in Figure 3.2, confirming the accentuated effect of solution concentration on the fiber morphology. The strong dependence of fiber diameter on material concentration has been reported by a number of studies for other materials [10-12]. In the electrospinning process, for fiber formation to occur, a minimum solution concentration is required. It has been found that solutions below 800 cP are too dilute to undergo chain entanglement and readily breakup into droplets [13]. In this case, a mixture of beads and fibers are obtained as observed in Figure 3.3 (a-b). However, it is difficult for the applied charged potential to overcome the surface tension of viscous solutions above 4000 cP [13]. In summary, the diameter of the electrospun

fibers correlates directly with polymer concentration. The upper and lower limits for solution concentration vary greatly and depend on the polymer type, its molecular weight, temperature and the polymer-solvent interaction.

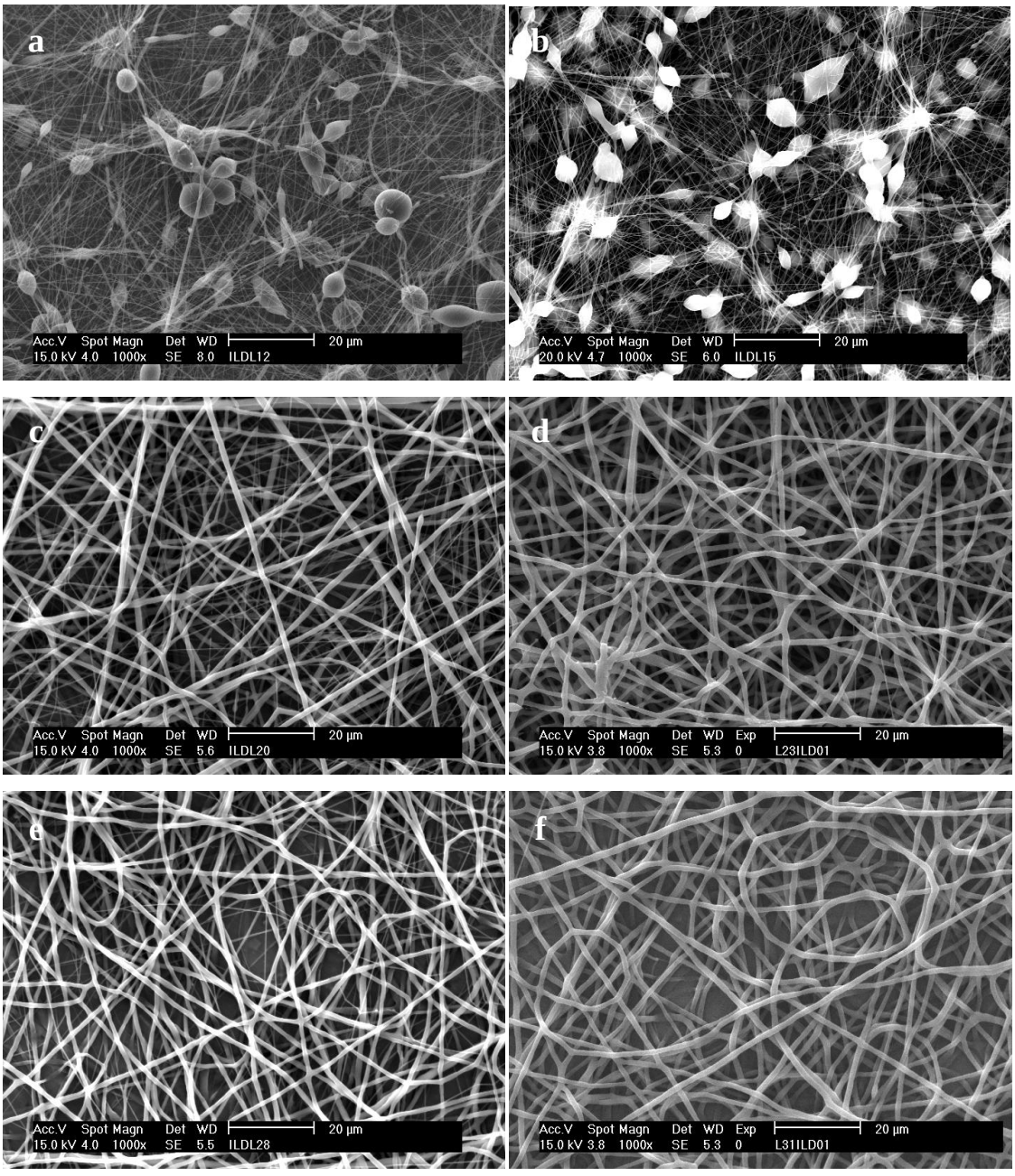

Figure 3.3: MEV of the PCL nanofiber mats: (a) PCL-12; (b) PCL-15; (c) PCL-20; (d) PCL-23; (e) PCL-28 and (f) PCL-31. (Magnification 10^3 X)

Figure 3.4 shows the effects of voltage on electrospun fiber morphology when the distance between the tip and the collector was raised to 15 cm at different PCL solution concentrations. As can be observed in Figure 3.4, in general, the nanofibers demonstrated the same previous behavior, i.e., larger fibers were formed when the voltage increased. The SEM micrographs presented in Figure 3.5 present the fibers when the distance between the tip and the collector was raised to 15 cm, and few differences from the previous images (Figure 3.3), where the distance was set to 12 cm, were observed.

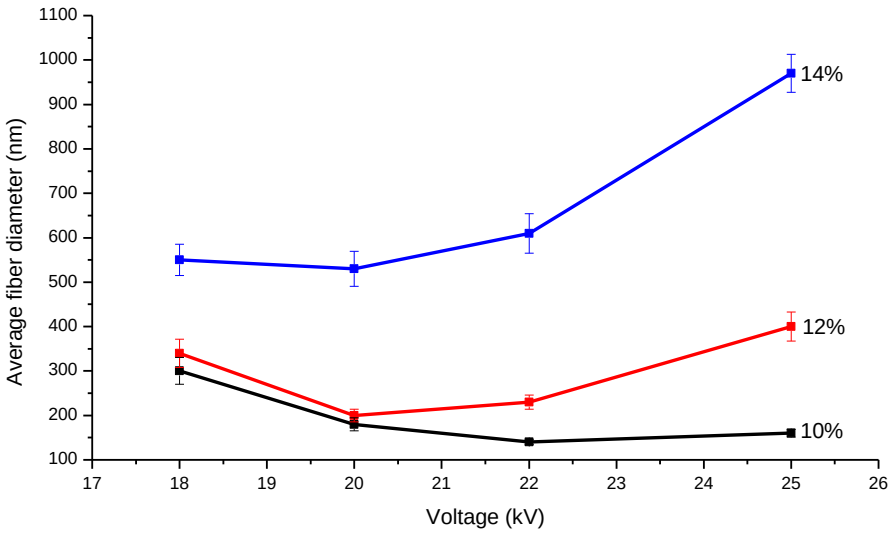

Figure 3.4: Graph showing fiber diameter vs. applied voltage for 10, 12 and 14% solutions of PCL in TFE. Samples used: PCL-16, PCL-17, PCL-18, PCL-19, PCL-24, PCL-25, PCL-26, PCL-27, PCL-32, PCL-33, PCL-34 and PCL-35. Distance from needle to collector of 15 cm and feed rate of 0.8 mL/hr. Error bars are ± standard deviation of sample population.

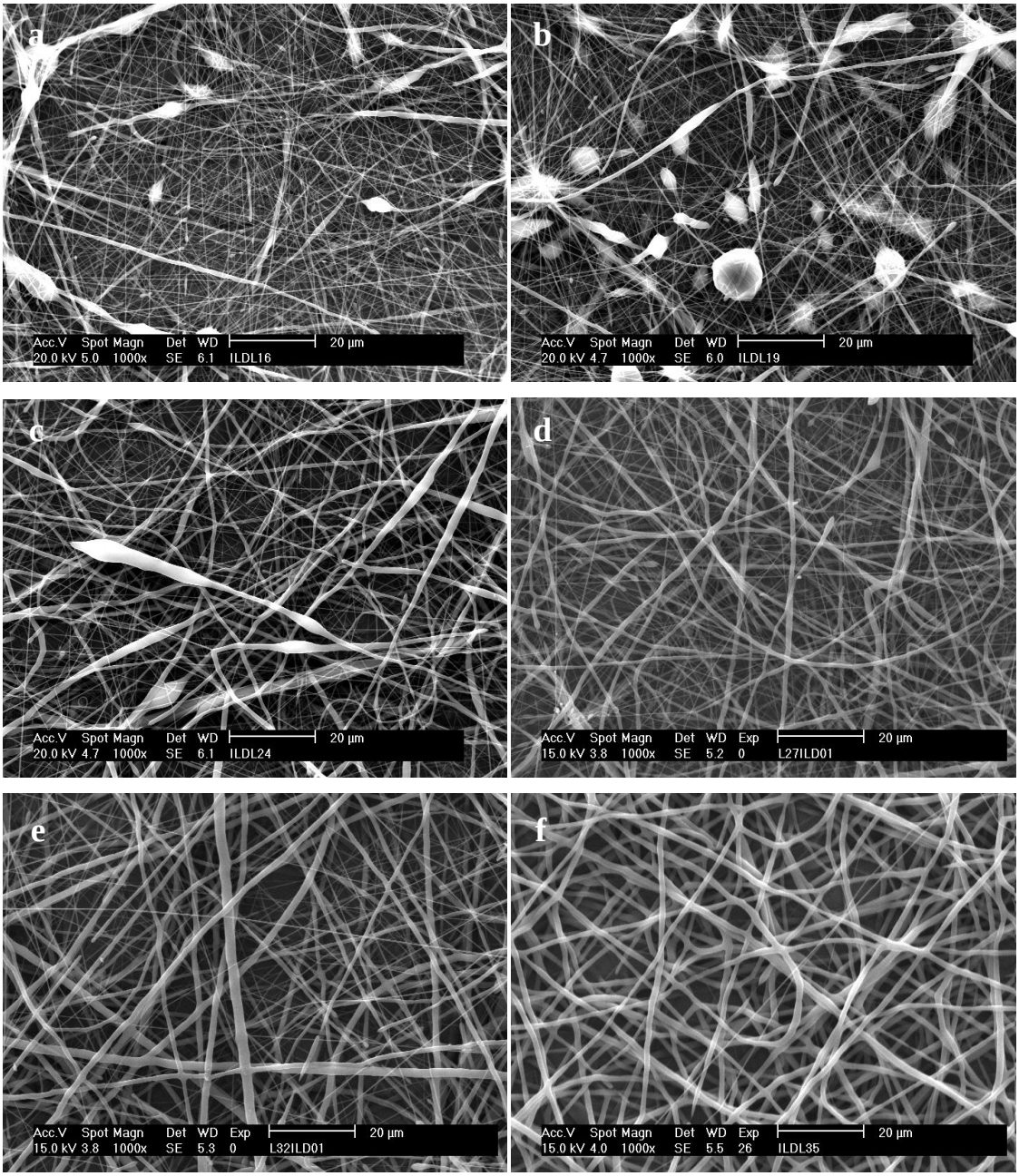

Figure 3.5: MEV of the PCL nanofibers mats: (a) PCL-16; (b) PCL-19; (c) PCL-24; (d) PCL-27; (e) PCL-32; (f) PCL-35. (Magnification 10^3 X**)**

The effect of increasing the distance between the tip and the collector on the morphology of PCL nanofibers is shown in detail in Figure 3.6. As can be observed in Figure 3.6, there seems to be a trend of smaller fiber diameters when the distance between the tip and the collector is raised from 12 cm to 15 cm. In view of this, it is reasonable to think that thinner fibers are produced using a higher distance, where less

solvent remains in the jet and more stretching occurs. However, Dougstani *et al*. [14] in their PCL electrospinning experiments with different parameter combinations found that the mean fiber diameter increased with the distance. According to them, by increasing the spinning distance, the electric field strength will decrease (E = V/d), resulting in less acceleration and, hence, less stretching of the jet, leading to thicker fiber formation. It is likely that the sum of these two opposite effects has an influence on the diameter of the fibers. However, due to the high sensitivity of the electrospinning process to small variations, the fiber diameter may be more influenced by one or the other depending on the experiment.

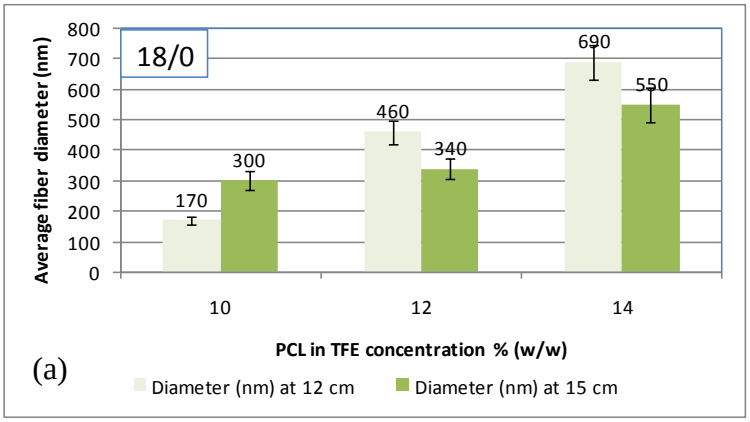

(a)

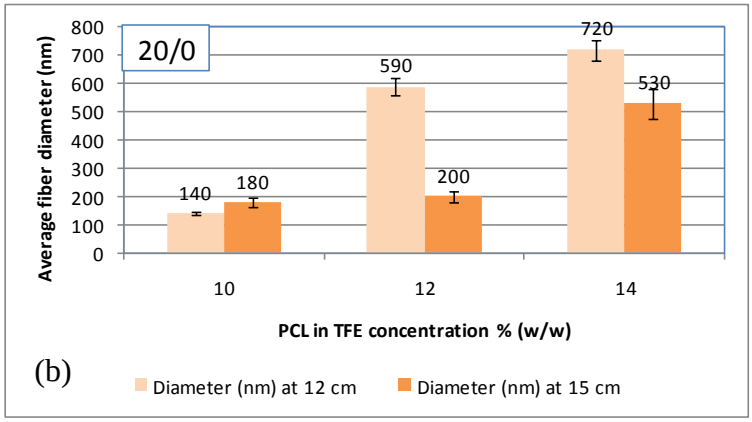

(b)

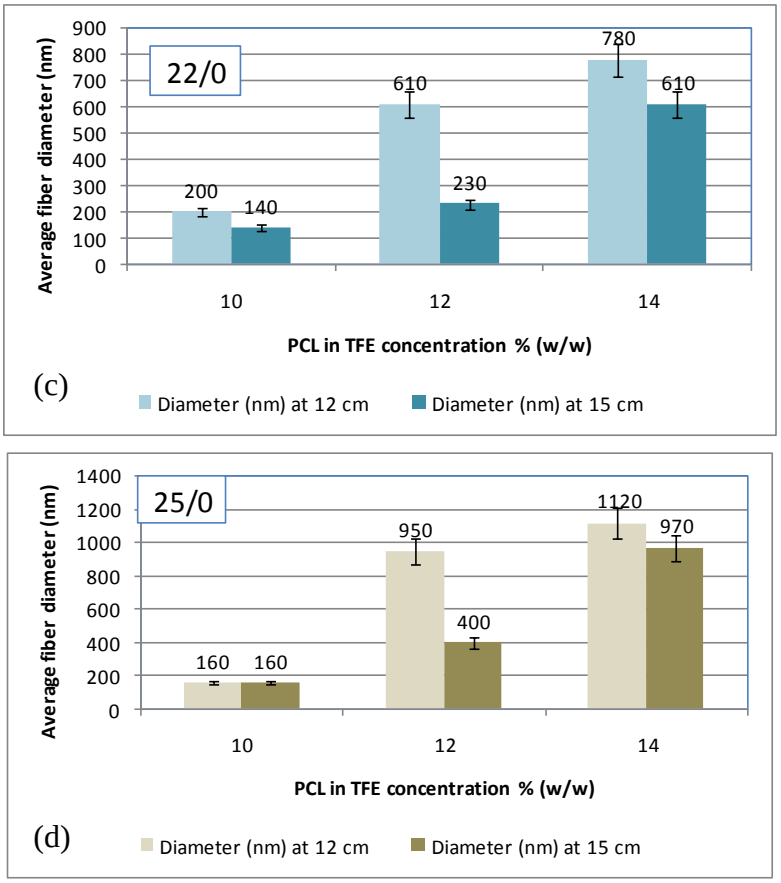

Figure 3.6: Comparison of the fiber diameter using distance between the tip and the collector of 12 cm (left) and 15 cm (right) for voltages of: (a) 18/0, (b) 20/0, (c) 22/0 and (d) 25/0 kV. Samples used: 18/0: PCL-12, PCL-20, PCL-28 (12 cm) and PCL-16, PCL-24, PCL-32 (15 cm); 20/0: PCL-13, PCL-21, PCL-29 (12 cm) and PCL-17, PCL-25, PCL-33 (15 cm); 22/0: PCL-14, PCL-22, PCL-30 (12 cm) and PCL-18, PCL-26, PCL-34 (15 cm); 25/0: PCL-15, PCL-23, PCL-31 (12 cm) and PCL-19, PCL-27, PCL-35 (15 cm).

In fact, it is very difficult to establish a reliable relation between the various electrospinning parameters and fiber diameter. An exception is the polymer solution concentration, which presents a direct response to the fiber diameter. Figure 3.7, for example, examines the behavior of the fiber diameter with increasing solution concentration for two different voltages. An opposite result to those of Figure 3.2 and Figure 3.4 is present in Figure 3.7. With these sets of samples, the mean fiber diameter decreased with an increase in voltage. As aforementioned, there are two factors

governing the relation between fiber diameter and voltage [1]. In the case of Figure 3.7, the predominant factor seems to be the increase of electric field strength and larger electrostatic stretching forces due to the increasing applied voltage that caused the jet to accelerate more in the electric field, thereby favoring thinner fiber formation.

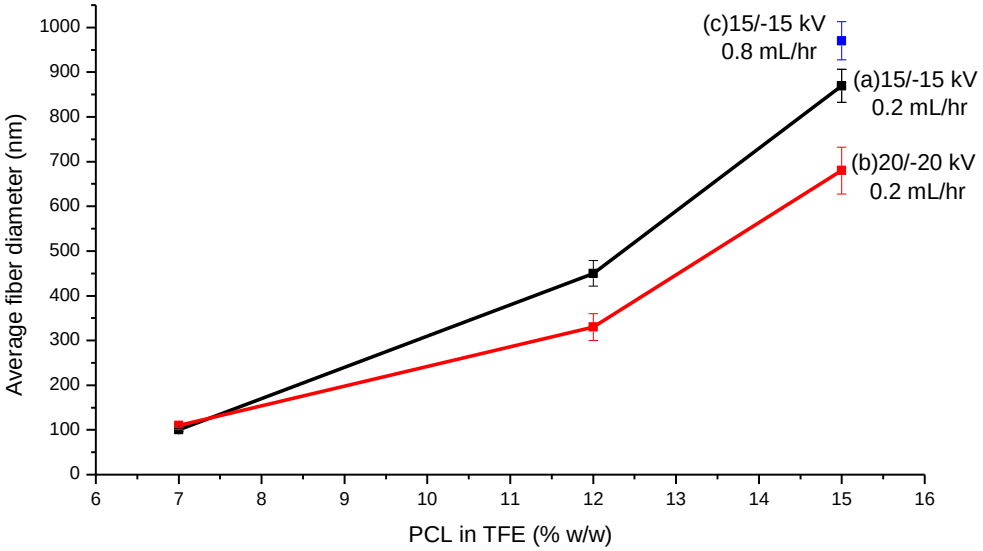

Figure 3.7: Graph showing average fiber diameter vs. solution concentration of PCL in TFE. Samples used: (a) PCL-70, PCL-75 and PCL-80; (b) PCL-71, PCL-76 and PCL-81; (c) PCL-35.

Figure 3.7 also shows that when the voltage is kept constant, the fiber diameter tends to increase with increase in the flow rate. This result is in agreement with Zhou *et al*. [15], who reported that the PCL single-fiber diameter increased from approximately 27 µm at 0.03 mL h^{-1} to 80 µm at 0.18 mL h^{-1}. The authors attributed this result to the deterioration of the stability of the jet due to solution dripping, which was noted at higher flow rates.

3.3.2. Nanofibers of PCL in acetic acid/formic acid (1:1)

In this work, a 1:1 (v/v) combination of acetic acid and formic acid was used as an alternative solvent to TFE. Among the solvents used for PCL electrospinning, acetic acid and formic acid are the least toxic [16]. Table 3.2 shows the various parameters used and their effect on the fiber diameter when this solvent system was used for PCL.

The average fiber diameter plotted versus PCL solution concentration in this solvent system can be seen in Figure 3.8.

Table 3.2: Electrospinning conditions for PCL solutions in acetic acid/formic acid 1:1 (v/v)

Sample	C%(wt)	U (kV)	d (cm)	FR	D (nm)	SD (nm)
ACETIC ACID/FORMIC ACID 1:1 (v/v)						
PCL-2	11.5	25/-1	14	0.4	120	67
PCL-3	11.5	25/0	14	0.4	120	55
PCL-4	13.1	25/-1	14	0.4	100	44
PCL-5	13.1	25/0	14	0.4	130	66
PCL-6	14.6	25/-1	14	0.4	130	62
PCL-7	14.6	25/0	14	0.4	110	52
PCL-8	14.6	25/-1	14	0.4	Failed	
PCL-9	17	25/-1	14	0.4	160	93
PCL-10	17	25/0	14	0.4	150	70
PCL-11	15	20/-10	14	0.4	Failed	
PCL-97	15	10/-10	15	0.4	Failed	
PCL-98	15	15/-15	15	0.4	130	61
PCL-99	15	20/-20	15	0.4	140	29
PCL-100	15	30/0	15	0.4	120	39
PCL-101	15	15/-20	15	0.4	150	39

C% (wt): solution concentration of PCL

d (cm): distance from needle to collector

U (kV): Voltage

FR: PCL solution feed rate (mL/h)

D (nm): Average fiber diameter

SD (nm): Standard deviation

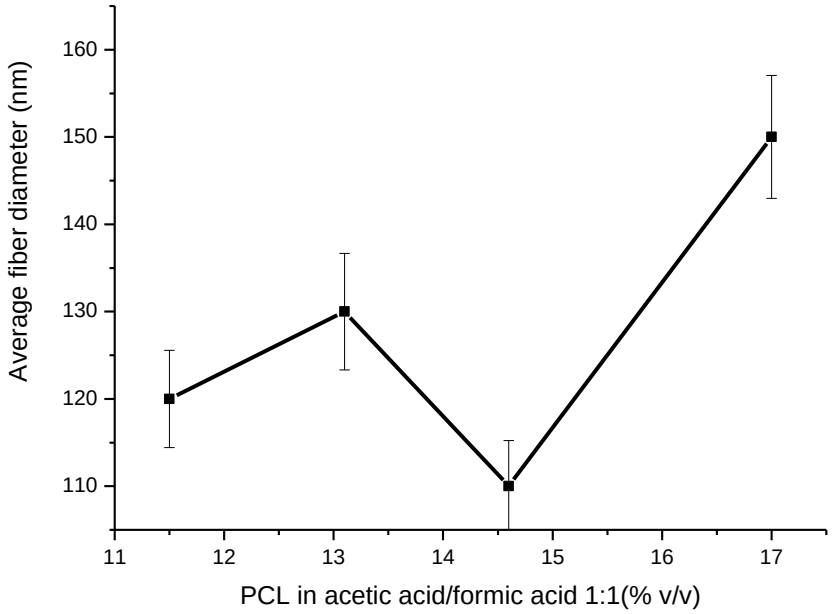

Figure 3.8: Graph showing fiber diameter vs. solution concentration of PCL in acetic acid/formic acid 1:1 (% v/v). Samples used: PCL-3, PCL-5, PCL-7, and PCL-10. Applied voltage of 25/0 KV, distance from needle to collector of 14 cm and feed rate of 0.4 mL/hr. Error bars are ± standard deviation of sample population.

As can be seen in Figure 3.8, with the exception of the point corresponding to the concentration of 14.6%, a trend of increase in the diameter with increase in the concentration of solution was maintained. Compared to TFE, the use of such acids as solvent gave rise to smaller fiber diameters. According to Raghavan *et al*. [17], the solution parameters have the most significant influence on the electrospinning process and electrospun fiber morphology. The viscosity of the solution and its electrical characteristics determine the extent of the elongation of the solution. This, in turn, has an effect on the diameter of the electrospun fiber. Table 3.3 shows the values of dielectric constant at 25 ^{0}C for some solvents [18].

Table 3.3: Dielectric constant (25 ºC) for some PCL electrospinning solvents

Solvent	Dielectric constant (ε)
Water	87.9
Acetic acid	6.15
Acetone	20.7
N,N-Dimethylformamide (DMF)	36.7
Formic acid	57.5
Methanol	32.7
Methylene chloride (MC)	9.1
Tetrahydrofuran (THF)	7.58
Toluene	2.4
2,2,2-Trifluoroethanol (TFE)	8.55

The behavior showed in Figure 3.8 coincides with the fact that the dielectric constant of formic acid is much higher than that of TFE, as shown in Table 3.3. In poly(ethylene oxide) electrospinning, for example, the higher is the dielectric constant of the solvent, the lower is the fiber diameter [17]. Sawada *et al*. [19] reported that the average diameter of the fibers electrospun from PVA aqueous solution was 580 ± 38 nm, which increased up to 1230 ± 254 nm when using 10 wt% DMF. However, the productivity defined as ([1 - (amount of polymer which did not come in contact with the collector) / (amount of polymer ejected from the needle for 30 min)] x 100) of electrospun PVA fibers increased from 15 to 92% by increasing the content of DMF from 0 to 10 wt%.

Lee *et al*. [20] have studied the effect of dielectric constant and electrical conductivity of solution on PCL electrospinning. They found that methylene chloride (MC), which has intermediate dielectric constant, was a good solvent for PCL but produced large fiber diameter. Although N, N-dimethylformamide (DMF) is not a solvent for PCL, it has a high dielectric constant and was used for improving electrospinning process. According to them, for the MC/DMF solvent systems, as the DMF volume fraction increased, solution electrical conductivity increased and the diameter of electrospun PCL fibers decreased conspicuously. Toluene reported as a poor solvent for PCL and with low dielectric constant did not impart the same effect. For MC/toluene systems, solution conductivity did not change as toluene increased. The authors interpreted that DMF has not only a high dielectric constant, but also polyelectrolyte behavior.

When non-conductive polymers such as PCL are used for electrospinning, the charges are solely accommodated for by the volatile solvent [12]. Therefore, a polymer solution with higher electrical conductivity would carry more charge, leading to a greater tensile force, which could lead to an increase in the stretching and splitting of the jet, resulting in a thinner fiber and broader diameter distribution [21]. In view of this one could suppose that the high dielectric constant of formic acid along with the polyelectrolyte character of the acids is responsible for thinner diameter of the fibers when compared with TFE.

Luong-Van *et al*. [22] found that the use of methanol, a poor solvent for PCL, improves the conductance of the polymer solution, which in turn affects the fiber diameter. According to them, the conductivity of the spinning solution can be altered by the addition of filler molecules such as ionic salts and drugs. The addition of salts (e.g., NaCl and KH_2PO_4) to polymer solutions have been found to affect the fiber diameter, with the presence of charged ions leading to fibers with substantially decreased diameter and with ions of small atomic radii (such as Na^+) having the larger effect. This observation was explained by the presence of the highly charged molecules in the spinning solution, resulting in an increase in the charge density on the surface of the ejected polymer jet. The increase in charge density imposes greater elongation and thinning forces on the jet as it travels through the electric field, resulting in fibers of smaller diameter.

Moghe *et al*. [23] describe a method to improve the electrospinnability of PCL to produce uniform ultra-fine nanofibers with narrow fiber diameter distribution. As reported by the authors, this was achieved by using a new solvent system that increases the conductivity of the solution. For this purpose, they used a fugitive salt that evaporates along with the solvent during electrospinning. Pyridine, an organic base compound, was used as an additive to accomplish this goal. According to them, when added to a solution of PCL in glacial acetic acid, pyridine is protonated and forms pyridinium acetate that evaporates during the electrospinning process. This results in pure polymeric nanofibers of smaller dimensions and superior uniformity than are otherwise possible.

3.3.3. Co-axial nanofibers of PCL/gelatin in acetic acid/formic acid (1:1)

Preliminary studies have shown that PCL/gelatin co-axial nanofibers provide a optimal solution for overcoming the shortcomings of natural and synthetic polymers, resulting in a new biomaterial with good biocompatibility and improved mechanical, physical and chemical properties [8, 24, 25]. The purpose of this work is to obtain PCL/gelatin co-axial nanofibers in the solvent system acetic acid/ formic acid 1:1 (v/v).

Because PCL and gelatin in solution have a threshold time for electrospinning before degradation, the rheological behavior of PCL and gelatin solution in these acids was initially studied. Rheograms for PCL and gelatin (15% wt) after different times are shown in Figure 3.9 and Figure 3.10, respectively.

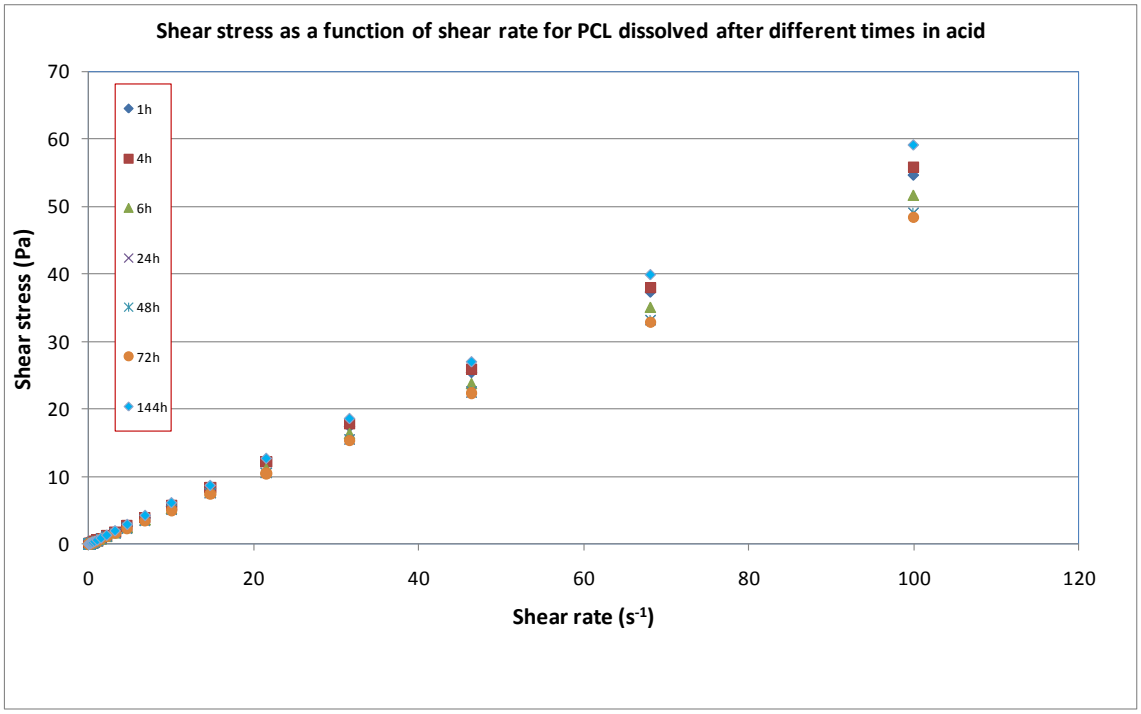

Figure 3.9: Rheograms for PCL solution (15% wt) after different times.

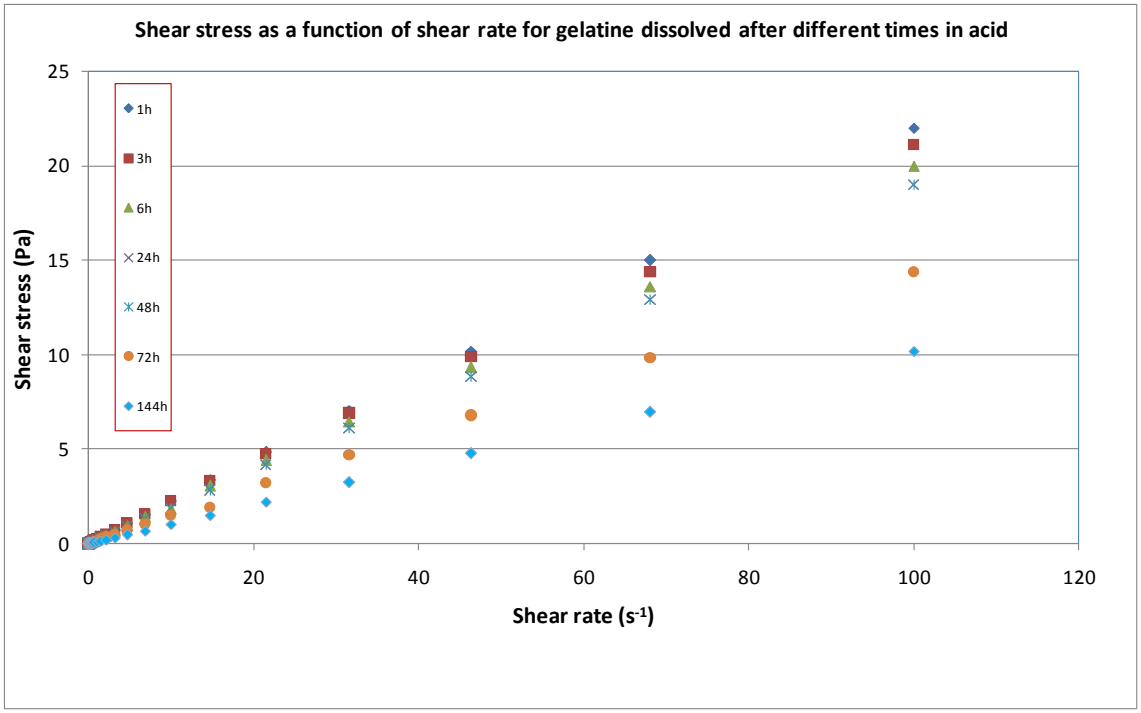

Figure 3.10: Rheograms for gelatin solution (15% wt) after different times.

Both polymer solutions presented rheological behavior close to Newtonian fluids, a slight shear-thinning was observed suggesting pseudoplastic behavior. Marcotte *et al*. [26] have shown that aqueous gelatin (2%) is Newtonian at most temperatures. According to them, just above the setting point, the viscosity becomes markedly time dependent, owing to the degree of aggregation taking place, which is accentuated by higher concentrations and high molecular weights.

The reduction in apparent viscosity with increasing shear rate is an alternative way to depict pseudoplastic behavior of the polymer solutions as shown in Figures 3.11, 3.12 and 3.13.

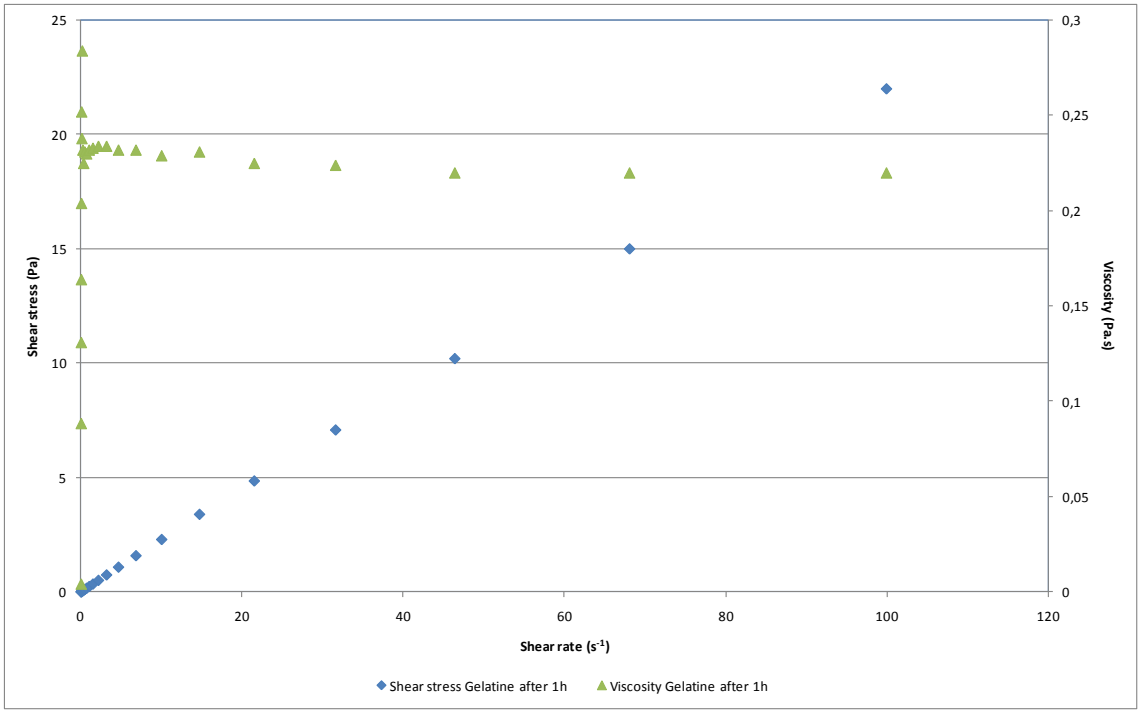

Figure 3.11: Viscosity for gelatin solution (15% wt) after 1 hour.

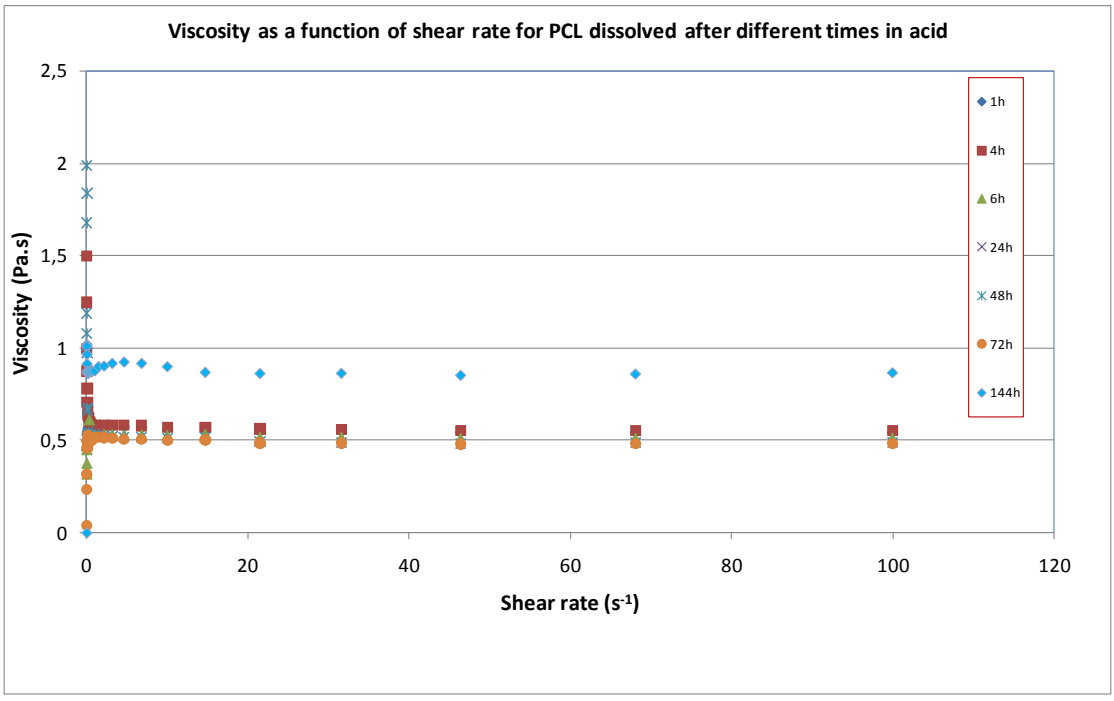

Figure 3.12: Viscosity/shear rate relationship for PCL solution (15% wt) after different times.

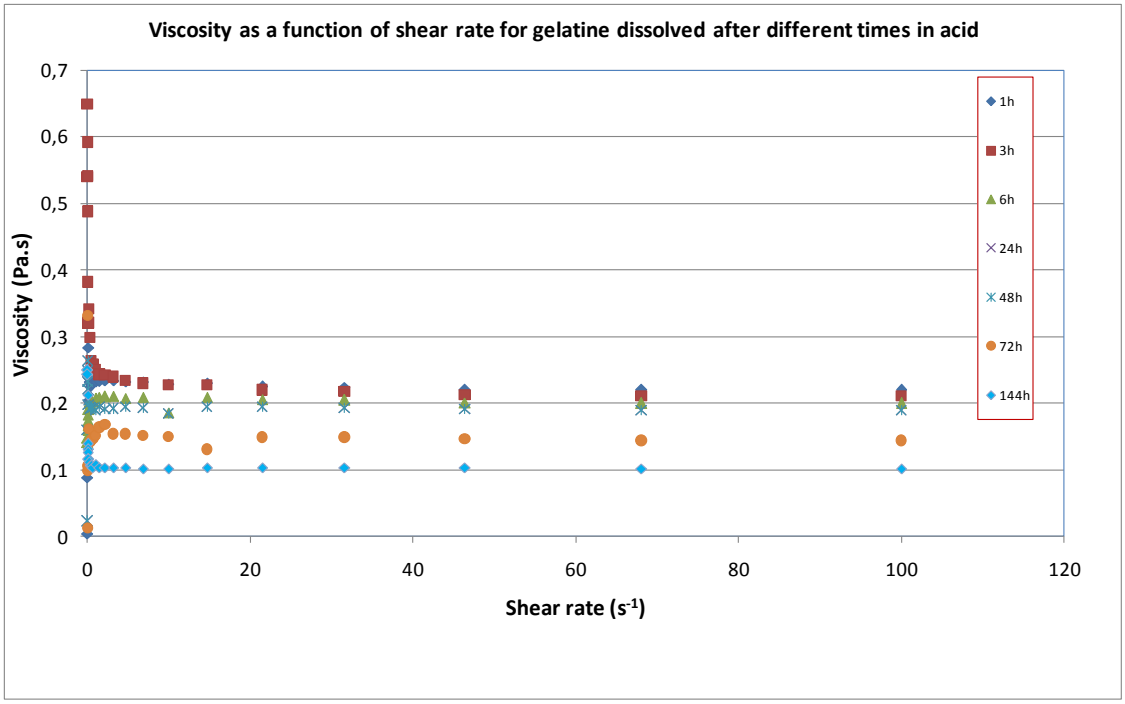

Figure 3.13: Viscosity/shear rate relationship for gelatin solution (15% wt) after different times.

The behavior of viscosity (η) with time is presented for both gelatin and PCL solution in Figure 3.14. As can be seen in Figure 3.14, for gelatin solution, a slight viscosity thinning with time occurred, whereas for PCL solution, the viscosity was maintained constant over time, except after 144 h, when an accentuated increase in viscosity was noted. This was probably due to solvent evaporation. The results in Figure 3.14 proved that minor degradation of the polymers in solution occurred at least for the first 48 hours after polymer dissolution.

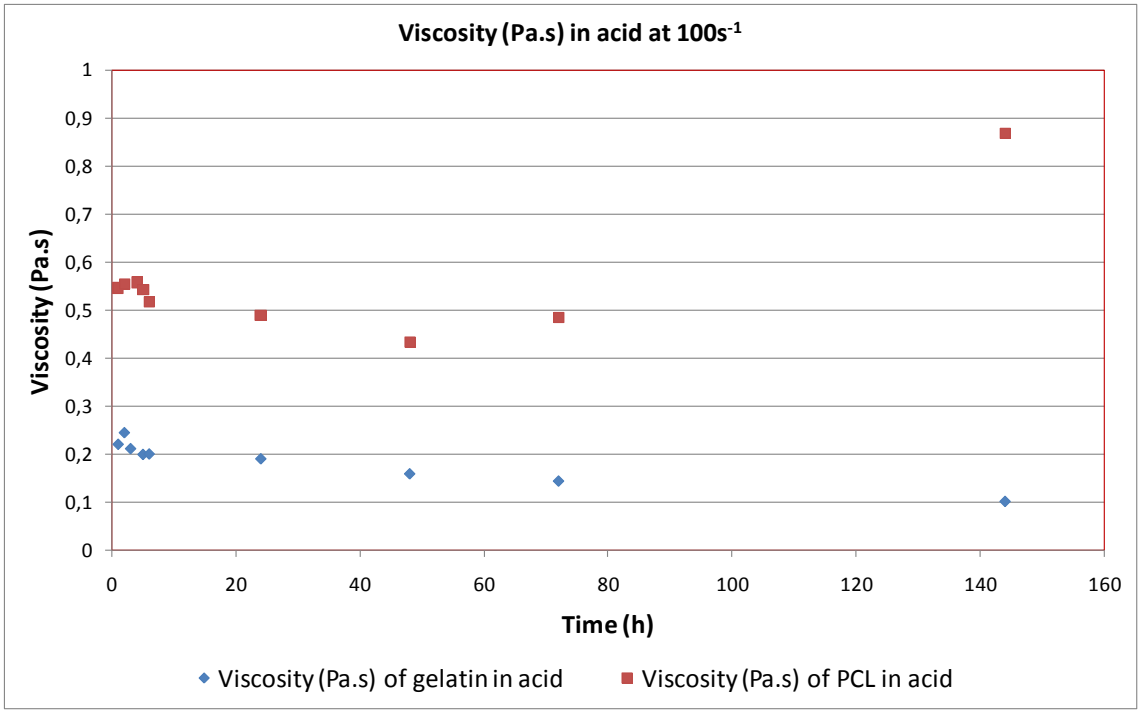

Figure 3.14: Viscosity versus time for gelatin and PCL solution (15% wt).

According to Tiwari *et al* [27], in the case of core-shell electrospinning, the ratio η_{core}/η_{shell} is of critical importance to obtain stable core-shell electrospinning, in addition to the individual viscosity requirements of core and shell solutions for electrospinning. For the shell solutions consisting of PLGA 80/20 (in 80:20 chloroform and DMF) and PVA solutions (in water) used in the core, the workable range is $\eta_{core}/\eta_{shell} \geq 0.55$. This range may vary for different polymer pairs, solvent types and interactions between core and shell solutions. Figure 3.15 shows the graph of the present system (PCL/gelatin 15% wt in acetic acid/formic acid 1:1), in which η_{core}/η_{shell} values were plotted against the time that polymer and solvent remained in contact before electrospinning. Adapting the Tiwari *et al* theory to the time of contact between the polymer and solvent to produce the solution for electrospinning, we can conclude that there should be a threshold time of polymer/solvent contact that, once exceeded, would result in unspinnable solutions. As can be seen in Figure 3.15, after 48 hours of contact between polymer and solvents, the conditions of spinnability were probably no longer suitable due to the high η_{core}/η_{shell}.

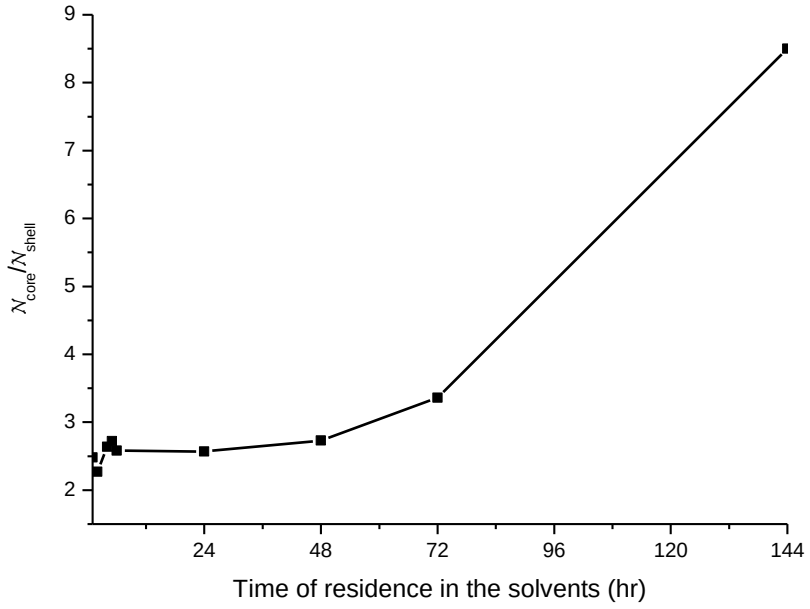

Figure 3.15: Time of residence in the solvents versus relative viscosities of the core and shell solutions.

Table 3.4 shows the various parameters used and their effect on fiber diameter when acid acetic/acid formic (1:1) was used as the solvent system for producing PCL/gelatin co-axial nanofibers. As can be seen in Table 3.4, the ratio of flow rates between the core and shell solutions profoundly affected the co-axial electrospinning. Nguyen *et al*. [28] focused on fabrication and characterization of porous core/shell structured composite nanofibers with a core of blended salicylic acid (SA) and poly(ethylene glycol) (PEG) and a shell of poly(lactic acid) (PLA). According to them, the stable core/shell structure of composite nanofibers is determined by the stability of the compound jet of two liquids, which in turn is strongly affected by the feed rates and applied voltage, among others parameters. Nanofibers obtained at core feed rates of 0.1–0.2 mL/h formed the core/shell structure, but when the core feed rate was increased to 0.4 mL/h, the PLA solution was insufficient for encapsulating core solutions. Chakraborty *et al* [13] stated that in this case, the resulting core/shell solutions form pendant drops at the needle, projecting only droplets under electrical gradient.

Table 3.2: Electrospinning conditions for co-axial fibers PCL/gelatin

Sample	U (kV)	FR_1	FR_2	D (nm)	SD (nm)
S_1=S_2= ACETIC ACID/FORMIC ACID 1:1 (v/v)					
PCL/G-116	30/0	0.3	0.13	190	60
PCL/G-117	30/0	0.2	0.2	400	144
PCL/G-118	30/0	0.2	0.3	350	72
PCL/G-119	25/0	0.3	0.13	270	117
PCL/G-120	25/0	0.2	0.2	Failed	
PCL/G-121	25/0	0.2	0.3	180	54
PCL/G-132	30/0	0.6	0.6	Failed	
PCL/G-133	30/0	0.3	0.3	Failed	
PCL/G-134	30/0	0.8	0.8	510	66
PCL/G-135	30/0	0.9	0.9	510	117
PCL/G-136	30/0	0.7	0.8	360	85
PCL/G-137	30/0	0.7	0.7	325	84

Solution concentration of PCL and gelatin: 15% (w/w)

Distance from needle to collector of 15 cm

U (kV): Voltage

FR_1: PCL solution feed rate

FR_2: Gelatin solution feed rate

D (nm): Average fiber diameter

SD (nm): Standard deviation

Figures 3.16 and 3.17 show SEM and TEM micrographs of co-axial PCL/gelatin nanofiber obtained in acetic acid/formic acid (1:1).

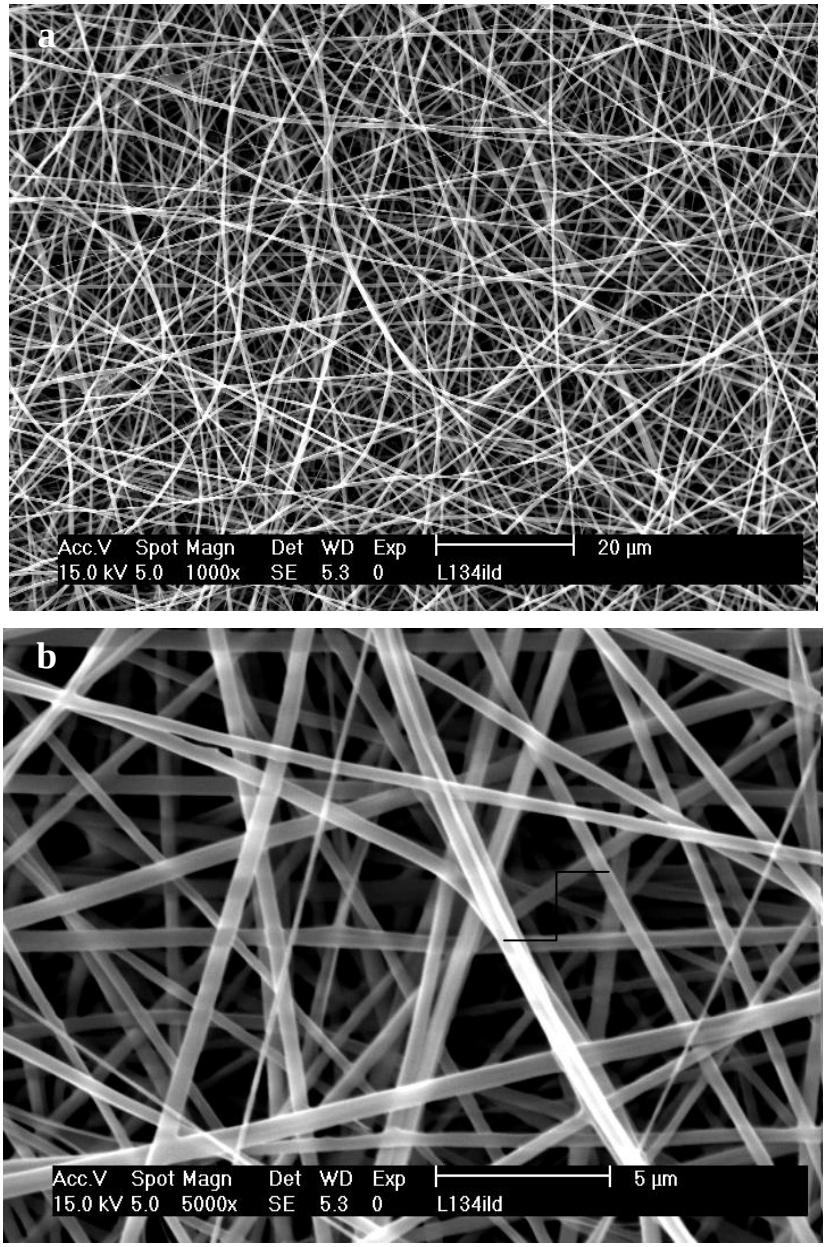

Figure 3.16: MEV of co-axial PCL/gelatin nanofibers in acetic acid/formic acid (1:1 v/v): The arrow highlights the PCL core of co-axial fiber. Sample used PCL/G-134. (Magnifications: (a) 10^3 X and (b) 5.10^3 X)

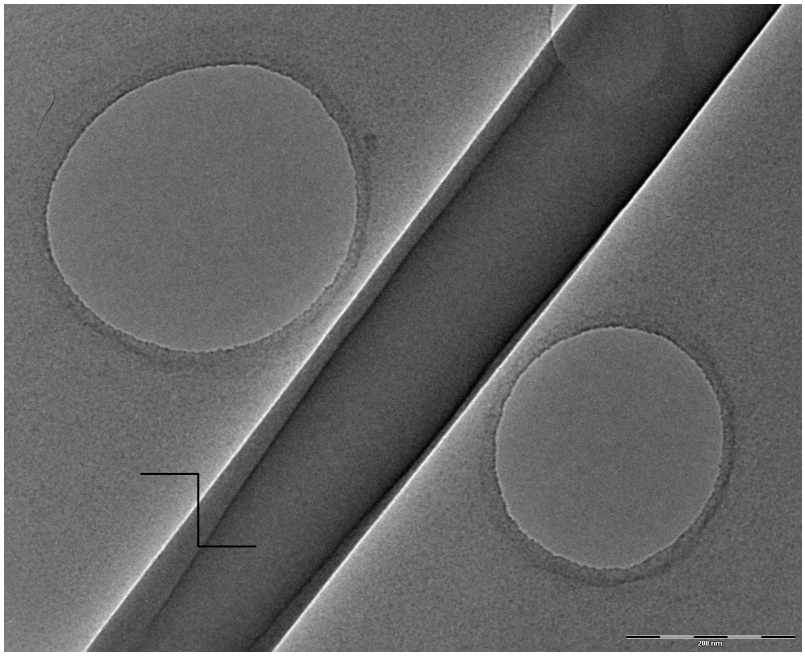

Figure 3.17: MET of co-axial PCL/gelatin nanofibers in acetic acid/formic acid (1:1 v/v): The arrow highlights the PCL core of co-axial fiber. Sample used PCL/G-134.

As can be seen from Figures 3.16 and 3.17, the co-axial morphology is well characterized.

3.4 Conclusions

It was shown through the electrospinning of PCL solution that such a process is governed by various parameters. Replacement of the solvent 2, 2, 2-trifluoroethanol (TFE) with a mixture 1:1 (v/v) of acetic acid and formic acid led to fibers with reduced diameter. PCL and gelatin solutions with a mixture 1:1 (v/v) of acetic acid and formic acid as solvent were also co-electrospun. In the case of core-shell electrospinning, the ratio η_{core}/η_{shell} is of critical importance in enabling stable core-shell electrospinning. PCL and gelatin in acid solution are to achieve a required threshold time for electrospinning before degradation.

References

1. Bhardwaj N, Kundu SC. Electrospinning: A fascinating fiber fabrication technique. Biotechnol. Adv 2010; 28:325-47.
2. Zhang Z, Hu J, Ma PX. Nanofiber-based delivery of bioactive agents and stem cells to bone sites. Adv. Drug Deliv. Rev 2012; 64:1129-41.
3. Rošic R, Pelipenko J, Kocbek P, Baumgartner S, Bešter-Rogač M, Kristl J. The role of rheology of polymer solutions in predicting nanofiber formation by electrospinning. Eur. Polym. J 2012; 48:1374-84.
4. Dash TK, Konkimalla VB. Poly-ϵ-caprolactone based formulations for drug delivery and tissue engineering: A review. J. Controlled Release 2012; 158:15-33.
5. Bosworth LA, Downes S. Physicochemical characterisation of degrading polycaprolactone scaffolds. Polym. Degrad. Stab 2010; 95:2269-76.
6. Jiang H, Hu Y, Li Y, Zhao P, Zhu K, Chen W. A facile technique to prepare biodegradable co-axial electrospun nanofibers for controlled release of bioactive agents. J. Controlled Release 2005; 108:237-43.
7. Ratanavaraporn J, Rangkupan R, Jeeratawatchai H, Kanokpanont S, Damrongsakkul S. Influences of physical and chemical crosslinking techniques on electrospun type A and B gelatin fiber mats. Int. J. Biol. Macromol 2010; 47:431-38.
8. Mobarakeh LG, Prabhakaran MP, Morshed M, Esfahani MHN, Ramakrishna S. Electrospun poly(ε-caprolactone)/gelatin nanofibrous scaffolds for nerve tissue engineering. Biomaterials 2008; 29:4532-39.
9. Veleirinho B, Ribeiro-do-Valle RM, Lopes-da-Silva JA. Processing conditions and characterization of novel electrospun poly (3-hydroxybutyrate-co-hydroxyvalerate)/chitosan blend fibers. Mater. Lett 2011; 65:2216-19.
10. Kong L, Ziegler GR. Quantitative relationship between electrospinning parameters and starch fiber diameter. Carbohydr. Polym 2013; 92:1416-22.
11. Theron SA, Zussman E, Yarin AL. Experimental investigation of the governing parameters in the electrospinning of polymer solutions. Polymer 2004; 45:2017-30.
12. Baji A, Mai YW, Wong SC, Abtahi M, Chen P. Electrospinning of polymer nanofibers: Effects on oriented morphology, structures and tensile properties. Compos. Sci. Technol 2010; 70:703-18.
13. Chakraborty S, Liao I-C, Adler A, Leong KW. Electrohydrodynamics: A facile technique to fabricate drug delivery systems. Adv. Drug Deliv. Rev 2009; 61:1043-54.
14. Doustgani A, Vasheghani-Farahani E, Soleimani M, Hashemi-Najafabadi S. Optimizing the mechanical properties of electrospun polycaprolactone and nanohydroxyapatite composite nanofibers. Composites Part B 2012; 43:1830-36.

15. Zhou F-L, Hubbard PL, Eichhorn SJ, Parker GJM. Jet deposition in near-field electrospinning of patterned polycaprolactone and sugar-polycaprolactone core-shell fibres. Polymer 2011; 52:3603-10.
16. Raghavan P, Lim D-H, Ahn J-H, Nah C, Sherrington DC, Ryu H-S, Ahn H-J. Electrospun polymer nanofibers: The booming cutting edge technology. React. Funct. Polym 2012; 72:915-30.
17. Sawada K, Sakai S, Taya M. Enhanced productivity of electrospun polyvinyl alcohol nanofibrous mats using aqueous N, N-dimethylformamide solution and their application to lipase-immobilizing membrane-shaped catalysts. J. Biosci. Bioeng 2012; 114:204-8.
18. Lee KH, Kim HY, Khil MS, Ra YM, Lee DR. Characterization of nano-structured poly(1-caprolactone) nonwoven mats via electrospinning. Polymer 2003; 44:1287-94.
19. Meng ZX, Zheng W, Li L, Zheng YF. Fabrication and characterization of three-dimensional nanofiber membrance of PCL–MWCNTs by electrospinning. Mater. Sci. Eng., C 2010; 30:1014-21.
20. Luong-Van E, Grøndahl L, Chua KN, Leong KW, Nurcombe V, Cool SM. Controlled release of heparin from poly(ε-caprolactone) electrospun fibers. Biomaterials 2006; 27:2042-50.
21. Moghe AK, Hufenus R, Hudson R, Gupta BS. Effect of the addition of a fugitive salt on electrospinnability of poly(ε-caprolactone). Polymer 2009; 50:3311-18.
22. der Schueren LV, Schoenmaker B, Kalaoglu OI, De Clerck K. An alternative solvent system for the steady state electrospinning of polycaprolactone. Eur. Polym. J 2011; 47:1256-63.
23. Huyskens P, Felix N, Janssens A, Van den Breck F, Kapubu F. Influence of the dielectric constant on the viscosity and on the formation of conducting ions in binary carboxylic acids-triethylamine mixtures. J. Phys. Chem 1980; 84:1387-93.
24. Drexler JW, Powell HM. Regulation of electrospun scaffold stiffness via co-axial core diameter. Acta Biomaterialia 2011; 7:1133-39.
25. Chong EJ, Phan TT, Lim IJ, Zhang YZ, Bay BH, Ramakrishna S, Lim CT. Evaluation of electrospun PCL/gelatin nanofibrous scaffold for wound healing and layered dermal reconstitution. Acta Biomaterialia 2007; 3:321-30.
26. Marcotte M, Hoshahili ART, Ramaswamy HS. Rheological properties of selected hydrocolloids as a function of concentration and temperature. Food Res. Int 2001; 34:695-703.
27. Tiwari SK, Venkatraman SS. Importance of viscosity parameters in electrospinning: Of monolithic and core-shell fibers. Mater. Sci. Eng., C 2012; 32:1037-42.
28. Nguyen TTT, Ghosh C; Hwang S-G, Chanunpanich N, Park JS. Porous core/sheath composite nanofibers fabricated by co-axial electrospinning as a potential mat for drug release system. Int. J. Pharm 2012; 439:296-306.

4 Elaboration and characterization of co-axial electrospun Poly(ε-Caprolactone)/Gelatin nanofibers for biomedical applications

Abstract. *Mats based on PCL/gelatin nanofibers are promising biomaterials for tissue engineering scaffolds because they exhibit morphological characteristics similar to the extracellular matrix for bone regeneration. For this purpose, novative coaxial poly(ε-caprolactone) (PCL)/gelatin nanofibers were successfully fabricated by electrospinning, using 2,2,2-trifluoroethanol (TFE) as a solvent. In such a multiphase system, the mechanical properties of the fibers are brought by the PCL core, a biocompatible polyester, and the bioactivity is linked to the gelatin skin. The morphology of the PCL/gelatin coaxial fibers was evaluated using attenuated total reflectance Fourier transform infrared spectroscopy (ATR-FTIR), scanning electron microscopy (SEM), transmission electron microscopy (TEM) and differential scanning calorimetry (DSC) experiments. The influences of PCL concentration, applied voltage and feed rate on the characteristics of the PCL core were analyzed in correlation with the fibers structure. The relation between the thickness of the gelatin shell and the diameter of the coaxial fibers was studied to demonstrate that this relationship is defined by the ratio between the gelatin and PCL feed rates.*

Keywords: *Co-axial nanofibers; Electrospinning; PCL; Gelatin.*

4.1 Introduction

Nonwoven fibrous mats obtained by electrospinning polymer solutions are characterized by an interconnected structure with small distance between the fibers and a large surface area per unit volume. These mats therefore resemble the natural extracellular matrix. These characteristics have made electrospun mats attractive mainly for biomedical applications [1].

Nanofibers can be generated from an electrostatically driven jet of polymer solution [2]. An electric field in the kilovolt range is usually generated by a high voltage power source between a capillary tip and a collector. As the electrostatic forces overcome the surface tension of the liquid, a Taylor cone is formed and a thin jet of the liquid is rapidly accelerated to a grounded or an oppositely charged collecting target. Solid nanofibers are formed due to solvent evaporation (Figure 4.1).

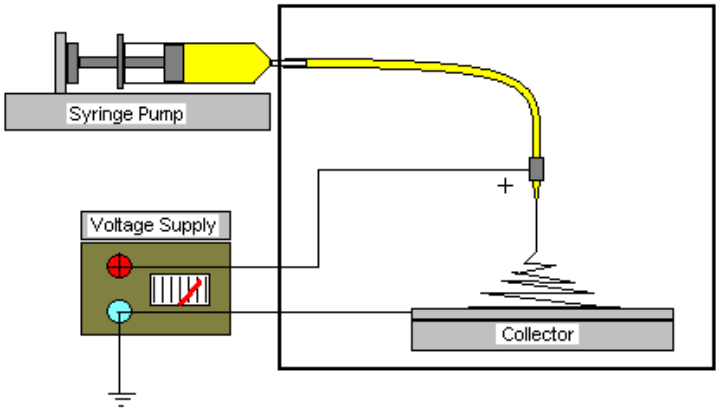

Figure 4.1: Scheme of the electrospinning setup.

Many electrospun polymers are biopolymers, such as zein [3], chitosan [4], collagen [5] and fibrinogen [6], because these polymers normally exhibit higher biocompatibility and lower toxicity than conventional polymers.

The present work includes a study on the electrospinning conditions of pure gelatin. Parameters, such as the voltage, polymer solution concentration and capillary-to-

collector distance, were varied to control the nanofiber size and morphology. Gelatin is a biopolymer that is derived from the controlled hydrolysis of native collagens and was selected due to its well-known suitability for promoting cell adhesion and proliferation [7]. Moreover, due to the large number of functional side groups in gelatin, it readily undergoes chemical cross-linking, which is very important for its use as a biomaterial. The ability of gelatin to be electrospun was also determined [8].

For many applications, such as tissue engineering, the nanofibers need to have sufficient strength and stiffness to withstand stresses in the host tissue environment [7]. This requirement cannot be met using pure gelatin.

Polycaprolactone (PCL) is one of the most commonly used synthetic polymer in the medical field because of good biocompatibility and slow biodegradability [9]. Some authors have combined the advantages of polycaprolactone (PCL) and gelatin (i.e., the mechanical strength of PCL and the bioactivity of the gelatin) using a coaxial electrospinning system [10-12].

Via coaxial electrospinning, two different polymer solutions can be simultaneously electrospun by using inner and outer coaxial capillaries and by applying the same voltage to both capillaries. As a result, fibers with cores of one polymer and with shells of the other are formed.

In this paper, obtained gelatin (shell)/PCL (core) coaxial nanofibers were extensively characterized. The relation between the feed rates of the polymer solutions and the morphology of the fibers was investigated. These findings will be useful for designing other complex multicomponent materials using electrospinning.

4.2 Materials and Methods

4.2.1 Materials

The chemicals and polymers used for nanofiber elaboration were as follows: Poly(ε-caprolactone) (PCL) (Sigma-Aldrich, St. Louis, MO, USA, Mn = 80,000 g/mol), gelatin powder (type A from porcine skin, gel strength of approximately 300 g Bloom) (Sigma-Aldrich, St. Louis, MO, USA), 2,2,2-trifluoroethanol (TFE) (99%, Sigma-Aldrich, St. Louis, MO, USA) and Glutaraldehyde (GTA) (50% solution, Merck Schuchardt OHG-Hoenbrunn, Germany). All of the chemicals were used as received without any further treatment.

4.2.2 *Electrospinning Setup*

The experimental setup used for the electrospinning process consisted of a syringe (2 mL and 7 mm in diameter) connected to a stainless steel needle (2 mm in diameter), with a polarity reversible high voltage power supply (Gamma High Voltage Research, USA) with one electrode directly clamped onto the metal needle and the other electrode clamped onto a static collector that was wrapped in aluminum foil. During the electrospinning process, the solution was ejected from the tip of the positively charged needle to form fibrous mats on the collector, which was connected to ground with a zero or negative polarity. The distance between the needle tip and the aluminum foil was 10, 12 or 15 cm. A syringe pump was connected to the syringe via a Teflon® tube and was used to push the syringe to deliver a constant and stabilized mass flow of the polymer solution. All of the experiments were conducted at 25°C and at less than 40% relative humidity.

4.2.3 Electrospinning of neat gelatin nanofibers

Preliminary tests have shown that to prepare spinnable solutions, the gelatin powder should be dissolved in TFE under stirring for 24 h at 40 °C. Different gelatin concentrations of 9%, 7%, 5% and 4% w/w were prepared to investigate the effect of the spinnability parameters on the nanofiber and mat morphology. A steel needle, 2 mm in diameter, is used. The electric potential was controlled between 15 and 40 kV. The

infusion rate was in the range of 0.2-0.5 mL/hr. Gelatin fiber mats that did not undergo crosslinking treatment were maintained in a sealed desiccator for further investigations.

4.2.4 Coaxial e*lectrospinning of PCL/gelatin nanofibers*

The two polymer solutions were independently fed through concentrically configured needles. The outer and inner diameters of the needles were 2 and 1.5 mm, respectively. The solution concentration of PCL in TFE was either 12% or 7% w/w. The concentration of gelatin in TFE was maintained at 5% w/w. Both PCL and the gelatin solutions were delivered using a programmable syringe pump. A collecting plate was placed on the grounded static collector that was wrapped in aluminum foil. The feed rates of both polymer solutions were varied by combining the feed rates over the range of 0.13-0.8 mL/hr. The needle was positively charged at 25 or 30 kV. The collector was connected to ground with zero polarity. Coaxial PCL/gelatin fiber mats that did no undergo crosslinking treatment were maintained in a sealed desiccator for further investigations.

4.2.5 Crosslinking of gelatin and coaxial PCL/gelatin fiber mats

The crosslinking process was conducted by placing the nanofibrous mats into a sealed desiccator containing a glutaraldehyde solution (50% w/v) in a Petri dish. The nanofibrous membranes were placed onto a holed ceramic plate in the desiccator and were crosslinked with glutaraldehyde vapor at room temperature for 1 h.

4.2.6 Washing procedure

A washing procedure was performed on the coaxial nanofibers. The samples crosslinked with glutaraldehyde and the uncrosslinked samples were washed with deionized water for 1 hour at room temperature to remove the gelatin shell.

4.2.7 Extraction of PCL

The extraction of the PCL cores in the crosslinked coaxial fibers was performed using dichloromethane by immersing the mats into this medium for 2 min.

4.2.8 Characterization of electrospun mats

The morphology of the gelatin and coaxial nanofibers were analyzed by scanning electron microscopy (SEM) (JEOL JSM 5600, Japan) at an accelerating voltage of 15 kV. The SEM samples were mounted onto metal stubs and coated with gold using a sputter coater (JEOL JFC-1200 fine coater, Japan). To determine the nanofiber average diameter and the corresponding standard deviation, the nonwoven mats were analyzed using 50 individual measurements, which were measured from the SEM micrographs by image analysis software (Image J, National Institutes of Health, USA). This analysis was repeated for a single electrospun fiber mat that was fabricated under a single set of constant conditions.

The nanofiber mats were also characterized using attenuated total reflectance Fourier transform infrared spectroscopy (ATR-FTIR) with a Golden Gate single reflection ATR accessory (containing a diamond crystal) in a Bruker IFS-spectrometer with a resolution of 4 cm^{-1} and with 256 co-added scans. The spectra were collected between 400 and 4,500 cm^{-1}.

A TA Instruments DSCQ200 (USA) was used for differential scanning calorimetry (DSC). For the tests with the uncrosslinked gelatin fibers, the sample was first heated from room temperature to 120°C at a rate of 10°C/min in a nitrogen atmosphere (50 mL/min) and held at this temperature for 2 min. Then, the sample was cooled to -80 °C at a rate of 10 °C/min in air (50 mL/min) and held at this temperature for 2 min. Finally, the sample was heated to 120°C at a rate of 10°C/min in air (50 mL/min) (second scan). The procedure for the crosslinked gelatin fibers, uncrosslinked coaxial fibers and crosslinked coaxial fibers was the same as described except the upper temperature was 200°C instead of 120 °C.

Transmission electron microscopy (TEM) (TOPCON 002B - Japan) performed at 200 kV was used to observe the core-shell structure of the fibers. The TEM samples were prepared by directly depositing the as-spun fibers onto copper grids. The samples were then dried in a vacuum oven for 48 h at room temperature prior to TEM imaging.

4.3 Results and Discussion

4.3.1 Neat gelatin nanofibers

The electrospinning process is controlled by many parameters, including the solution parameters, the processing parameters and the ambient parameters [13]. In this study, the effect of different processing parameters, such as the voltage applied, the tip-to-collector distance and the solution concentration, on the final fiber diameter were investigated. Three different voltages were applied with a fixed tip-to-collector distance of 15 cm for the 5 and 4% (w/w) solutions. Three tip-to-collector distances were examined with a fixed voltage for the 5% (w/w) solution: 10, 12 and 15 cm, respectively. The details of the parameters used to produce the gelatin nanofiber samples in this study are given in Table 4.1.

Table 4.1: Electrospinning parameters for different gelatin nanofiber samples

Sample	C(%w/w)	U (kV)	d (cm)	D (nm)	SD (nm)
GEL-41	9	30/0	15	-	-
GEL-48	7	30/0	15	-	-
GEL-43	5	30/0	12	192	52
GEL-62	5	15/-15	15	190	63
GEL-64	5	15/-20	15	180	74
GEL-65	5	20/-20	15	150	51
GEL-50	5	20/-10	15	160	34
GEL-51	5	20/-10	12	160	49
GEL-52	5	20/-10	10	160	54
GEL-44	5	30/0	10	195	57
GEL-67	4	30/0	15	110	29
GEL-58	4	20/-15	15	100	29
GEL-61	4	20/-20	15	100	37

C (%w/w): concentration of the gelatin solution

d (cm): distance between the needle tip and the collector

D (nm): average fiber diameter
SD (nm): standard deviation
Flow rate of the gelatin solution: 0,2 mL/h
Average humidity (%): 40
Average temperature (°C): 20ºC

To evaluate the effect of solution concentration on the morphology of the gelatin fibers, various concentrations in the range of 4 to 9% (w/w) gelatin solution were electrospun.

The solution viscosity is strongly related to the solution concentration. According to Bhardwaj *et al.* [13], there should be an optimum solution concentration for the electrospinning process because beads are formed at low concentrations instead of fibers. Continuous fibers cannot be formed at high concentrations due to the inability of the solution to keep flowing at the tip of the needle, resulting in the formation of larger fibers. Huang *et al*. [14] have shown that the electrospinning of gelatin was achieved by using gelatin solutions in the range of 5–12.5% (w/w) with 2,2,2-trifluoroethanol. These authors reported that lower or higher concentrations were difficult to process.

Gelatin solutions at 4-9% (w/w) were successfully electrospun into nanofibers. Figure 4.2 shows SEM micrographs of the electrospun gelatin fibers.

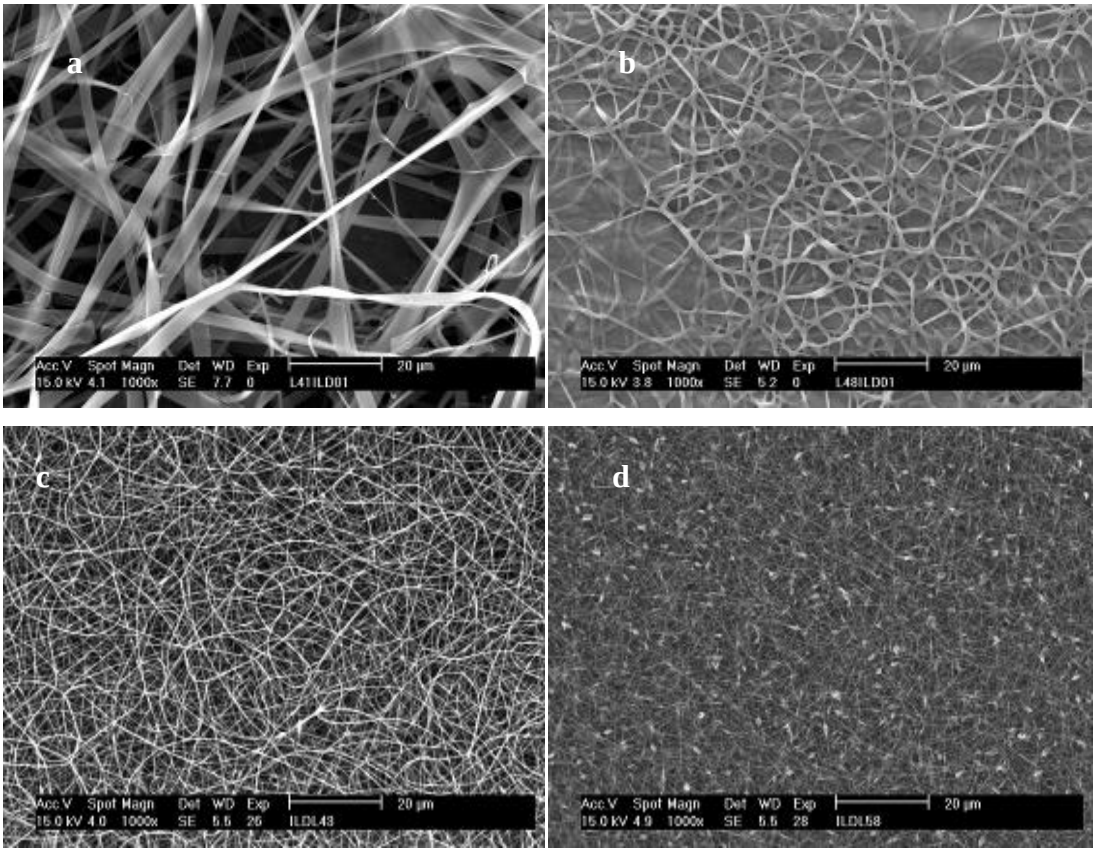

Figure 4.2: Scanning electron microscope photographs of electrospun gelatin nanofibers for various concentrations (magnification of 10^3): (a) 9%, (b) 7%, (c) 5% and (d) 4%. The applied solution voltage and the tip-to-collector distance were 30 kV and 10 cm, respectively. Samples used: GEL-41, GEL-48, GEL-43 and GEL-58.

As shown in Figure 4.2, at a low concentration (4% (w/w)), many beads were formed (Figure 4.2 d). Ki *et al*. [15] found a similar result for the 7% (w/w) concentration. They electrospun gelatin nanofibers in formic acid solutions at 7-12% (w/w). According to these authors, the formation of beads at low concentrations is due to the low viscosity of the solution and to a relatively high surface tension. Therefore, the solution jet, which should form a nanofiber, could not maintain its shape at the end of tip and then formed small drops. Conversely, the fibers obtained from 9 to 7% (w/w) solutions (Figure 4.2 a and b) exhibit specific fibers morphology as flat belts. Flattened fibers are obtained because a fraction of the solvent was trapped inside the fiber, after electrospinning step. When the solvent evaporated, the fiber collapsed, resulting in flat fiber belts [16].

Among the conditions that were evaluated in Figure 4.2, 5% (w/w) was shown to be the optimum solution concentration for the electrospinning process of gelatin nanofibers.

According to the review of Bhardwaj *et al.* [13], some researchers suggested that there is more polymer ejected when higher voltages are applied, which would facilitate the formation of a larger diameter fiber. Other authors have reported that an increase in the applied voltage (i.e., an increase in the electric field strength) increases the electrostatic repulsive force on the fluid jet, which favors the narrowing of the fiber diameter. In Figure 4.3, the average diameters of gelatin fibers obtained using the 4 and 5% (w/w) solutions were plotted as a function of the applied voltage.

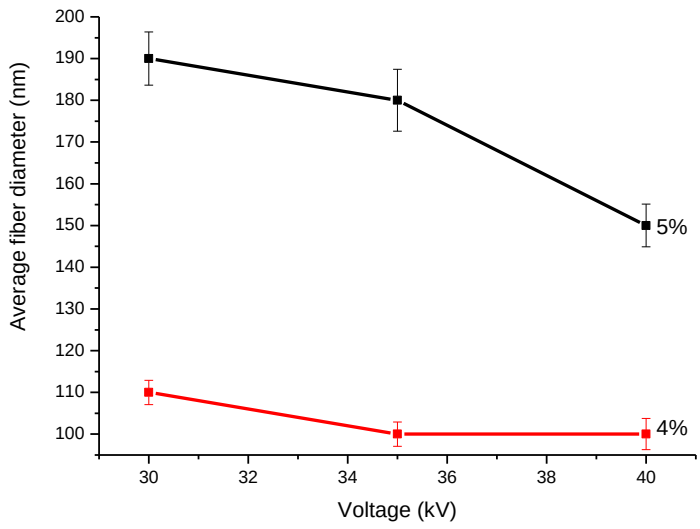

Figure 4.3: Fiber diameter vs. applied voltage for the 4 and 5% solutions of gelatin in TFE. Samples used: GEL-58, GEL-61, GEL-62, GEL-64, GEL-65 and GEL-67.

According to Figure 4.3, under the conditions used in this study, the average fiber diameter decreases with increasing voltage, and smaller diameters are achieved with more dilute solutions. This result does not agree with the one obtained by Ki *et al.* [15]; they found that the electric field did not significantly affect the size of the nanofiber. Moreover, the authors achieved gelatin nanofibers with mean diameters of approximately 80 nm using an 8% (w/w) concentration with an electric field of 1.0 kV and a spinning distance of 10 cm, which corresponds to smaller fibers than the ones

produced in the present work. The values of the diameters determined in this work are closer to those found by Ratanavaraporn *et al*. [17], who reported that the electrospinning of a type A gelatin solution in formic acid at various concentrations (2.5–60% w/v) produced fibers with diameters that ranged from 190–300 nm. However, the results of these authors is partially in good agreement with the previous ones of Ki *et al*. [15] since they observed that gelatin fibers prepared at 25% w/v with a 10 to 25 kV, resulted in smooth fibers without any beads.

The distance between the tip and the collector has been also analyzed for controlling the fiber diameters and morphology, as reported by Bhardwaj *et al.* [13]. According to these authors, a minimum distance is required to give the fibers sufficient time to dry before reaching the collector.

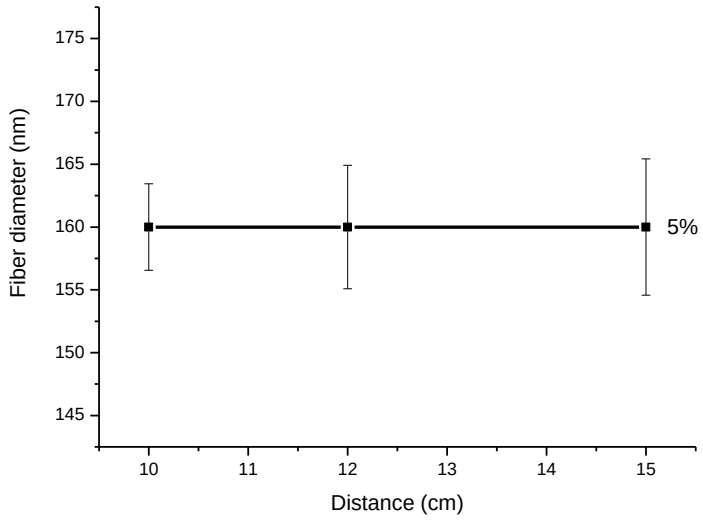

Figure 4.4: Fiber diameter vs. needle-to-collector distance at a fixed voltage for the 5% solution of gelatin in TFE. Samples used: GEL-50, GEL-51 and GEL-52. The error bars are the ± standard deviations of the sample population.

As shown in Figure 4.4, for our process conditions the effect of the tip-to-collector distance on the fiber morphology was not as significant as the other studied parameters. Other parameters, such as the type of solvent and the solution feed rate, affect significantly the fiber morphology. It is worth noting that Ki *et al.* [15] worked with

formic acid to obtain thin fibers, as did Ratanavaraporn *et al*. [17], who used higher solution concentrations. As stated by Wang *et al*. [18], a gelatin solution with formic acid has a large conductivity due to the high dielectric constant of formic acid, which favors the formation of thinner fibers.

An example of the influence of the solution feed rate on the fiber morphology was given by Montero *et al*. [19]. They reported nanofibers from gelatin in 1,1,1,3,3,3 hexafluoro-2-propanol. These authors obtained electrospun nanofibers using an applied voltage and a tip-to-collector distance of 20 kV and 15 cm, respectively. Under these conditions, for a 5% (w/w) precursor solution and a feed rate of 1 mL/hr, they found an average diameter of 240 ± 60 nm. When the authors increased the feed rate to 8 mL/hr, they found an average diameter of 390 ± 26 nm.

With close conditions, using gelatin in 2,2,2-trifluoroethanol and a feed rate of 0.2 mL/h, we found an average diameter of 160 ± 34 nm. From this observation, we can infer that the fiber diameter tends to increase with increasing feed rate. The same observation was reported by Bhardwaj *et al.* [13] in the case of polystyrene fibers. According to the authors, the fiber diameter and the pore diameter increase with an increase in the polymer flow rate. Additionally, a lower feed rate is more desirable because the solvent will have enough time to evaporate.

In summary, approaches in this work, such as decreasing the polymer concentration and increasing the net charge density of the solution, were utilized to reduce the diameter of the electrospun gelatin nanofibers. Although the objective of reducing the fiber diameter down to less than 100 nm was not achieved, nanoscale gelatin fibers were conveniently obtained.

Figure 4.5 shows the wide scan FTIR spectra for the electrospun gelatin nanofibers (sample GEL-44). In Figure 4.5, the characteristic absorption bands of gelatin can be observed i.e., the amide I band (antisymmetric stretching vibration of the carboxyl group or C=O vibration) at 1642 cm^{-1} [20] and the amide II band (N-H bending vibration) at 1530 cm^{-1} [20]. The spectrum also exhibited the characteristic absorption

band at 3290 cm^{-1} that is associated with the N–H stretching vibration in gelatin [8]. According to Choi *et al*. [8], a free N–H stretching vibration occurs in the range 3400-3440 cm^{-1}, and, when the N–H group of the peptides is involved in hydrogen bonding, the position of this band is shifted to lower frequencies, usually to approximately 3300 cm^{-1}.

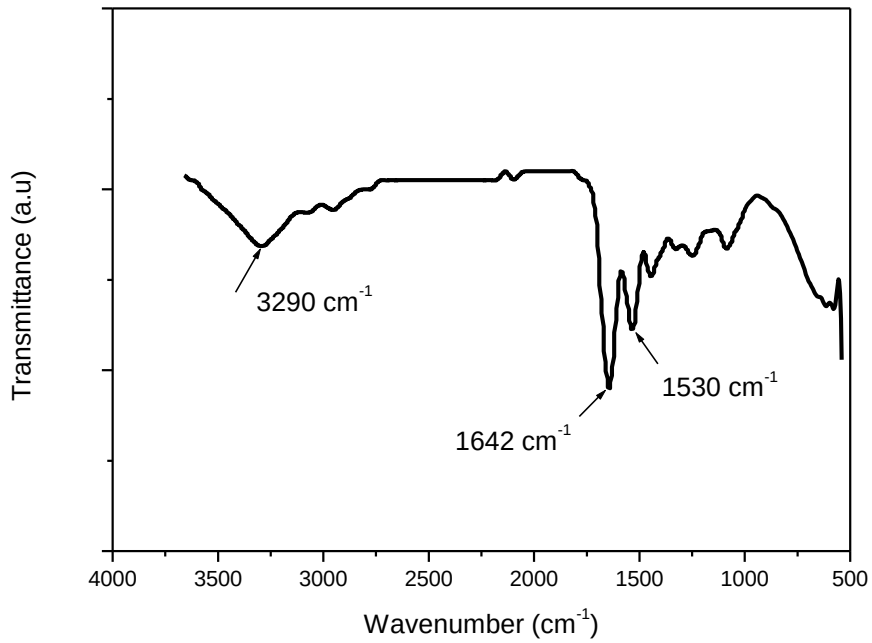

Figure 4.5: FTIR spectrum of gelatin nanofibers. Sample used: GEL-44.

It is well known that gelatin is water soluble and mechanically weak [21]. For scaffold applications, electrospun gelatin nanofibers must be crosslinked to stabilize the nanofibers structure, to maintain their morphology even after exposure to an aqueous solution. Otherwise, it is impossible to culture cells in an aqueous environment.

Glutaraldehyde (GTA) is by far the chemical most widely used as a crosslinking agent due to its high efficiency in stabilizing collagenous materials. The GTA-based crosslinking of collagenous materials significantly reduces their biodegradation rates, making the materials biocompatible and nonthrombogenic while preserving their biological integrity, strength and flexibility [21]. Although other crosslinking agents have been reported to reduce cytotoxicity [22], they usually cannot match GTA in collagen stabilization [21].

4.3.2. PCL/Gelatin coaxial nanofibers

Although gelatin has been successfully electrospun into nanofibers, pure gelatin mats did not produce completely satisfactory results for use in tissue engineering. According to Almeida *et al*. [8], amongst the other requirements, an ideal scaffold must have sufficient strength and stiffness to withstand the stresses in the host tissue environment. Based on these requirements, gelatin and PCL were co-electrospun to produce PCL/gelatin core-shell nanofibers. PCL was used to form the core structure of the fibers while gelatin was used as the shell, thus forming PCL fibers coated with gelatin, which are able to meet the requirements for use in tissue engineering.

The electrospinning conditions, such as the different concentrations of the core and shell solutions, the voltage and the feed rates of both polymer solutions, are listed in Table 4.2.

Table 4.2: Electrospinning parameters for coaxial PCL/gelatin nanofibers

Sample	C1	C2	FR1	FR2	U (kV)
PCL/G-85	12	5	0.2	0.3	25/0
PCL/G-86	12	5	0.2	0.2	25/0
PCL/G-87	12	5	0.3	0.13	25/0
PCL/G-88	12	5	0.2	0.3	30/0
PCL/G-89	12	5	0.2	0.2	30/0
PCL/G-90	12	5	0.13	0.3	30/0
PCL/G-91	12	5	0.3	0.13	30/0
PCL/G-92	7	5	0.2	0.3	30/0
PCL/G-93	7	5	0.2	0.2	30/0
PCL/G-94	7	5	0.13	0.3	30/0
PCL/G-95	7	5	0.3	0.13	30/0
PCL/G-122	7	5	0.5	0.5	30/0
PCL/G-123	7	5	0.4	0.4	30/0
PCL/G-124	7	5	0.8	0.8	30/0
PCL/G-125	7	5	0.5	0.8	30/0

PCL/G-126	7	5	0.4	0.7	30/0
PCL/G-127	7	5	0.4	0.6	30/0
PCL/G-128	7	5	0.4	0.5	30/0
PCL/G-129	7	5	0.3	0.6	30/0
PCL/G-130	7	5	0.2	0.5	30/0

C1 (%w/w): concentration of the core solution (PCL)
C2 (%w/w): concentration of the shell solution (Gelatin)
FR1: flow rate (mL/hr) of the core solution (PCL)
FR2: flow rate (mL/hr) of the shell solution (Gelatin)
Distance between the needle tip and the collector: 15 cm
Average relative humidity: 26%
Average temperature: 19.3 °C

Based on the previously obtained electrospun gelatin fibers, a 5% w/w gelatin/TFE solution was selected and used for all of the coaxial experiments. The effect of varying the concentration of the PCL/TFE solution is illustrated in the SEM micrographs in Figure 4.6. The diameters of the coaxial fibers increase from 744 ± 237 nm (figure 4.6b) to 893 ± 286 nm (figure 4.6a) with increasing core solution concentration. Schueren *et al*. [23] reported that this behavior was due to the increase in viscosity with the increase in PCL, which they determined during their study for an alternative solvent system for use in steady-state PCL electrospinning. According to the authors, the higher amount of entanglements discourages the bending stability of the jet at long distances from the needle, thus causing thicker fibers. The same trend in coaxial PCL/gelatin fibers was previously observed by other authors [24].

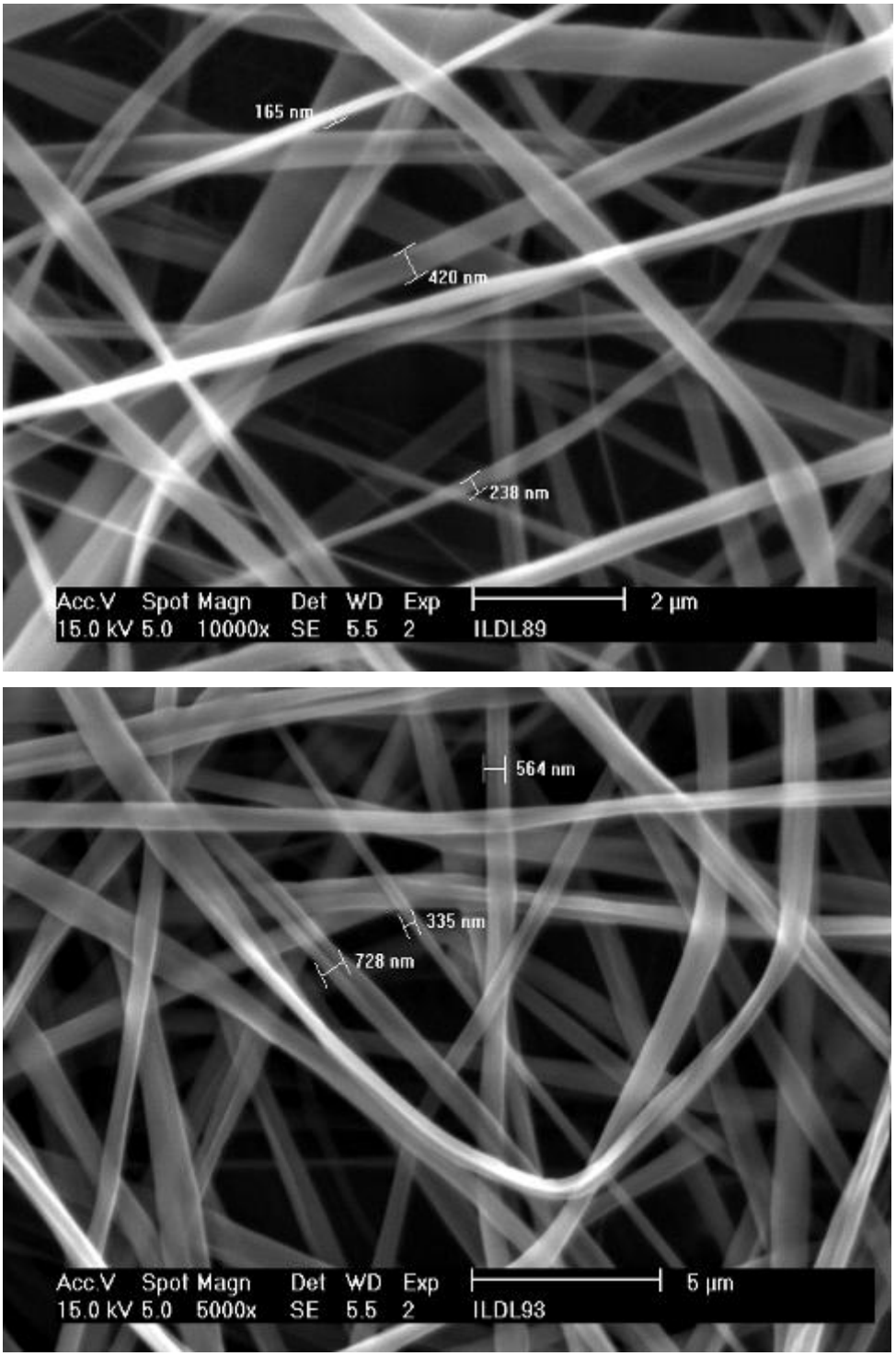

Figure 4.6: Scanning electron microscope photographs of electrospun coaxial PCL/gelatin nanofibers for PCL solution concentrations of: (a) 12% (w/w) and (b) 7% (w/w). The gelatin solution concentrations of 5% (w/w) with a feed rate of 0.2 mL/hr

for both solutions and a voltage of 30 kV were used. Samples used: (a) PCL/G-89 and (b) PCL/G-93. (Magnification of 5.10^3).

Figure 4.7 shows the transmission electron microscopy (TEM) image of the electrospun coaxial nanofiber structure for the 7% (w/w) and 5% (w/w) solution core and shell concentration, respectively. A distinct boundary between PCL and gelatin can be observed, indicating a clear core-shell structure.

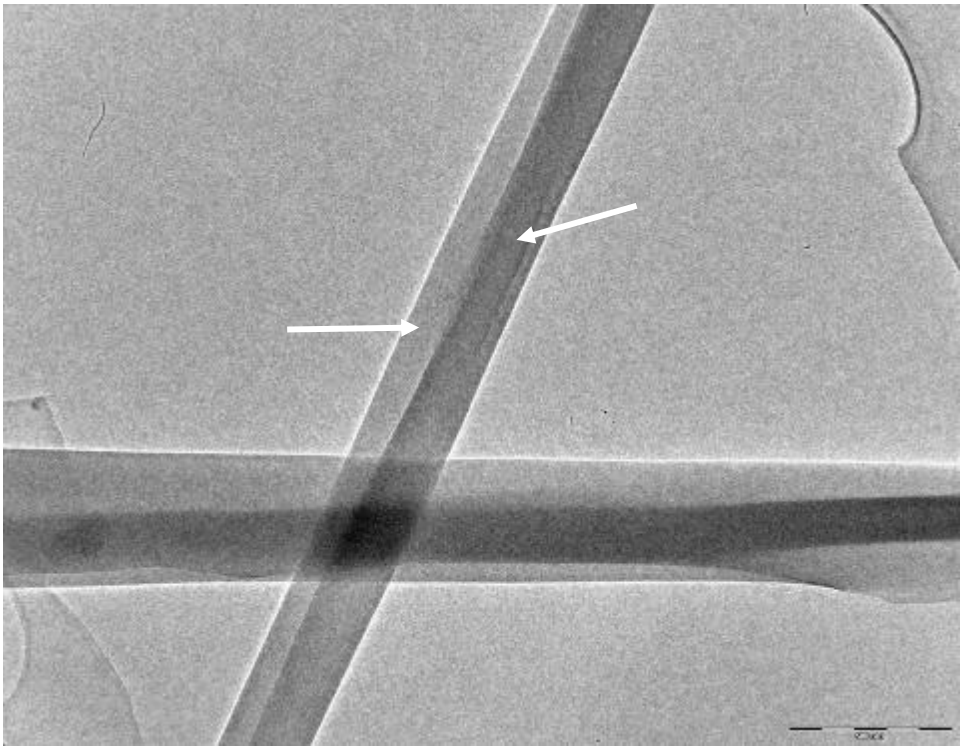

Figure 4.7: TEM of the core-shell morphology of the PCL/gelatin nanofibers obtained by electrospinning the 7% (w/w) PCL/TFE solution (core) and the 5% (w/w) gelatin/TFE solution (shell). The feed rates of the core solution and shell solution were 0.2 mL/hr and the applied voltage was 30 kV. Sample used: PCL/G-93

After washing the coaxial fibers with dionized water, we observed that the diameters of the coaxial fibers of the PCL/G-93 reduced from 744 ± 237 nm to 619 ± 182 nm, and the corresponding mat was examined using FTIR spectroscopy. The gelatin uncrosslinked nanofiber spectrum was used to control as a reference (Figure 4.8).

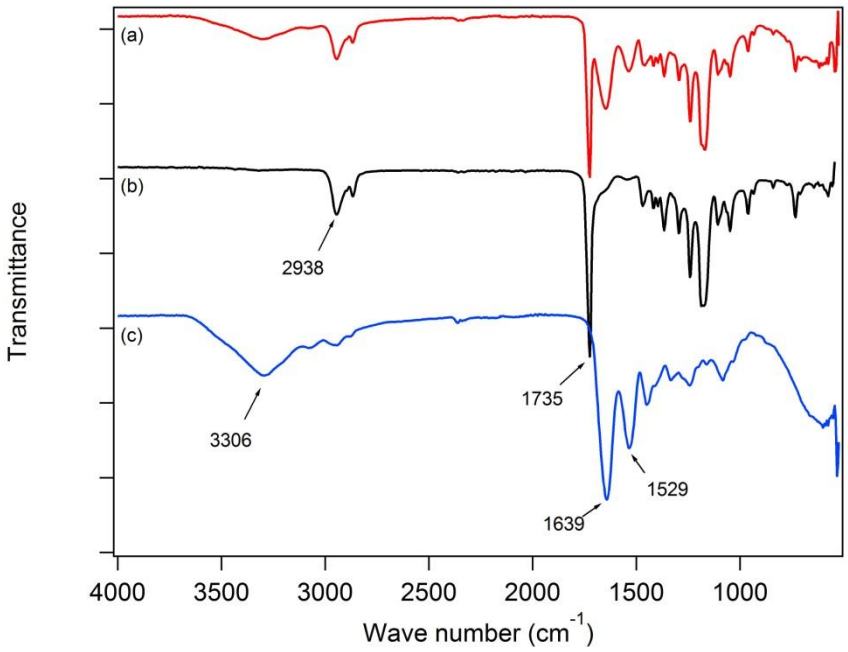

Figure 4.8: FTIR spectra of uncrosslinked coaxial PCL/gelatin nanofibers (a) before washing and (b) after washing and (c) of single gelatin nanofibers (control). Samples used: PCL/G-93 and PCL/G-44

The spectrum of the control exhibited the characteristic absorption band at 3306 cm^{-1} that is associated with the N-H stretching vibration in gelatin. According to a previous report, a free N-H stretching vibration occurs in the range from 3400-3440 cm^{-1}, and, when the N-H group of the peptides is involved in hydrogen bonding, this band is shifted to lower frequencies, approximately 3300 cm^{-1} [8]. This band is not observed in the spectra of the washed mat. Besides common protein bands appeared at approximately 1639 cm^{-1} (amide I) and 1529 cm^{-1} (amide II), corresponding to the stretching vibration of C=O bond and to coupling of the bending of N-H bond with the stretching vibration of C-N bond, respectively [8, 15]. These bands were also not observed for the washed nanofibers. Conversely, the characteristic band at 1735 cm^{-1}, which is related to the stretching vibration of the carbonyl groups associated with the ester bonds in PCL [25], was observed in the spectrum of the washed coaxial fibers, as was the band corresponding to CH_2 absorption (2938 cm^{-1}). All these data indicate the disappearance of gelatin and the appearance of PCL after mat washing step.

Because gelatin is hydrolytically unstable, for future applications of the core-shell mats as scaffolds in tissue engineering, it is essential to stabilize the gelatin shell by crosslinking. We used glutaraldehyde for this purpose. The crosslinking process was studied using FTIR. Figure 4.9 shows the FTIR spectra of the crosslinked coaxial fibers before and after water washing and the Figure 4.10 show the SEM micrographs of the crosslinked coaxial fibers.

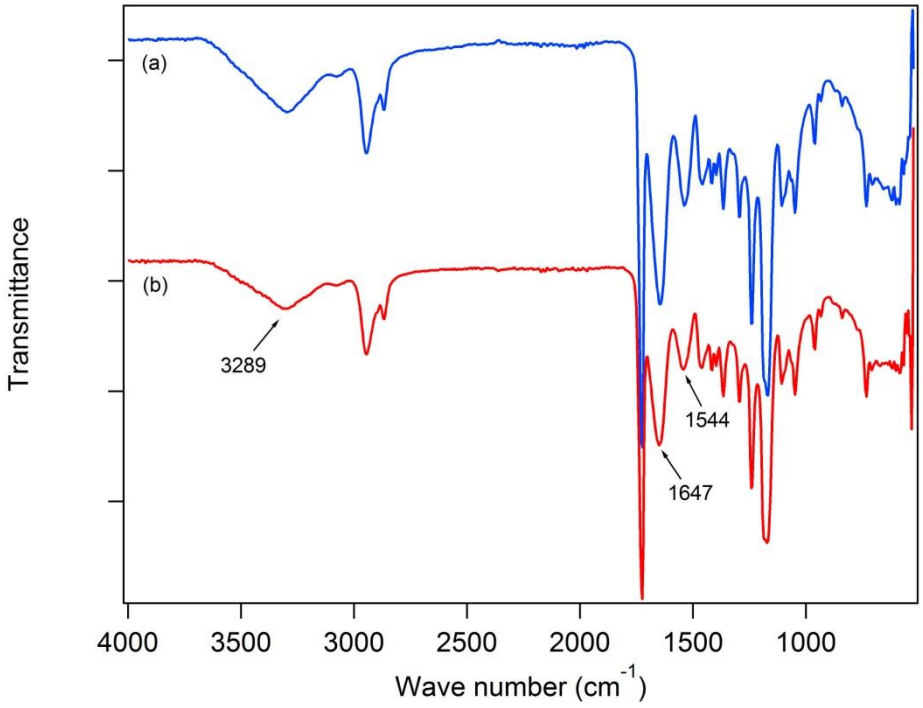

Figure 4.9: FTIR spectra of coaxial PCL/gelatin nanofibers crosslinked with GTA: (a) before washing and (b) after washing. Sample used: PCL/G-93

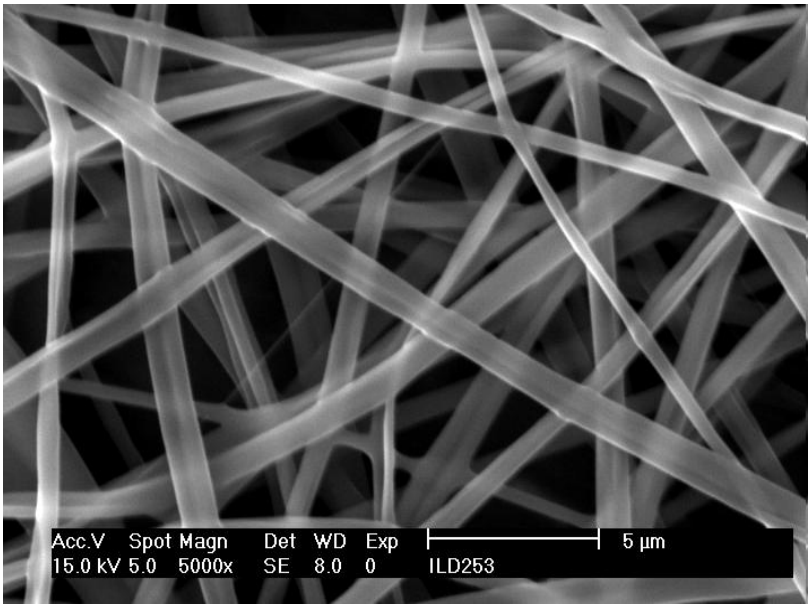

Figure 4.10: Scanning electron microscope photographs of coaxial PCL/gelatin nanofibers crosslinked with GTA. Sample used: PCL/G-93 (Magnification of 5.10^3).

After treatment with GTA vapor for one hour, the gelatin main bands were maintained in the spectrum after washing the coaxial fibers, in contrast to what was observed in the figure 4.8. This result proves that one hour was enough time to crosslink the gelatin shell and does not agree with the results of *Lu et al*. [26]. The authors found that coaxial PCL/gelatin membranes were crosslinked after being exposed to GTA vapor for 2 h and that serious fiber damage occurred when the exposure time was 8 h.

Figure 4.11 shows the DSC of the crosslinked coaxial fibers. The melting and crystallization peaks of PCL in the core/shell nanofibers are not shifted compared to those of pure PCL nanofibers [27]. This result indicates weak interactions between the shell and the core in the coaxial nanofibers.

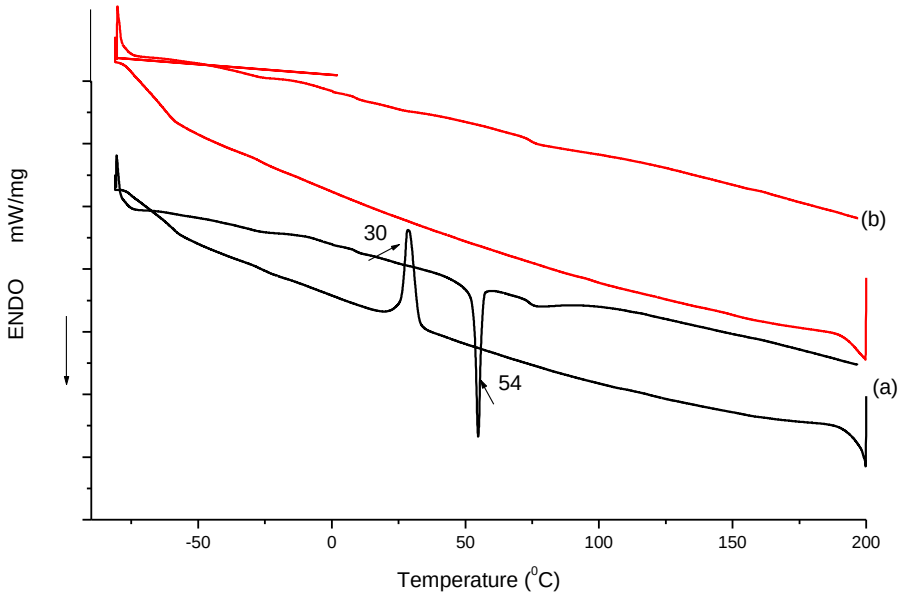

Figure 4.11: DSC curves (cooling and 2nd scan heating) of: (a) GTA crosslinked PCL/gelatin coaxial nanofibers and (b) GTA crosslinked gelatin nanofibers (control). Samples used: PCL/G-129 and PCL/G-44

The selective extraction of the PCL core using dichloromethane was performed for the crosslinked coaxial fibers, producing the hollow structure shown in Figure 4.12. This test verified again the core-shell morphology of the fibers obtained by coaxial electrospinning.

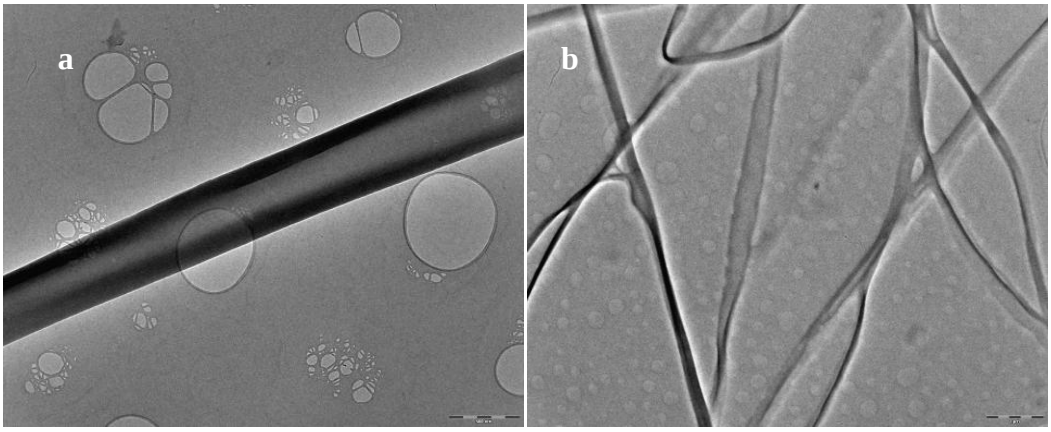

Figure 4.12: TEM of coaxial nanofibers: (a) before extraction (control) and (b) after extraction of the PCL core using dichloromethane. Sample used: PCL/G-129

Figure 4.13 shows the SEM micrographs of the coaxial nanofibers for different applied voltages.

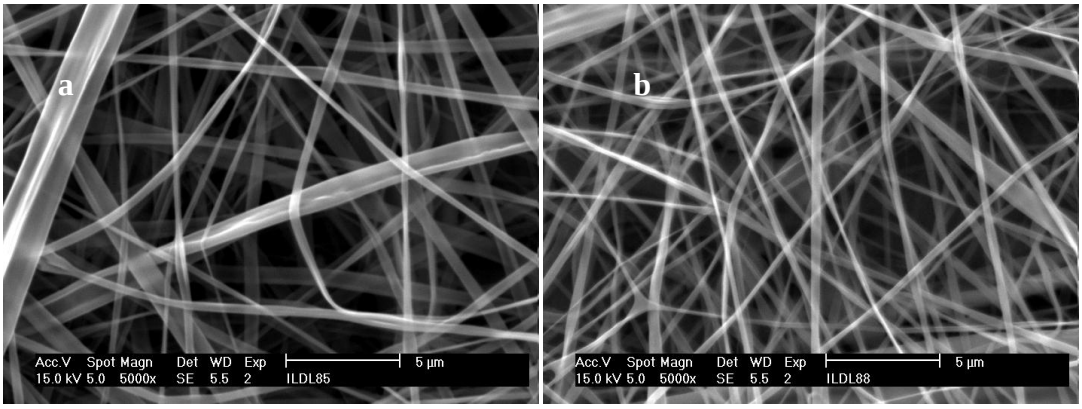

Figure 4.13: Scanning electron microscope photographs of electrospun coaxial PCL/gelatin nanofibers at voltages of: (a) 25/0 and (b) 30/0. The PCL solution concentration of 12% (w/w) and a feed rate of 0.2 mL/hr were used for the PCL solution and 0.3 mL/hr for the Gelatin solution. Samples used: (a) PCL/G-85 and (b) PCL/G-88 (Magnification of 5.10^3).

According to the micrographs shown in Figure 4.13, the effect of varying the voltage on the coaxial fiber morphology and on the average diameters is not as noticeable as in the case of the pure gelatin fibers. Nevertheless, we can observe a trend toward more

uniform fibers with higher applied voltages. Zhang *et al*. [11] reported that increasing the feed rate of the PCL core solution required a corresponding increase in the applied voltage to achieve stable jets. Drexler *et al*. [24] found that the coaxial electrospinning parameters significantly affected the core diameter of the PCL/gelatin fibers but had little effect on the as-spun total fiber diameter.

Possible changes in the morphology of the coaxial fibers were also investigated by varying the feed rate of the PCL core solution. According to the micrographs shown in Figure 4.14, no significant difference in the fiber diameters was found with the reduction in the core feed rate from 0.4 to 0.3 mL/hr, respectively. This observation is in agreement with Drexler *et al.* [24]. As reported by these authors, reducing the core feed rate from 2 to 1 mL/hr produced a 23.4% reduction in the core diameter, but the variation of the total fiber diameter didn't exhibit explicit trend.

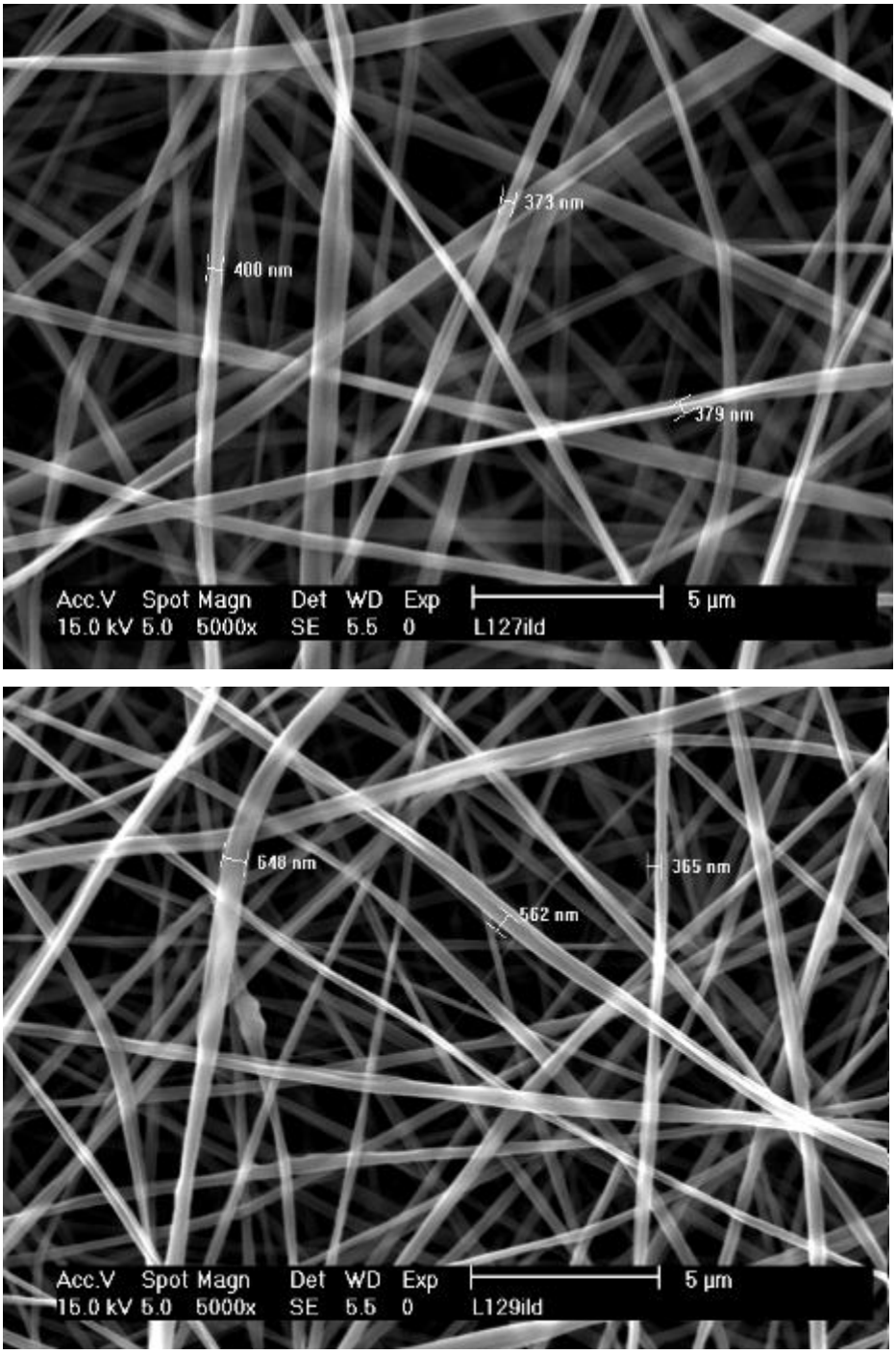

Figure 4.14: Scanning electron microscope photographs of electrospun coaxial PCL/gelatin nanofibers for different feed rates of the PCL solution: (a) 0.4 mL/hr (b) 0.3 mL/hr. The PCL solution concentration of 7% (w/w), a gelatin solution feed rate of 0.6 mL/hr and a voltage of 30 kV were used. Samples used: (a) PCL/G-127 and (b) PCL/G-129. (Magnification of 5.10^3).

4.4 Conclusions

Core/shell nanofibers, in which the core is formed by PCL and the shell is formed by glutaraldehyde-crosslinked gelatin, were successfully fabricated via coaxial electrospinning using TFE as a solvent. TEM revealed the coaxial morphology of the obtained fibers. The results from experiments, such as FTIR of washed and unwashed fibers and extraction of the PCL core using dichloromethane, confirmed the coaxial morphology. The morphology of the coaxial fibers was affected by changes in the PCL solution concentration. However, changes in the applied voltage and in the core feed rate do not appear to significantly affect the morphology of the fibers. The fabricated core/shell nanofibers are good candidates for use in biomedical fields because they combine the bioactivity of gelatin with the mechanical strength and biodegradability of PCL.

References

1. Lannuttti J, Reneker D, Ma T, Tomasko D, Farson D. Electrospinning for tissue engineering scaffolds. Mater. Sci. Eng., C 2007; 27(3):504-9.
2. Beachley V, Wen X. Polymer nanofibrous structures: Fabrication, biofunctionalization, and cell interactions. Prog.Polym.Sci 2010; 35:868-92.
3. Kayaci F, Uya T. Electrospunzein incorporating cyclodextrins. Carbohydr.Polym 2012; 90(1):558-68.
4. Elsabee MZ, Naguib HF, Mors RE. Chitosan based nanofibers review. Mater. Sci. Eng., C 2012; 32(7):1711-26.
5. TengSH, Lee EJ, Wang P, Kim HE. Collagen/hydroyapatite composite nanofibers by electrospinning.Mater.Lett 2008; 62(17-18):3055-58.
6. Baker S, Sigley J, Helms CC, Stitzel J, Berry J, Bonin K, Guthold M. The mechanical properties of dry, electrospun fibrinogen fibers. Mater. Sci. Eng., C 2012; 32(2):215-21.
7. Almeida HA, Bártolo PJS. Virtual topological optimization of scaffolds for rapid prototyping. Med. Eng.&Phys 2010; 32:775-82.
8. Choi MO, Kim YJ. Fabrication of gelatin/calcium phosphate composite nanofibrous membranes by biomimetic mineralization.Int. J. Biol. Macromol2012; 50:1188-94.
9. Woodruff MA, HutmacherDW. The return of a forgotten polymer-Polycaprolactone in the 21st century. Prog. Polym. Sci 2010; 35(10):1217-56.
10. Zhang Y, Ouyang H, Lim CT, Ramakrishna S. Electrospinning of gelatin fibers and gelatin/PCL composite fibrous scaffolds. J Biomed Mater 2005; 72:156-165.
11. Zhao P, Jiang H, Pan H, Zhu K, Chen W. Biodegradable fibrous scaffolds composed of gelatin coated poly(ε-caprolactone) prepared by coaxial electrospinning. J Biomed Mater 2007; 83:372-382.
12. Mobarakeh LG, Prabhakaran MP, Morshed M, Esfahani MHN, Ramakrishna S. Electrospun poly(ε-caprolactone)/gelatin nanofibrous scaffolds for nerve tissue engineering. Biomaterials 2008; 29:4532-39.
13. Bhardwaj N, Kundu SC. Electrospinning: A fascinating fiber fabrication technique. Biotechnol. Adv 2010; 28:325-47.
14. Huang ZM, Zhang YZ, Ramakrishna S, Lim CT. Electrospinning and mechanical characterization of gelatin nanofibers. Polymer 2004; 45:5361-68.
15. Ki CS, Baek DH, Gang KD, Lee KH, Um IC, Park YH. 2005 Characterization of gelatin nanofiber prepared from gelatin–formic acid solution. Polymer 2005; 46:5094-102.
16. Baji A, Mai YW, Wong SC, Abtahi M, Chen P. Electrospinning of polymer nanofibers: Effects on oriented morphology, structures and tensile properties. Compos. Sci. Technol 2010; 70:703-18.

17. Ratanavaraporn J, Rangkupan R, Jeeratawatchai H, Kanokpanont S, Damrongsakkul S. Influences of physical and chemical crosslinking techniques on electrospun type A and B gelatin fiber mats. Int. J. Biol. Macromol 2010; 47:431-38.
18. Wang X, Ding B, Yu J; Yang J. Large-scale fabrication of two-dimensional spider-web-like gelatin nano-nets viaelectro-netting. Colloids Surf., B 2011; 86:345-52.
19. Montero RB, Vial X, Nguyen DT, Farhand S, Reardon M, Pham SM, Tsechpenakis G, Andreopoulos FM. bFGF-containing electrospun gelatin scaffolds with controlled nano-architectural features for directed angiogenesis. Acta Biomaterialia 2012; 8:1778-91.
20. Xu J, Yan J, Gu Q, Li J, Wang H. Preparation of fluoride-containing gelatin nanofiber scaffold. Mater.Lett 2011; 65:2404-6.
21. ZhangYZ, Venugopal J, Huang ZM, Lim CT, Ramakrishna S. Crosslinking of the electrospun gelatin nanofibers. Polymer 2006; 47:2911-17.
22. PanzavoltaS, GioffrèM, Focarete ML, Gualandi C, Foroni L. Electrospun gelatin nanofibers: Optimization of genipin cross-linking to preserve fiber morphology after exposure to water. Acta Biomaterialia 2011; 7:1702-9.
23. Schueren LVD, Schoenmaker B, Kalaoglu OI, De ClerckK. An alternative solvent system for the steady state electrospinning of polycaprolactone. Eur. Polym. J 2011; 47:1256-63.
24. Drexler JW, Powell HM. Regulation of electrospun scaffold stiffness via coaxial core diameter. Acta Biomaterialia 2011; 7:1133-39.
25. Kim MS, Jun I, Shin YM, Jang W, Kim SI, Shin W. The Development of Genipin-Crosslinked Poly(caprolactone) (PCL)/Gelatin Nanofibers for Tissue Engineering Applications. Macromol. Biosci 2010; 10:91–100
26. Lu Y, Jiang H, Tu K, Wang L. Mild immobilization of diverse macromolecular bioactive agents onto multifunctional fibrous membranes preparedby coaxial electrospinning. Acta Biomaterialia 2009; 5:1562-74.
27. Zamani M, Morshed M, Varshosaz J, Jannesari M. Controlled release of metronidazole benzoate from poly e-caprolactone electrospun nanofibers for periodontal diseases. Eur. J. Pharmac. Biopharmac 2010; 75:179-85.

5 *In vitro* biocompatibility and osteogenesis of mineralized electrospun co-axial Poly(ε-caprolactone) (PCL)/Gelatin nanofibers

Abstract. *Mineralized poly(ε-caprolactone) (PCL)/gelatin core–shell nanofibers were prepared via co-axial electrospinning and subsequent incubation in biomimetic simulated body fluid containing 10 times the calcium and phosphate ion concentrations found in human blood plasma (SBF10). The deposition of calcium phosphate on the nanofiber surfaces was investigated through scanning electronic microscopy (SEM) and X-ray diffraction (XRD). Energy dispersive spectroscopy (EDS) results indicated that calcium-deficient hydroxyapatite (HA) had grown on the fibers. Fourier transform infrared spectroscopy (FTIR) analysis suggested the presence of hydroxyl-carbonate-apatite. The results of a viability assay (MTT) and alkaline phosphatase activity (ALP) analysis suggested that these mineralized matrices promote osteogenic differentiation of human adipose-derived stem cells (hASCs) when cultured in an osteogenic medium and have the potential to be used as a scaffold in bone tissue engineering. hASCs cultured in the presence of nanofibers in endothelial differentiation medium showed lower rates of proliferation than cells cultured without the nanofibers. However, endothelial cell markers were detected in cells cultured in the presence of nanofibers in endothelial differentiation medium.*

Keywords*: Coaxial nanofibers; PCL; Gelatin; Mineralization; In vitro tests*

5.1 Introduction

Bone tissue is composed of a heterogeneous mixture of cell types as osteoid and endothelial lineages, embedded within a mineralized extracellular matrix (ECM), which serves to maintain its structural integrity [1]. An important strategy in tissue engineering is the fabrication of scaffolds that can mimetize the ECM. The function of such scaffolds is to stimulate and support the growth of new tissues until the cells produce their own ECM. Culture of adult mesenchymal stem cells (MSCs) on such scaffolds and subsequent differentiation of these cells into osteogenic lineages is an approach that is considered to be of great importance in bone tissue engineering, as this strategy can circumvent drawbacks such shortages of donors cells, tissues, and organs, which are the major problems in transplantation medicine [1].

Human adipose tissue, obtained via liposuction, contains multipotent cells that may represent an alternative to bone marrow-derived MSCs as a stem cell source [2]. MSCs derived from human adipose tissue (hASCs) have been successfully differentiated into bone cells [3, 4]. This type of cell source has the advantage of being a discard product, mainly from liposuction surgeries with an aesthetic purpose. Furthermore, the creation of an endothelial network from MSCs has been reported to improve the vascularization of engineered bone tissue and, hence, could favor the growth and proliferation of bone cells [5].

An ideal scaffold must satisfy certain biological and mechanical requirements [6]. In addition, geometric factors are of great importance for the adhesion and proliferation of cells. To meet these requirements, scaffolds produced with polymer nanofibers obtained via electrospinning have been generated and reported to show clear benefits [7]. Among the polymers that can be electrospun, poly(ε-caprolactone) (PCL) has been found to be cyto-compatible when in contact with several types of body tissues, which makes it an ideal material for tissue engineering [8].

In the case of bone tissue engineering, recent studies have focused on the importance of incorporating an inorganic phase to better mimic the native bone tissue [9]. Among the

strategies for such incorporation, direct deposition of minerals on the nanofiber surface has been reported to provide a favorable substrate for cell proliferation and osteogenic conduction [9]. However, the attachment of an inorganic phase to polymeric fibers produced with a hydrophobic polymer such as PCL requires surface treatment.

To be used as a scaffold for tissue engineering applications, PCL has been surface modified with aqueous NaOH to introduce carboxylate groups, which facilitate the binding of a bonelike apatite layer to its surface [10]. The purpose of surface modification is to improve the adhesion of minerals (inorganic phase) to fibers (organic phase). These modifications can be either chemical or physical and can alter the compounds or molecules on the existing surface, or they may be achieved via coating the existing surface with a different material [10]. In this context, the use of a core-shell structure with two different polymers may represent a functional strategy for surface modification.

Gelatin, a hydrophilic biopolymer, is derived from the partial hydrolysis of collagen and is known for its wealth of benefits, such as its biological origin, biocompatibility, bioresorbability, non-immunogenicity, biodegradability and commercial availability [11]. Several researchers have produced PCL/gelatin nanofibers via the co-axial electrospinning method, mostly with the purpose of improving the mechanical, physical and chemical properties of gelatin, or with the aim of circumventing the poor hydrophilicity of PCL [12-14]. Recently, Gautam *et al*. [15] reported that there are interactions, such as hydrogen bonds, between the ester groups of PCL and the amine groups of gelatin molecules, which are beneficial for cell attachment and proliferation.

In the present study, the ability of a gelatin shell to promote the adhesion of an apatite-related mineral to the surface of co-axial fibers was examined. A simulated body fluid (SBF) solution was used to induce the deposition of calcium phosphate, generating the desired mineral coating on a nonwoven mat [16]. To this end, Tas *et al*. [17] used an SBF containing 10 times the calcium and phosphate ion concentrations found in human blood plasma (SBF10). According to these authors, the use of SBF10 leads to linear and rapid coating kinetics. In the present study, the process developed by Tas *et al*. [17] was

chosen to induce the adhesion of an apatite-related material to the surface of electrospun mats.

In summary, the main aim of the present study was to produce and characterize mineralized electrospun co-axial PCL/gelatin nanofibers. An additional aim of this study was to evaluate the potential of such nanofiber mats to be used as a scaffold for hASC growth and differentiation into osteogenic cells through *in vitro* tests.

5.2 Materials and Methods

5.2.1 Materials

The following materials were used for nanofiber fabrication: poly(ε-caprolactone) (PCL) (Sigma-Aldrich, St. Louis, MO, USA, Mn = 80,000), gelatin powder (type A from porcine skin, gel strength approx. 300 g Bloom) (Sigma-Aldrich, St. Louis, MO, USA), 2,2,2-trifluoroethanol (TFE) (99%) (Sigma-Aldrich, St. Louis, MO, USA), glutaraldehyde (GTA) (50% solution, Merck Schuchardt OHG - Hohenbrunn, Germany). All chemicals were used without any further treatment.

5.2.2 Co-axial electrospinning of PCL/gelatin nanofibers

The two polymer solutions were independently fed through concentrically configured needles. The outer and inner diameters of the needles were 2.0 and 1.5 mm, respectively. The concentrations of the PCL and gelatin solutions in 2, 2, 2-trifluoroethanol (TFE) were maintained at 7% w/w and 5% w/w, respectively. For each solution, 10 mL was fed into a glass syringe, where the feed rates were controlled by a syringe pump at 0.3 mL/h for PCL and 0.6 mL/h for gelatin. The needle was positively charged with a voltage of 30 kV. The static collector was connected to the ground with a zero polarity. The distance from the tip of the needle to the collector was maintained at 15 cm. The electrospinning process was carried out at 21.5ºC under 37.5% relative humidity. After the electrospinning process was complete, the nanofibrous membrane was carefully collected in a Petri dish, wrapped with aluminum foil and placed in a sealed desiccator to be further treated with glutaraldehyde and subjected to mineralization.

5.2.3 Crosslinking of co-axial PCL/gelatin fiber mats

The crosslinking process was carried out by placing a Petri dish containing the nanofibrous mats on a holed ceramic plate in a sealed desiccator containing a glutaraldehyde solution (50% w/v). The nanofibrous membranes were crosslinked in the glutaraldehyde vapor at room temperature for 1 h.

5.2.4 Preparation of a 10x concentrated SBF (SBF10) solution

Concentrated simulated body fluid (SBF10) was prepared according to Tas *et al*. [17]. Briefly, for a total aqueous volume of 2 L a stock solution containing in grams NaCl (116.8860), KCl (0.7456), $CaCl_2 \cdot 2H_2O$ (7.3508), $MgCl_2 \cdot 6H_2O$ (2.0330) and Na_2HPO_4 (2.3996) was prepared in advance (pH of 4.35–4.40). An appropriate amount of $NaHCO_3$ powder was added just prior to the coating procedure to raise the pH to 6.5. Reagent-grade chemicals and deionized water (Millipore, USA) were used to prepare this solution. The final solution was filtered to eliminate impurities.

5.2.5 Coating process for mineralization

Co-axial PCL/gelatin mats were immersed in SBF10 and held at room temperature for 2 hours. When the coating process was complete, the samples were collected, extensively washed with deionized water and placed in a sealed desiccator for further characterization.

5.2.6 Characterization of non-coated and coated electrospun co-axial PCL/gelatin nanofibers

5.2.6.1 Scanning electronic microscopy (SEM) and transmission electron microscopy (TEM)

The morphology of the non-coated and coated PCL/gelatin co-axial nanofibers was analyzed via scanning electron microscopy (SEM) (JEOL JSM 5600, Japan) at an accelerating voltage of 15 kV. Samples for SEM were coated with gold using a sputter coater. Transmission electron microscopy (TEM) (TOPCON 002B) at 200 kV was performed to observe the core-shell structure of the non-coated PCL/gelatin co-axial nanofibers. Samples for TEM observation were prepared by directly depositing the as-spun fibers onto copper grids. The samples were dried in a vacuum oven for 48 h at room temperature prior to TEM imaging.

5.2.6.2 Energy dispersive spectroscopy (EDS)

To evaluate the composition of the coating on the nanofibers, EDS of coated fibers was performed using an energy dispersive X-ray microanalyzer (Voyager, Noran) connected to an SEM. During collection of the spectra, the accelerating voltage was set to 10 kV.

5.2.6.3 X-ray diffraction (XRD)

The crystallographic structure of the coated nanofibers was verified using a Philips PW3710 with Cu K-radiation (λ=1.54 Å). The scanning range was from 2θ=10 to 90º, with a step size of 0.06º.

5.2.6.4 Fourier transform infrared spectroscopy (FTIR)

The coated PCL/gelatin co-axial nanofibers were also characterized via attenuated total reflectance Fourier transform infrared spectroscopy (ATR-FTIR) using a Golden gate single-reflection ATR in a Nicolet model 6700 spectrometer at a resolution of 4 cm^{-1} with 256 co-added scans. The spectra were collected from 400 – 4,500 cm^{-1}.

5.2.7 In vitro tests

5.2.7.2 Basal medium

Dulbecco's modified Eagle's medium (DMEM) (Sigma-Aldrich) was supplemented with 5 mM sodium bicarbonate (Cinética Química Ltda), 10% serum: FBS (Cripion Biotecnologia Ltda), penicillin (100 U/mL), streptomycin (0.1 mg/mL), amphotericin B (0.25 µg/mL) (Sigma-Aldrich) and gentamicin (60mg/L; Schering-Plough). The pH was adjusted to 7.2, and the medium was then filtered through a 0.22 µm polyvinylidene difluoride membrane (Milipore).

5.2.7.3 Osteogenic differentiation medium (OM)

Dulbecco's modified Eagle's medium (DMEM) (Sigma-Aldrich) was supplemented with 50 µg/mL ascorbate-2-phosphate (Ecibra), 10mM β-glycerophosphate (Sigma-Aldrich), and 0.1 µM dexamethasone (Ache´). The pH was then adjusted to 7.2, and the medium was filtered through a 0.22 µm polyvinylidene difluoride membrane (Milipore).

5.2.7.4 Endothelial differentiation medium

Dulbecco's modified Eagle's medium (DMEM) (Sigma-Aldrich - St. Louis, MO) was supplemented with 5 mM sodium bicarbonate (Cinética Química Ltda), 2% serum: FBS (Cripion Biotecnologia Ltda), 50 ng/mL Vascular Endothelial Growth Factor (VEGF)

(Invitrogen), Basic Fibroblast Growth Factor (bFGF) (Invitrogen), penicillin (100 U/mL), streptomycin (100 U/mL), amphotericin B (0.25 µg/mL) (PSA, Gibco). The pH was adjusted to 7.2, and the medium was then filtered through a 0.22 µm polyvinylidene difluoride membrane (Millipore).

5.2.7.5 Sterilization method

Prior to the *in vitro* tests, the mineralized PCL/gelatin mats were sterilized with ultraviolet radiation for 60 minutes.

5.2.7.6 Isolation of human adipose-derived stem cells (hASCs)

Adipose tissue obtained from liposuction was used as the source of the stem cells (approved by the Ethics Committee for Research (COEP) of the UFMG, no. ETIC 0023.0.203.000-11). The isolation and culture of human adipose-derived stem cells (hASCs) were performed based on the procedure described by Zuk *et al*. [2]. Briefly, human adipose tissue was obtained from elective liposuction procedures performed on healthy patients aged between 20 and 30 years. The raw lipoaspirate was conditioned in sterile syringes and subsequently transferred to polyethylene tubes (50 cc) to be washed extensively with equal volumes of phosphate-buffered saline (PBS) (0.15 M, pH 7.2), followed by centrifugation at 1400 x g for 6 min at 20ºC. A biphasic solution was formed in which the bottom layer consisted of PBS with blood cells, and the upper layer consisted of adipose tissue. The upper layer was transferred to polyethylene tubes (50 cc) to be enzymatically digested with 0.10% collagenase type I (Life Technologies) in 0.15 M PBS (pH 7.4) (1:1) at 37ºC under 5% CO_2 in a humidified atmosphere. During this period, the tubes were shaken vigorously every 15 minutes. To isolate the stromal vascular fraction (SVF), after 2 h of incubation, the tubes were centrifuged at 1400 x g for 10 min at 20 ºC. The pellet was resuspended in basal medium and plated in cell culture flasks (T-75-Sarstedt). The flasks were incubated at 37ºC under 5% CO_2 in a humidified atmosphere. After 48 h of culture, the contents of the flasks were transferred to polyethylene tubes (50 cc) and centrifuged as detailed above. The supernatant was discarded, and the pellet was resuspended in basal medium, followed by plating in new cell culture flasks (T-75-Sarstedt). Every 2 days, the cells were washed extensively with PBS to remove residual nonadherent red blood cells, and any plastic adherent cells that

remained, i.e., the hASCs, were maintained in new basal medium. When the cells reached 70-80% confluence, the basal medium was removed, and the cells were washed with PBS and treated with 0.05% trypsin-ethylenediaminetetraacetic acid (EDTA) (Invitrogen) for 5 min, followed by inactivation of trypsin with basal medium. The resulting suspension was replated in new cell culture flasks. The cells were expanded this way until passage 4 before they were used in assays.

5.2.7.7 Viability assay and cells proliferation analysis

A viability assay was performed, and cell proliferation was examined during osteogenic and endothelial differentiation using an MTT-based colorimetric assay (3-(4, 5-dimethylthiazol-2-yl) 2, 5-diphenyl tetrazolium bromide) (Invitrogen). This method is based on the fact that the mitochondrial enzyme succinate-dehydrogenase within viable cells is able to cleave the tetrazolium salt MTT into a blue-colored product (formazan). The formazan derivatives are then excreted into the culture medium, and the optical density can be measured. The amount of formazan produced is correlated with the number of living cells in a sample [18]. Briefly, hASCs at a density of 5×10^4 cells/well, both with and without nanofibers, were seed in 24-well plates (Thermo Scientific Nunc) in the different media described above (osteogenic, endothelial and basal) and incubated at 37ºC under 5% CO_2 in a humidified atmosphere for 2, 7, 14, or 21 days. After these various incubation times, the culture media were replaced with fresh media (210 µL/well), and MTT (5 mg/mL) was added to each well. After two hours of incubation at 37 ºC under 5% CO_2 in a humidified atmosphere, the cell morphology and formazan salt production were visualized using an optical microscope (OLYMPUS IX70). The formazan salts were solubilized in 210 µL/well of 10% sodium dodecyl sulfate - 0.01 M hydrochloric acid (SDS-HCl) and maintained for 18 h at 37 ºC under 5% CO_2 in a humidified atmosphere. Then, 100 µL of the solution in each well was transferred in duplicate to a 96-well plate (flat bottom), and metabolic activity was determined based on the optical density at 595 nm using a spectrophotometer (Elx800, Bio-Tek, Instruments Inc.). Cell viability was determined by comparison of the optical densities of the cultures with a standard curve of 10^3 to 10^6 cells per well. The data were analyzed via two-way analysis of variance (ANOVA), followed by Bonferroni's post-hoc test (GraphPad, San Diego, CA). The results are presented with the mean ± standard

deviation of duplicates assays, and significance was determined at $p<0.05$. hASCs cultivated in the presence of nanofibers in the basal medium (i.e., without any factor to induce differentiation) were used as a control.

5.2.7.8 Alkaline phosphatase (ALP) activity

Alkaline phosphatase activity was examined to evaluate cell differentiation in osteogenic cells. The alkaline phosphatase production by the cells in culture was assayed using an alkaline phosphatase assay kit (BCIP-NBT) (Gibco). This assay is based on a chromogenic reaction initiated by the cleavage of the phosphate group of BCIP (5-bromo-4-chloro-3'-indolyphosphate p-toluidine) dihydrogen phosphate by the alkaline phosphatase present in the cells. This reaction produces a proton, which reduces NBT (nitro-blue tetrazolium chloride), yielding an intense, insoluble black-purple precipitate. Briefly, the same procedure described above was employed here, but instead of adding MTT, 210 µL/well of a BCIP-NBT solution (prepared according to the manufacturer's instructions) was added. After two hours of incubation at 37ºC under 5% CO_2 in a humidified atmosphere, the black-purple precipitate was observed using an optical microscope (OLYMPUS IX70). The black-purple precipitate was then solubilized in 210 µL/well of 10% sodium dodecyl sulfate - 0.01 M hydrochloric acid (SDS-HCl) and maintained for 18 h at 37 ºC under 5% CO_2 in a humidified atmosphere. Subsequently, 100 µL of the solution in each well was transferred in duplicate to a 96-well plate (flat bottom). The optical density of the solution was measured at 595 nm using automatic reading equipment (Elx800, Bio-Tek, Instruments Inc.). Electrospun mineralized nanofibers containing hASCs cultured in basal medium were used as a control. To prevent interference of the electrospun nanofibers with the colorimetry process, the mean value obtained for electrospun nanofibers without hASCs was subtracted from the optical density values obtained at different times for nanofibers with hASCs. The obtained data were analyzed using two-way analysis of variance (ANOVA), followed by Bonferroni's post-hoc test (GraphPad, San Diego, CA). The results are presented as the mean ± standard deviation of duplicate assays, and significance was determined at $p<0.05$.

5.2.7.9 Endothelial cell marker expression (immunofluorescence assay)

To analyze the differentiation of the cells towards an endothelial phenotype, an immunofluorescence assay was performed to examine the expression of endothelial markers. Briefly, hASCs seeded onto the electrospun fiber mesh and cultured in endothelial differentiation medium for different incubation periods were fixed in 4% paraformaldehyde in 100 mM sodium phosphate buffer (pH 7.0) for 15 min. at room temperature. The cells were then washed three times in PBS, followed by permeabilization of the plasmatic membrane with PBS containing 0.1% Triton X-100 for 10 minutes. The cells were washed again three times for 5 minutes each and then blocked for 1 h at room temperature in 1% bovine serum albumin (BSA)/PBS and 5% goat serum. The cells were subsequently incubated overnight with a mouse monoclonal antibody against von Willebrand Factor (VW92-3, primary antibody-vWF, *Abcam),* an endothelial marker expressed in hASCs, at a dilution of 1:100 in 1% PBS/BSA. After incubation, the cells were washed again three times and incubated for 1 h with Alexa Fluor® 488 Goat Anti-Mouse IgG (secondary antibody-Cat. A11001; Invitrogen) diluted 1:500 in 1% PBS/BSA. Negative controls were performed using only the secondary antibody. To stain nuclei, the cells were incubated for 20 minutes with 0.2 μg/mL Hoeschst 33258 pentahydrate, (Cat. H3569; Invitrogen). After washing with PBS (three times/10 min), the slides were mounted with Hydramount Aqueous medium (Cat. HS-106; National diagnostics) and analyzed with a Zeiss LSM 510 Meta confocal microscope.

5.3 Results and Discussion

5.3.1 Mineralization of co-axial PCL/Gelatin nanofibers

The extracellular matrix (ECM) is a complex fibrous network that provides structure and support for cells and tissues. Structures designed to mimic and replace the native ECM in damaged or diseased tissues are a key factor in tissue engineering. It is widely accepted that electrospinning technique generates structures that resemble native ECM [19].

In spite of all of the advantages reported for PCL [10], the development of scaffolds using a core-shell structure with two different polymers is more likely to be successful. In the case of tissue engineering, the main drawback of PCL nanofibrous scaffolds is their hydrophobicity, which hinders adhesion and cell proliferation. In addition, due to this lack of hydrophilicity, for scaffolds to be applied in bone tissue engineering, surface treatments are required to improve the stage of mineralization [20, 21, 9].

Type I collagen is a major organic component of the mineralized ECM of bone tissue, comprising 90–95% of its organic material, and serves as a template upon which minerals are deposited [7]. Sionkowska [22] described the structure of collagen and the numerous intra- and intermolecular forces that stabilize it in detail. Briefly, the autors described how collagen, like most proteins, loses all of its structure during heating. The triple helix unwinds, and the chains separate. Then, when this denatured mass of tangled chains cools down, it absorbs all of the surrounding water like a sponge, forming gelatin. Therefore, gelatin itself is a mixture of water-soluble proteins derived primarily from collagen [23]. Thus, nanofibrous scaffolds of gelatin have been reported to mimic not only the topography, but also the chemical composition of the ECM [24]. In the present work, we first produced co-axial PCL/gelatin nanofibers, and mineralization was subsequently carried out. Figure 5.1 shows SEM micrographs of the generated PCL/gelatin mats before mineralization.

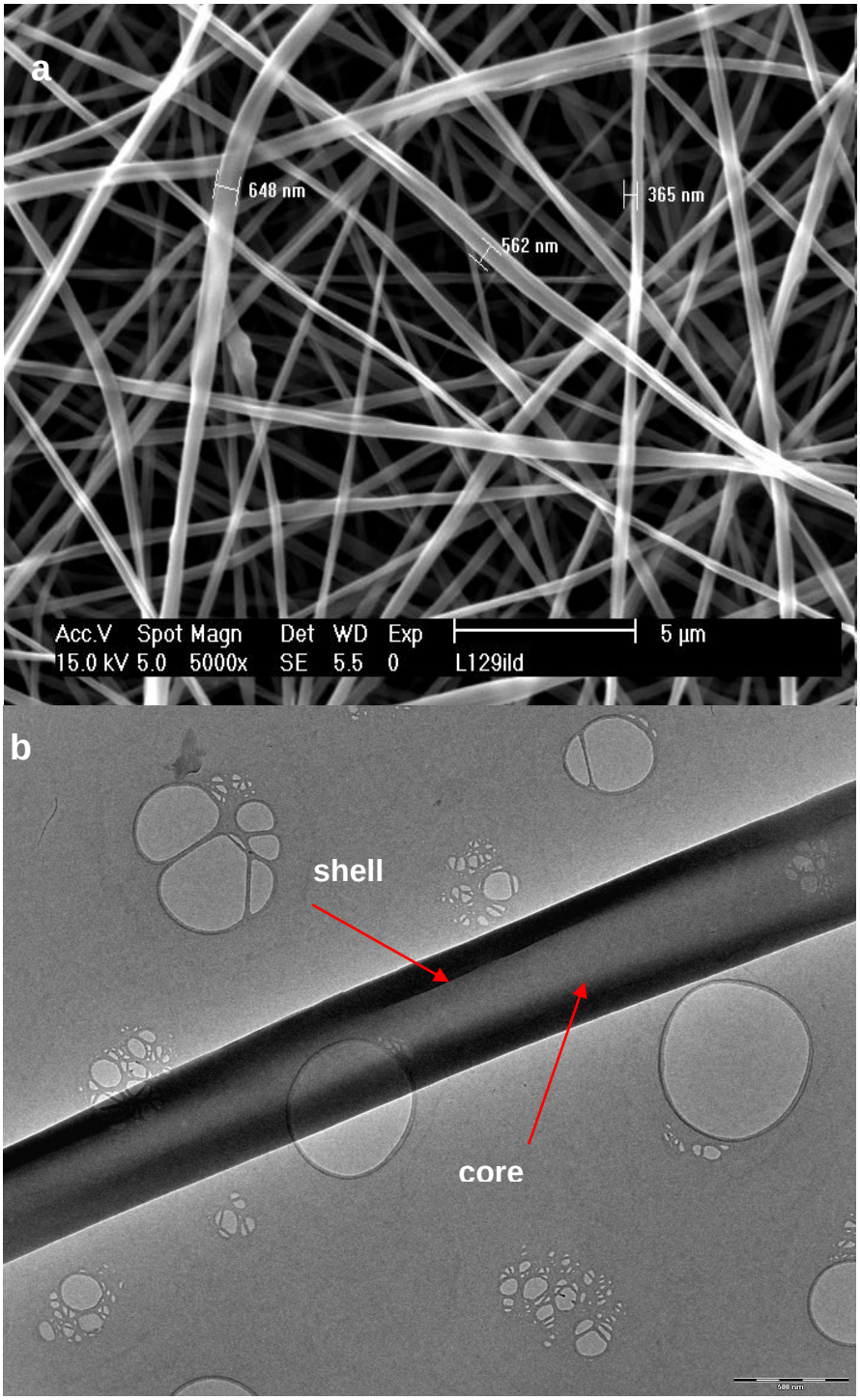

Figure 5.1: Co-axial PCL/gelatin nanofibers crosslinked with glutaraldehyde prior to mineralization. (a) SEM and (b) TEM. PCL in TFE (7%w/w; core), flow rate of 0.3 mL/hr; and gelatin in TFE solution (5%w/w; shell), flow rate of 0.6 mL/hr. Voltage: 30/0 kV; distance between the needle tip and the collector: 15 cm; relative humidity: 37.5%; temperature: 21.5 ºC.

Various approaches for surface mineralization have been reported. Fu *et al*. [25] produced electrospun poly(ε-caprolactone)-poly(ethylene glycol)-poly(ε-caprolactone) (PCL-PEG-PCL, PCEC) containing 30 wt.% of nano-hydroxyapatite (n-HA). They incorporated n-HA powder into the PCEC solution with the aid of an ultrasonic vibrator to disrupt agglomerated HA particles as much as possible. Choi *et al*. [26] mixed gelatin dissolved in TFE with 0.3 M $CaCl_2$ and 0.3 M Na_2HPO_4 (1:1 ratio) prior to the electrospinning process. The formation of bone-like apatite on the surface of composite membranes immersed in SBF with ionic concentrations nearly equal to those of human blood plasma was examined. Cai *et al*. [27] used poly(L-lactic acid) (PLLA)/gelatin electrospun nanofibers as a template to produce biomimetic hexagonal HA. For this purpose, they soaked the nanofibers in SBF five times to induce apatite deposition, followed by calcination to remove the organic fibers. Jaiswal *et al*. [28] reported a technique, referred to as the alternate soaking method, that forms apatite via incubation of the substrate alternately in Ca^{+2} and PO_4^{-3} solutions for a certain number of cycles. Yang *et al*. [21] adopted the method reported by Tas *et al*. [17], in which a new SBF solution containing 10 times the calcium and phosphate ion concentrations found in human blood plasma was used. This last method is the same method adopted in the present study to mineralizate the PCL/gelatin nanofibers. Figure 5.2 presents SEM micrographs of the fibers coated by immersing them for 2 h in SBF10 without any previous treatment. Compared with SEM images of non-coated fibers, the SEM image shown in Figure 5.2 suggests that mineralization of the fibers took place.

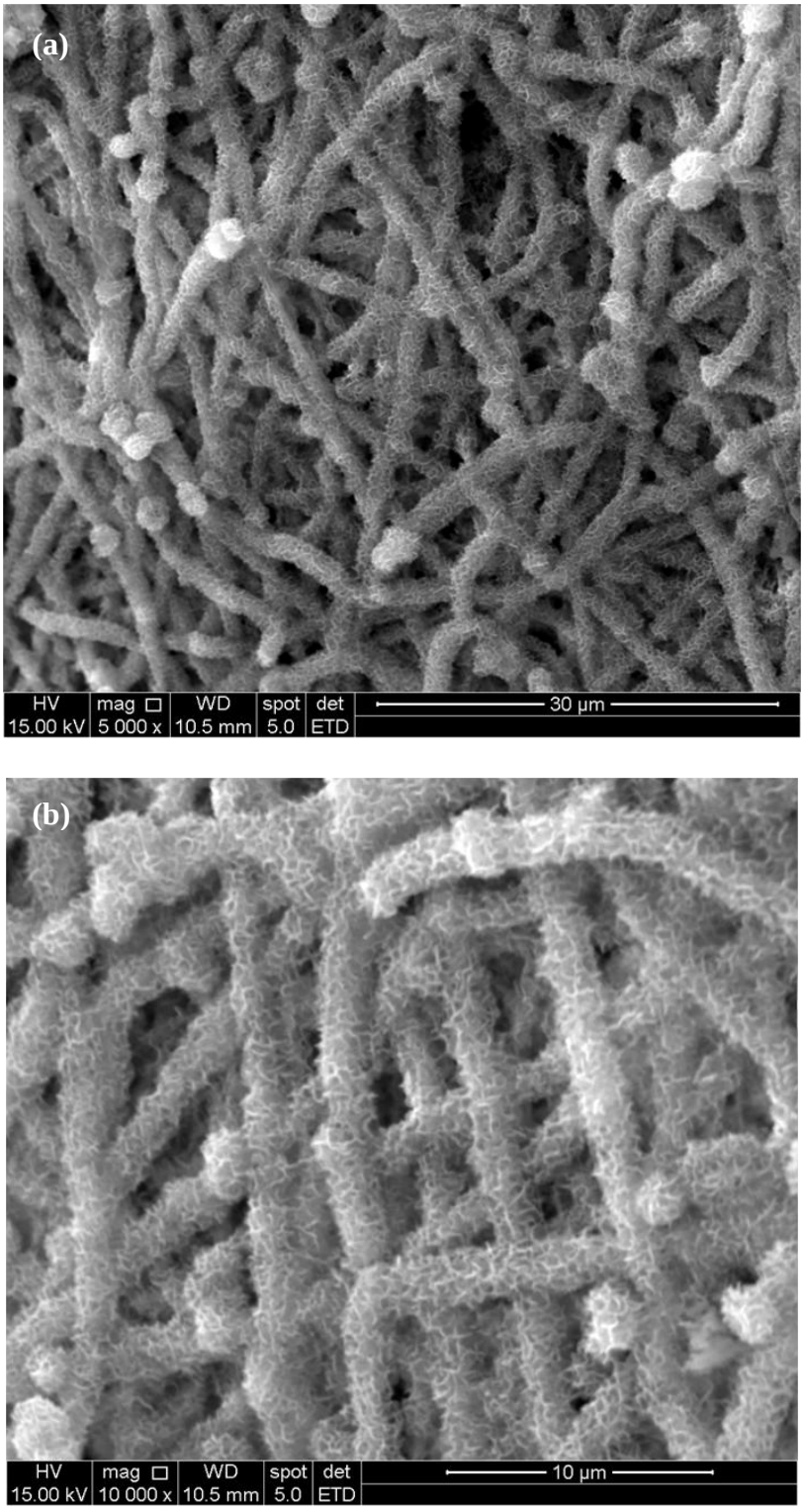

Figure 5.2: SEM micrographs showing the surface of the co-axial PCL/gelatin nanofibers after coating with SBF10 for 2h: (a) 5000X magnification; (b) 10000X magnification.

5.3.2 Characterization of mineralized co-axial-PCL/Gelatin nanofibers

To evaluate the composition of the coating observed under SEM (Figure 5.2), the coated fibers were first analyzed via energy-dispersive X-ray spectroscopy (EDS). This analysis, whose spectrum is shown in Figure 5.3, detected the presence of Ca and P, among other elements.

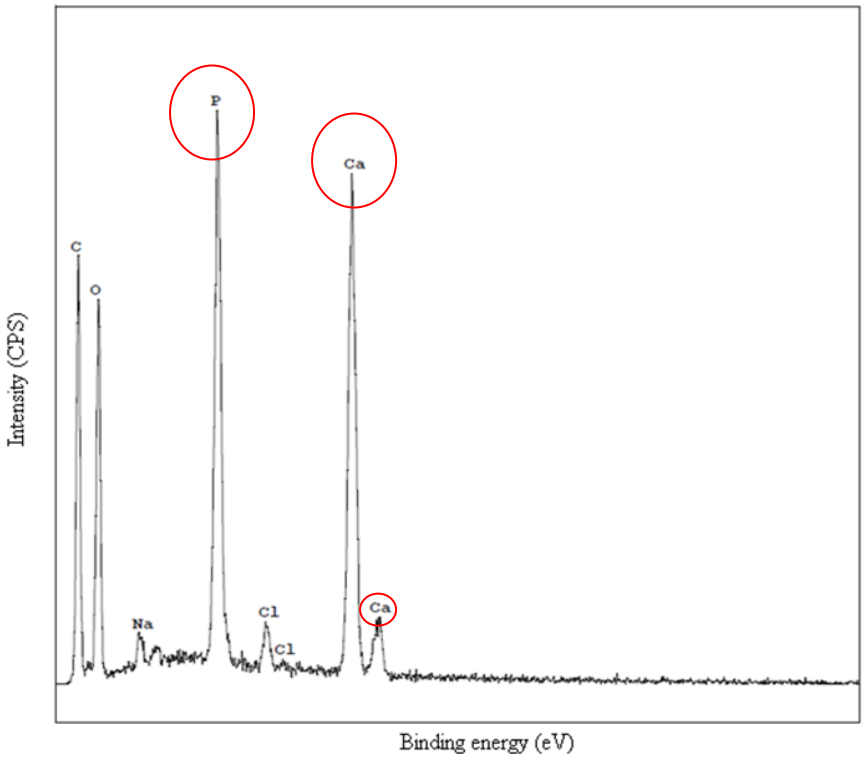

Figure 5.3: EDS spectrum for coated co-axial PCL/gelatin nanofibers after mineralization.

As the formula of hydroxyapatite is $Ca_5(PO_4)_3(OH)$ and the fibers were washed extensively with water before being analyzed, this result was considered to indicate the presence of hydroxyapatite on the fiber surface. According to the above formula, the theoretical mass percentages of Ca and P were 39.84% and 18.52%, respectively. A quantitative composition microanalysis conducted on the measured X-ray intensities using ZAF software indicated percentages of 39.29% and 20.74% for Ca and P, respectively. Such values are close to those of hydroxyapatite.

On the other hand, the Ca/P atomic ratio of stoichiometric hydroxyapatite is 1.67 [29], and the value of the Ca/P atomic ratio determined here using EDS data was 1.46, which falls within the range of 1.31-1.48 reported for amorphous calcium phosphates produced in aqueous media [29].

Raynaud *et al*. [30] synthesized single-phase calcium phosphate apatites with variable Ca/P atomic ratios within the range of 1.50–1.667 by changing the synthesis conditions. According to these authors, a Ca/P = 1.5, corresponding to pure apatitic tricalcium phosphate (TCP), was not obtained, instead, they generated biphasic mixtures composed of a calcium apatite and $CaHPO_4$ at Ca/P < 1.50 or $Ca(OH)_2$ at Ca/P>1.667. In light of this finding, we can infer that the co-axial PCL/gelatin nanofibers produced in the present work were coated with a biphasic mixture of HA and more soluble phosphates.

XRD analysis of the coated fibers was performed in an attempt to better characterize the coating on the fibers. The most remarkable peaks in the X-ray diffraction pattern were found in the 2θ angle range between 20 and 45º and are indicated in Figure 5.4.

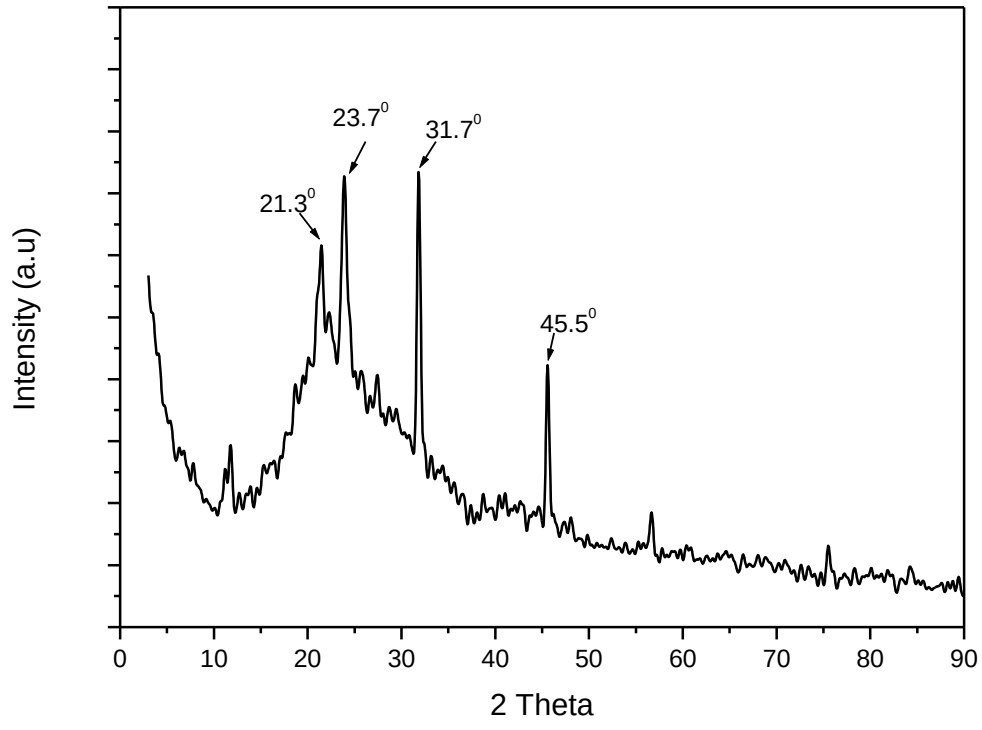

Figure 5.4: XRD pattern obtained for SBF10-coated co-axial PCL/gelatin nanofibers.

In the case of the PCL, it is also known that its crystalline phase diffracts at 21.3º (110) and at 23.8º (200) [31]. Both peaks were found and as gelatin is amorphous, the peaks found at 31.7 and 45.5º may be attributed to the mineral coated onto the fibers.

Strong peaks in the region of 30 and 35° are characteristic of bone apatite [32]. Ribeiro Neto *et al*. [31] found peaks at 25.8 (002), 31.8 (211), 32.9 (112) and 40.0º (130) corresponding to diffraction planes of the nano-hydroxyapatite. Correa *et al*. [33] stated that calcium phosphate with hydroxyapatite structure has its main diffraction peaks in the 2θ angle range between 20 and 60º. The XRD pattern depicted in Figure 5.4 clearly shows the peak at 31.7º but is not conclusive regarding other peaks.

Liao *et al*. [34] compared the mineralization processes onto collagen nanofibers with that onto poly (lactic-co-glycolic acid) (PLGA) nanofibers. Their study revealed that the mineral coating composition is dependent on the material coated. For instance, they observed the formation of nanosize carbonated hydroxyapatite during collagen mineralization, whilst nanosize hydroxyapatite was observed during PLGA mineralization.

From the obtained XRD patterns, the crystallite size of HA, i.e., the thickness of the mineralized layer, can be estimated using Scherrer's equation [33]:

$$D = \frac{k\,\lambda}{\beta \cos\theta} \qquad (1)$$

where k is a constant (the value generally = 0.9); λ is the X-ray wavelength (nm); β is the width of the XRD peak (in radian unit), measured as the full width at half maximum; and θ is the XRD peak position. Using this approach, the estimated size of the crystallites based on the peak at 31.8º (211) was found to be 19.53 nm (Figure 5.5). By using the same procedure based on the peak at 45.5^0 the estimated size of the crystallites was found to be 21.07 nm (Figure not shown).

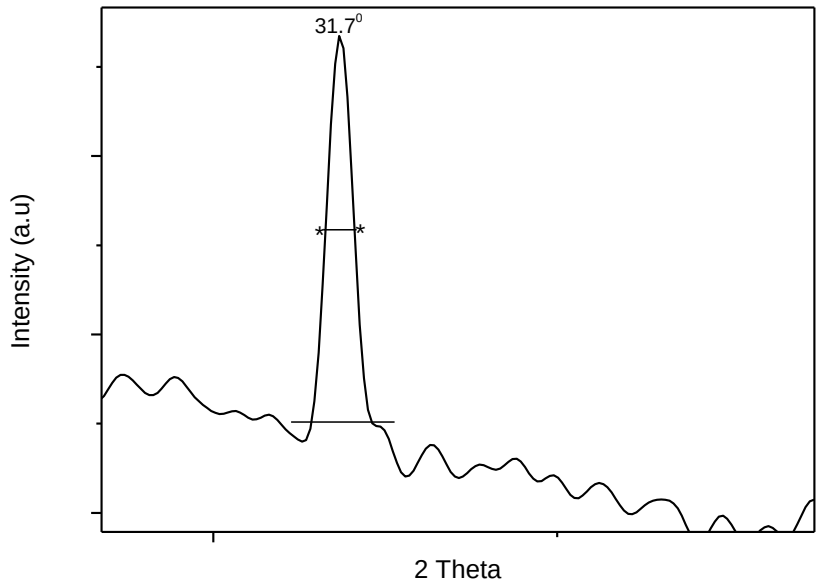

Figure 5.5: Peak at 31.7° expanded from the XRD pattern and used in the Scherrer equation.

Using the Scherrer equation, other authors have estimated the size of HA crystals. Correa *et al*. [33] reported a value of approximately 75 nm for calcium phosphate with a hydroxyapatite structure synthesized via the continuous precipitation method (2θ = 25.9º). Liao et al. [34] estimated the average crystal size with respect to the (002) peak fitting of HA grown on different electrospun nanofibers. These authors observed values of 11.5 nm for HA on collagen nanofibers and 12.5 nm or 15.7 nm for HA on PLGA nanofibers. They associated this size variation with the different kinetics of mineral formation on each material.

The FTIR spectrum of the mineralized fibers is shown in Figure 5.6. The following bands were described as being characteristic of PCL by Gautam *et al* [15]: 2949 cm^{-1} (asymmetric CH_2 stretching), 2865 cm^{-1} (symmetric CH_2 stretching), 1727 cm^{-1} (carbonyl stretching), 1293 cm^{-1} (C-O and C-C stretching), 1240 cm^{-1} (asymmetric C-O-C stretching) and 1170 cm^{-1} (symmetric C-O-C stretching). The following bands for gelatin were described by the same authors: 3443 cm^{-1} due to N-H stretching of amide bonds, C-O stretching at 1640 cm^{-1}, N-H bending at 1543 cm^{-1}, and N-H out-of-plane wagging at 670 cm^{-1}. According to these authors, all the characteristic bands for PCL and gelatin are observed in PCL/gelatin nanofibers, but the bands are shifted towards

lower wavenumbers due to interactions between PCL and gelatin. Other bands attributed to PCL described by others authors [31] were found at 1360, 1290 and 1240 cm^{-1}, corresponding to CH_3 group folds, and at 1190-1170 cm^{-1}, corresponding to C-O-C stretching vibrations.

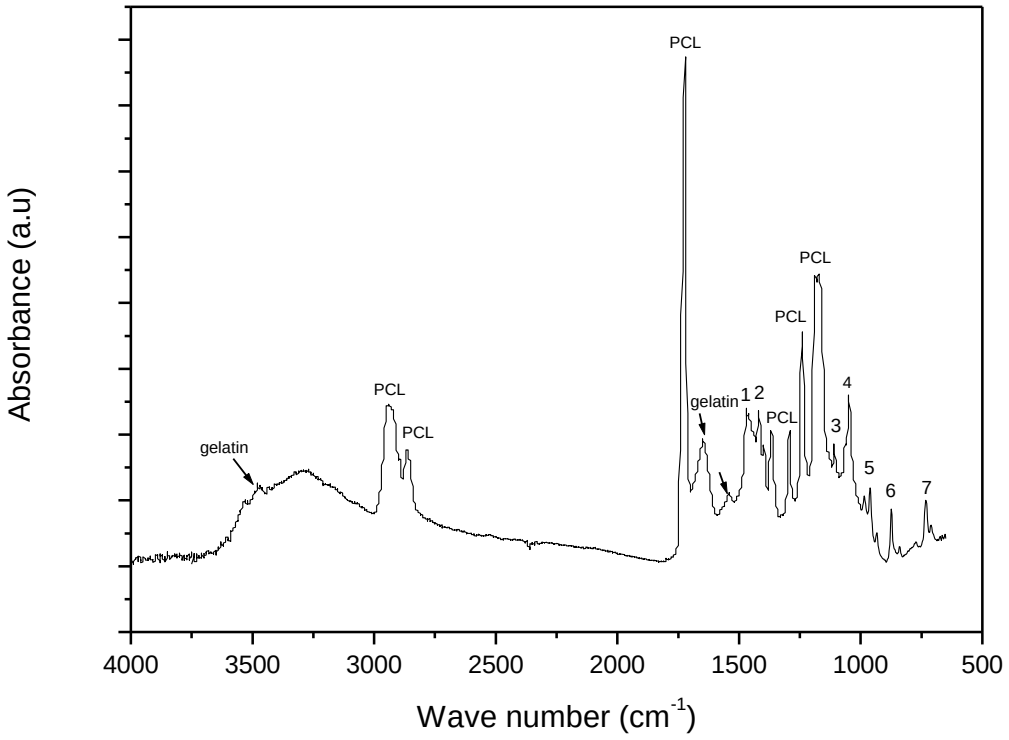

Figure 5.6: FTIR spectrum of mineralized co-axial PCL/gelatin nanofibers.

Among the bands described for PCL and gelatin, other accentuated absorptions that can be observed in Figure 5.6 were attributed to the mineral coating, which are located at (1) 1463 cm^{-1}, (2) 1420 cm^{-1}, (3) 1110 cm^{-1} (4) 1048 cm^{-1}, (5) 961 cm^{-1}, (6) 874 cm^{-1}, and (7) 731 cm^{-1}. Regarding the hydroxyapatite FTIR spectra that have been reported in the literature, the main findings are described hereafter. The band at 720 cm^{-1} has been attributed to a $P_2O_7^{4-}$ group [35]. The bands at 962.6 and 1040 cm^{-1} were assigned by Correa *et al*. [33] to the fundamental frequencies of the PO_4^{3-} group, and the same authors described a low intensity band at 957 cm^{-1} as a P-OH group.

Absorption bands in the range of 1411 cm^{-1}-1450 cm^{-1} have been assigned to B-type CO_3 [35]. Franco *et al*. [36] observed bands at 1462 and 870 cm^{-1}, suggesting the

presence of carbonate hydroxyapatite. According to Rehman *et al*. [37], a hydroxyl stretch is observed at 3569 cm^{-1} within the spectrum of carbonated apatite and shows a lower intensity compared to that from hydroxyapatite. However, in our spectrum, the peaks located in this region overlapped due to the absorption of gelatin.

On the other hand, Yang *et al*. [21] confirmed the presence of HPO_4 based on P-OH stretching at 874 cm^{-1} and suggested that dicalcium phosphate dihydrate ($CaHPO_4.2H_2O$) (DCPD) had formed. According to these authors, an obvious feature of DCPD is the occurrence of two intense doublets in the O-H stretching region: one with components at 3541 and 3488 cm^{-1} and the other with components at 3286 and 3162 cm^{-1}. As mentioned above, this absorption region is not clear in the spectrum presented in Figure 5.6.

The EDS results showed that the Ca/P ratio of the coating was approximately 1.46 (calcium-deficient HA), which is above the Ca/P molar ratio of DCPD (1.0) [21]. This may be due to the contribution from apatite, whose stoichiometric Ca/P molar ratio is 1.67, indicating the formation of HA along with DCPD.

Based on the above discussion, it may be suggested that the coating of the co-axial PCL/gelatin nanofibers consisted of a mixture hydroxyapatite, carbonate hydroxyapatite and dicalcium phosphate dehydrate. Brushite ($CaHPO_4.2H_2O$*)* is known to be a precursor to HA [38]. It is likely that if the nanofibers remained immersed in SBF10 for a longer period, more pure hydroxyapatite would be formed on the mats.

5.3.3 Cell viability

Heng *et al*. [1] pointed out that *in vitro* tests based directly on human-derived cells and tissues are much more clinically relevant, timely, and accurate as well as more cost-effective in comparison with laboratory testing performed in animal cell/tissue cultures or live animals. Among the various tissue types from which adult stem cells can be obtained, adipogenic tissue was chosen as the source of these cells (hASCs) in the present study. The results of MTT assays, shown in Figure 5.7, demonstrated that

hASCs seeded in basal medium (control) and on mineralized PCL/gelatin mats were able to metabolize MTT into formazan crystals.

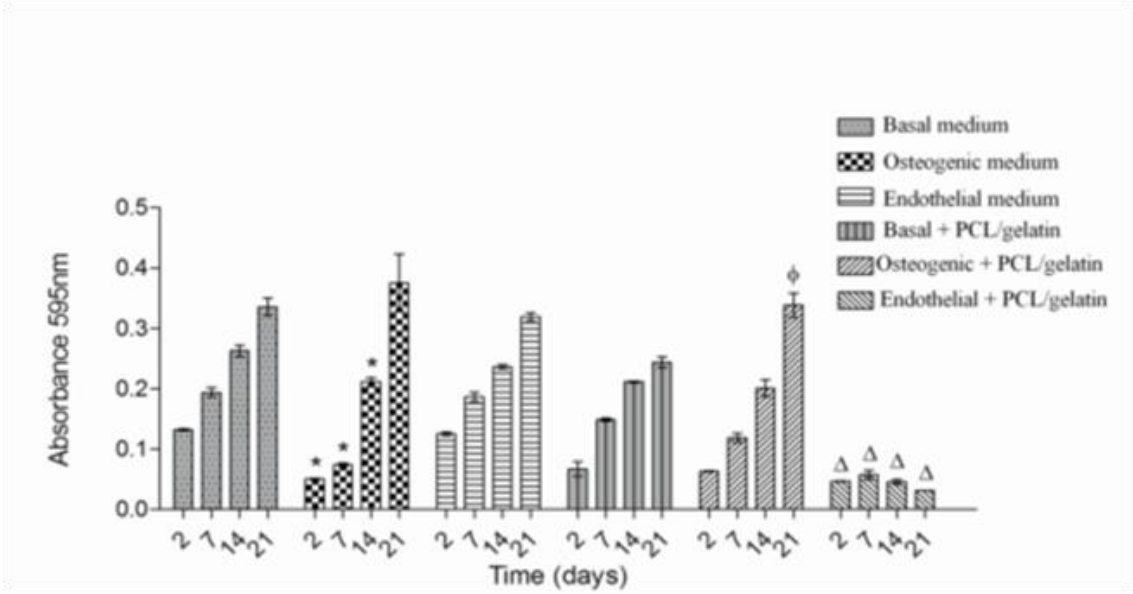

Figure 5.7: MTT proliferation assays performed 7, 14 and 21 days after hASCs were seeded and cultured in three specific media: basal medium, osteogenic medium and endothelial differentiation medium. The results are expressed as the mean ± SD; (*) indicates a significant difference at $p<0.05$ for basal x osteogenic medium; (Φ) indicates a significant difference at $p<0.05$ for basal + PCL/gelatin x osteogenic + PCL/gelatin, (Δ) $p<0.05$ basal + PCL/gelatin x endothelial + PCL/gelatin.

As can be seen in Figure 5.7, when seeded in basal medium, the hASCs exhibited reduced proliferation in the presence of mineralized PCL/gelatin mats when compared to the control. Some reduction of cell proliferation rates is not unexpected when cells are placed in contact with implant material. This type of behavior does not mean that the material is incompatible, as it can be observed that the hASCs continued to proliferate over time.

Initially, the hASCs cultivated in osteogenic medium displayed less proliferation than those seeded in basal medium. However, at 21 days, the same level of cell growth was

observed in both types of media. During the osteogenic induction of hASCs, there was no significant difference observed in the results regarding the optical density (OD) due to the presence of mineralized PCL/gelatin mats in basal medium. PCL/gelatin mats did not affect the proliferative capacity of these cells, in which superior cell proliferation was observed after 21 days. This suggests that the PCL/gelatin mats promote cell proliferation and are able to create a favorable environment for the cells. This effect may be partly attributed to the hydroxyapatite layer on the fiber surface, which helped to mimetize the native environment of osteogenic cells.

The importance of blood vessels in the formation of the bone tissue has been described by various authors. For example, Zonari *et al*. [5] highlighted the role played by the vascularization of cell-seeded implants in cell survival. According to these authors, the efficient supply of nutrients to the cells and metabolite diffusion allow bone tissue engineering products to be used in clinical practice. Jang *et al*. [7] stated that scaffolds that are capable of releasing an active angiogenic factor will promote early vascularization and attract osteogenic precursor cells.

With respect to the present study, Figure 5.7 shows that there was no significant difference observed when the hASCs were cultured in a basal culture medium versus an endothelial differentiation medium. The results indicated that the hASCs proliferated in both types of medium. However, the hASCs cultured on PCL/gelatin mats showed less proliferation in endothelial differentiation medium compare to the hASCs cultured on PCL/gelatin mats in basal medium and the hASCs cultured without fiber mesh in endothelial differentiation medium. A similar result was found by Zonari *et al*. [5] in a study addressing hASC endothelial differentiation in the presence of poly(3-hydroxybutyrate-co-3-hydroxyvalerate) (PHB/PHB-HV) mats. These authors reported that the capacity to self-renew is unique to stem cells, and as the stages of differentiation progress, the proliferative potential diminishes. According to these investigators, mature cells are unable to proliferate; however, the majority of lineages exhibit a precursor or committed progenitor stage in which proliferation and differentiation are balanced. They suggested that PHB/PHB-HV was contributing to compromising the differentiation of the cells into an endothelial lineage.

Our research demonstrated a clear interference of the PCL/gelatin mats with hASC proliferation in the endothelial differentiation medium. The observed reduction in the proliferation rate of cells cultured in endothelial differentiation medium when in contact with nanofibers may also be associated with reduction of the proliferative ability of stem cells during differentiation. This result is dissimilar to that obtained using osteogenic medium. It is reasonable to assume that the presence of hydroxyapatite deposited over a large surface area formed by a group of nanofibers can favor osteostimulation more than other types of differentiation.

5.3.4 Alkaline phosphatase (ALP) activity

Alkaline phosphatase (ALP) activity is an indicator of osteoblast phenotypic activity [20]. Increasing ALP activity has been considered to be an early marker of osteogenic differentiation for hASCs [4]. The results of the ALP assays are shown in Figure 5.8.

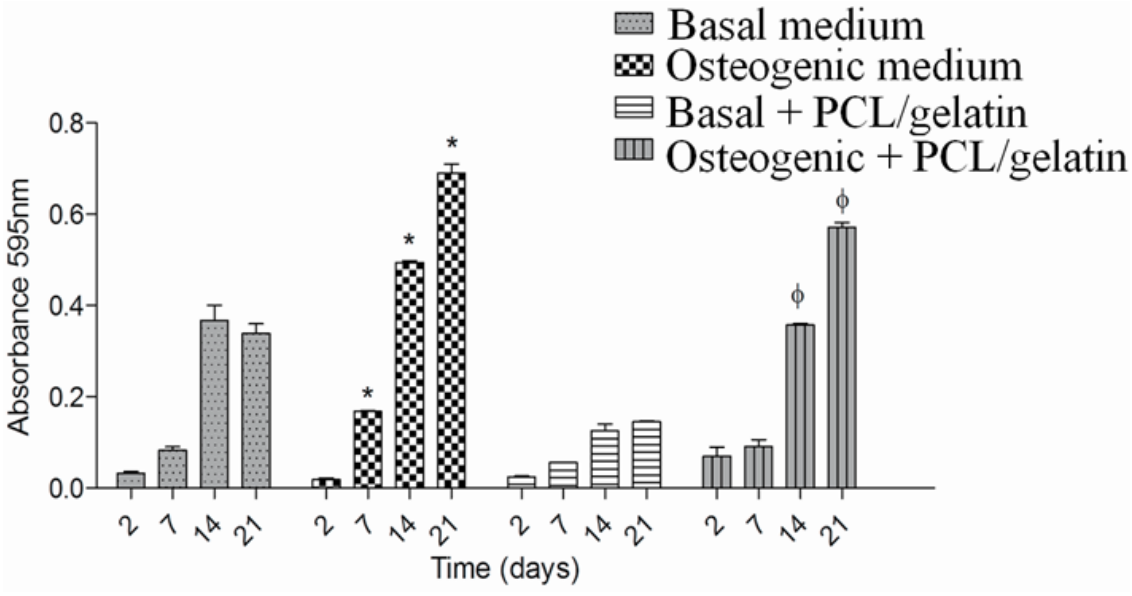

Figure 5.8: ALP activity assays performed 7, 14 and 21 days after hASCs were seeded and cultured in two specific media: basal medium and osteogenic differentiation medium. The results are expressed as the mean ± SD; (*) and (Φ) indicate a significant difference at $p<0.05$.

It was observed that the ALP activity in hASCs cultured in osteogenic medium was higher than the ALP activity in the control cells (basal medium), with the activity observed to increase progressively for up to 21 days. This result is in agreement with the findings of Jaiswal *et al*. [32], who cultured human mesenchymal stem cells *in vitro*. According to these authors, approximately 30–40% of the cells were ALP positive when cultured in osteogenic medium, whereas control cultures contained ALP positive cells at a much lower frequency.

A slight delay in the more pronounced ALP activity was observed for hASCs cultured on PCL/gelatin mats in osteogenic medium. In this case, the onset of increased ALP activity was observed only after 14 days. In spite of this, a continuous increase in cell viability was observed in hASCs cultured on PCL/gelatin mats in osteogenic medium (Figure 5.7). It is likely that the presence of the fibers caused some delay in hASC differentiation, although they continued to produce alkaline phosphatase after 21 days.

It was also observed that ALP was affected by the PCL/gelatin mats in basal medium compared with pristine basal medium (control). Jaiswal *et al*. [32] pointed out the importance of the culture medium for achieving optimal osteogenic differentiation and, thus, greater numbers of ALP-positive cells. In this case, it may be suggested that, without the aid of osteogenic differentiation factors, when the hydroxyapatite-coated fibers were cultured in basal medium, they did not lead to major cellular differentiation towards bone-type cells. It appears that providing an optimum combination of differentiation factors, together with a suitable surface for cell attachment (such as a large mineralized surface area), is important for achieving high levels of osteogenesis.

5.3.5 Endothelial cell marker expression (immunofluorescence assay)

The von Willebrand factor (vWF) glycoprotein acts as both an antihemophilic factor carrier and a platelet-vessel wall mediator in the blood coagulation system. It participates in platelet-vessel wall interactions by forming a noncovalent complex with coagulation factor VIII at the site of vascular injury [39]. It is a useful marker for

endothelial cells and was used as a laboratory test to confirm whether the hASCs were induced to undergo endothelial differentiation when they were cultured in endothelial medium. After 21 days of cell culture on co-axial PCL/gelatin nanofibers in endothelial medium, the hASCs were observed to express vWF, which can be detected as a green glow when observed microscopically, as shown in Figure 5.9-b. Under the other examined conditions, cells cultivated in basal medium did not show evidences of endothelial differentiation (Figure 5.9-a).

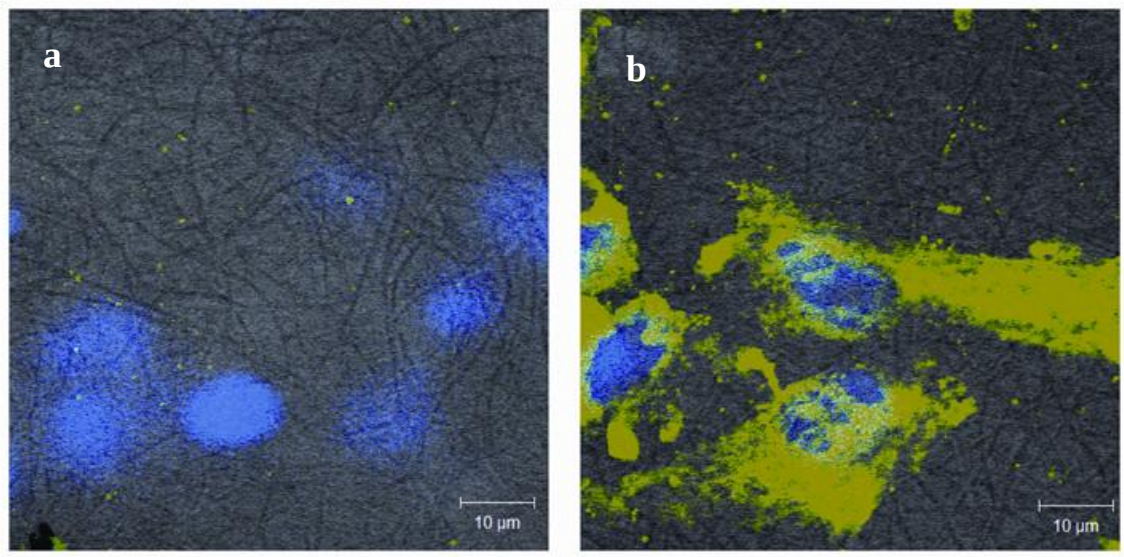

Figure 5.9: Confocal images of the expression of the vWF factor of hASCs after 21 days cultured on the electrospun PCL/gelatin mats in: (a) basal medium (control) and (b) endothelial differentiation medium.

5.4 Conclusions

Co-axial PCL/gelatin nanofibers were successfully produced via electrospinning and biomimetically coated by immersing them in SBF10 for 2 h. At this time, the coating on the fibers was found to be composed of a mixture of hydroxyapatite (HA), carbonate

hydroxyapatite and dicalcium phosphate dihydrate (DCPD). The results of MTT assays demonstrated that the human adipose-derived stem cells (hASCs) seeded on mineralized PCL/gelatin mats in basal medium (control), osteogenic medium and endothelial differentiation medium were viable and could proliferate. The same levels of alkaline phosphatase (ALP) activity were observed in hASCs cultured on mineralized PCL/gelatin mats without nanofibers in osteogenic medium. These results suggest that osteogenic differentiation of hASCs occurred on the mineralized matrices, enabling them to be used as bone scaffold material. The rate of cell proliferation was clearly reduced when the hASCs were cultured on nanofibers in endothelial differentiation medium. This result may be attributed to the decrease in the proliferation ability of stem cells during differentiation. On the other hand, the expression of endothelial cell markers could be detected in cells cultured in the presence of nanofibers in endothelial differentiation medium, thus confirming the differentiation of hASCs into endothelial cells.

References

1. Heng BC, Cao T, Stanton LW, Robson P, Olsen B. Strategies for Directing the Differentiation of Stem Cells Into the Osteogenic Lineage In Vitro. J. Bone Miner. Res 2004; 19:1379-94.
2. Zuk PA, Zhu M, Mizuno H, Huang J, Futtrel JW, Katz AJ, Benhaim P, Lorenz HP, Hedrick MH. Multilineage Cells from Human Adipose Tissue: Implications for Cell-Based Therapies. Tissue Eng 2001; 7:211-28.
3. Wen Y, Jiang B, Cui J, Li G, Yu M, Wang F, Zhang G, Nan X, Yue W, Xu X, Pei X. Superior osteogenic capacity of different mesenchymal stem cells for bone tissue engineering. Oral Surg. Oral Med. Oral Pathol. Oral Radiol 2012; article in press.
4. Paula ACC, Zonari AAC, Martins TMM, Novikoff S, Silva ARP, Correlo VM, Reis RL, Gomes DA, Goes AM. Human Serum is a Suitable Supplement for the Osteogenic Differentiation of Human Adipose-Derived Stem Cells Seeded on Poly-3-Hydroxibutyrate-Co-3-Hydroxyvalerate Scaffolds. Tissue Eng.: Part A 2012; 19:1-13.
5. Zonari A, Novikoff S, Electo NRP, Breyner NM, Gomes DA, Martins A, Neves NM, Reis RL, Goes AM. Endothelial Differentiation of Human Stem Cells Seeded onto Electrospun Polyhydroxybutyrate/Polyhydroxybutyrate-Co-Hydroxyvalerate Fiber Mesh. www.plosone.org 2012; 7:e35422.
6. Almeida HA, Bártolo PJS. Virtual topological optimization of scaffolds for rapid prototyping. Med. Eng. & Phys 2010; 32:775-82.
7. Jang JH, Castano O, Kim HW. Electrospun materials as potential platforms for bone tissue engineering. Adv. Drug Deliv. Rev 2009; 61:1065-83.
8. Dash TK, Konkimalla VB. Poly-ϵ-caprolactone based formulations for drug delivery and tissue engineering: A review. J. Controlled Release 2012; 158:15-33.
9. Xie J, Zhong S, Ma B, Shuler FD, Lim CT. Controlled biomineralization of electrospun poly(e-caprolactone) fibers to enhance their mechanical properties. Acta Biomater 2013; 9:5698-5707.
10. Woodruff MA, Hutmacher DW. The return of a forgotten polymer-Polycaprolactone in the 21st century. Prog. Polym. Sci 2010; 35(10):1217-56.
11. Ratanavaraporn J, Rangkupan R, Jeeratawatchai H, Kanokpanont S, Damrongsakkul S. Influences of physical and chemical crosslinking techniques on electrospun type A and B gelatin fiber mats. Int. J. Biol. Macromol 2010; 47:431-38.
12. Zhang Y, Ouyang H, Lim CT, Ramakrishna S. Electrospinning of gelatin fibers and gelatin/PCL composite fibrous scaffolds. J. Biom. Mater. Res 2005; 72B:156-165.
13. Chong EJ, Phan TT, Lim IJ, Zhang YZ, Bay BH, Ramakrishna S, Lim CT. Evaluation of electrospun PCL/gelatin nanofibrous scaffold for wound healing and layered dermal reconstitution. Acta Biomater 2007; 3:321-30.
14. Mobarakeh LG, Prabhakaran MP, Morshed M, Esfahani MHN, Ramakrishna S. Electrospun poly(ε-caprolactone)/gelatin nanofibrous scaffolds for nerve tissue engineering. Biomaterials 2008; 29:4532-39.

15. Gautam S, Dinda AK, Mishra NC. Fabrication and characterization of PCL/gelatin composite nanofibrous scaffold for tissue engineering applications by electrospinning method. Mater. Sci. Eng., C 2013; 33:1228-1235.
16. Chen J, Chu B, Hsiao BS. Mineralization of hydroxyapatite in electrospun nanofibrous poly(L-lactic acid) scaffolds. J. Biomed. Mater. Res., Part A 2006; 79A:307-17.
17. Tas AC, Bhaduri SB. Rapid coating of Ti6Al4V at room temperature with a calcium phosphate solution similar to 10× simulated body fluid. J. Mater. Res 2004; 19:2742-49.
18. Mosmann T. Rapid colorimetric assay for cellular growth and survival: Application to proliferation and cytotoxicity assays. J. Immunol. Mater 1983; 65:55-63.
19. Fleischer S, Dvir T. Tissue engineering on the nanoscale: lessons from the heart. Curr. Opin. Biotechnol 2012; 24:1-8.
20. Choong C, Triffitt JT, Cui ZF. Polycaprolactone Scaffolds for Bone Tissue Engineering: Effects of a Calcium Phosphate Coating Layer on Osteogenic Cells. Food and Bioproducts Processing 2004; 82:117-125.
21. Yang F, Wolke JGC, Jansen JA. Biomimetic calcium phosphate coating on electrospun poly (ε-caprolactone) scaffolds for bone tissue engineering. Chem. Eng. J 2008; 137:154-161.
22. Sionkowska A. Current research on the blends of natural and synthetic polymers as new biomaterials: Review. Prog. Polym. Sci 2011; 36:1254-76.
23. Elzoghby AO, Samy WM, Elgindy NA. Protein-based nanocarriers as promising drug and gene delivery systems. J. Controlled Release 2012; 161:38-49.
24. Lu Y, Jiang H, Tu K, Wang L. Mild immobilization of diverse macromolecular bioactive agents onto multifunctional fibrous membranes prepared by coaxial electrospinning. Acta Biomater 2009; 5:1562-74.
25. Fu SZ, Ni PY, Wang BY, Xu BY, Peng JR, Zeng L, Zhao X, Luo F, Wei YQ, Qian ZY. In vivo biocompatibility and osteogenesis of electrospun poly(ε-caprolactone)-poly(ethylene glycol)-poly(ε-caprolactone)/nano-hydroxyapatite composite scaffold. Biomaterials 2012; 33:8363-71.
26. Choi MO, Kim YJ. Fabrication of gelatin/calcium phosphate composite nanofibrous membranes by biomimetic mineralization. Int. J. Biol. Macromol 2012; 50:1188-94.
27. Cai Q, Feng Q, Liu H, Yang X. Preparation of biomimetic hydroxyapatite by biomineralization and calcination using poly(L-lactide)/gelatin composite fibrous mat as template. Mater. Lett 2013; 91:275-78.
28. Jaiswal AK, Kadam SS, Sony VP, Bellare JR. Improved Functionalization of Electrospun PLLA/Gelatin Scaffold by Alternate Soaking Method for Bone Tissue Engineering. Appl. Surf. Sci doi:10.1016/j.apsusc.2012.12.152.
29. Takadama H, Kim HM, Kokubo T, Nakamura T. TEM-EDX study of mechanism of bonelike apatite formation on bioactive titanium metal in simulated body fluid. J. Biomed. Mater. Res 2001; 57:441-48.

30. Raynaud S, Champion E, Assollant BD, Thomas P. Calcium phosphate apatites with variable Ca/P atomic ratio I. Synthesis, characterization and thermal stability of powders. Biomaterials 2002; 23:1065-72.
31. Ribeiro Neto WA, Pereira IHL, Ayres E, Paula ACC, Averous L, Góes AM, Oréfice RL, Bretas RES. Influence of the microstructure and mechanical strength of nanofibers of biodegradable polymers with hydroxyapatite in stem cells growth. Electrospinning, characterization and cell viability. Polym. Degrad. Stab 2012; 97:2037-51.
32. Jaiswal N, Haynesworth SE, Caplan AI, Bruder SP. Osteogenic Differentiation of Purified, Culture-Expanded Human Mesenchymal Stem Cells In Vitro. J. Cell. Biochem 1997; 64:295-312.
33. Correa FG, Martínez JB, Gómez JS. Synthesis and characterization of calcium phosphate and its relation to Cr (VI) adsorption properties. Rev. Int. Contam. Ambient 2010; 26:129-34.
34. Liao S, Murugan R, Chan CK, Ramakrishna S. Processing nanoengineered scaffolds through electrospinning and mineralization suitable for biomimetic bone tissue engineering. Journal of the mechanical Behavior of Biomedical Materials I 2008; 252-60.
35. Li J. Structural characterization of apatite like materials. Thesis submitted to the School of Metallurgy and Materials of University of Birmingham (2009); pp 56-60. Available in inhttp://etheses.bham.ac.uk/618/1/Li10MRes.pdf (accessed in 01/31/2013).
36. Franco PQ, Silva JC, Borges JP. Produção de fibras de hidroxiapatite por electrofiação. Ciência & Tecnologia dos Materiais 2010; 22:57-64.
37. Rehman I, Bonfield W. Characterization of hydroxyapatite and carbonated apatite by photo acoustic FTIR spectroscopy. J. Mater. Sci.: Mater. Med 1997; 8:1-4.
38. Xie J, Riley C, Chittur K. Effect of albumin on brushite transformation to hydroxyapatite. J. Biomed. Mater. Res 2001; 57:357-65.
39. Sadler JE. Von Willebrand factor assembly and secretion. Journal of Thrombosis and Haemostasis 2009; 7:24-7.

6 Conclusão

Neste estudo, nanofibras coaxiais de policaprolactona (PCL) formando o núcleo, e gelatina formando a casca, foram produzidas e caracterizadas. PCL fornece características de biodegradabilidade, bioreabsorção e propriedades mecânicas superiores, e a gelatina melhora a biocompatibilidade, favorecendo a adesão e proliferação celular. Para restringir a solubilidade da gelatina suas cadeias foram reticuladas com glutaraldeído. Conforme mostrado, foi possível também produzir e caracterizar nanofibras de PCL e gelatina separadamente utilizando a eletrofiação convencional, mas para estes materiais serem usados na regeneração de tecido ósseo, o idealizado é um biomaterial que possa fornecer características semelhantes ao osso, o que poderá ser mais garantido agregando as características dos dois materiais. Após mudanças nos parâmetros da solução e processamento durante a eletrofiação, a morfologia obtida das fibras foi caracterizada, provando que estas alterações podem modificar substancialmente a forma e a aplicabilidade de cada material. Para a aplicação em Engenharia de Tecido Ósseo, fosfatos de cálcio foram depositados na superfície das fibras pela mineralização induzida após imersão das fibras em solução SBF10. A gelatina facilitou a homogênea cobertura. Difração de Raios X indicou a composição do depósito mineral por fosfatos de cálcio e hidroxiapatita, principal constituinte da matriz inorgânica dos ossos. O material desenvolvido por esta técnica apresentou adequada estrutura, sendo ainda não-tóxico e favoreceu o crescimento e proliferação de células-tronco (hASCs) *in vitro*, assim como revelou indícios de diferenciação em osteoblastos, tornando esta estratégia viável e uma alternativa segura para aplicação em Engenharia de Tecido Ósseo.